Sara Raquel Gemelgo Pereira

Mestre em Engenharia Biomédica

Study of the Effects of Cold Atmospheric Plasmas on Skin Cancer Cells

Dissertação para obtenção do Grau de Doutor em

Biofísica e Bioquímica da Radiação:
Especialização em Biofísica

Orientador: Susana Isabel dos Santos Silva Sério Venceslau, Professor Auxiliar, Faculdade de Ciências e Tecnologia, Universidade NOVA de Lisboa, FCT/UNL

Co-orientador: Paulo António Martins Ferreira Ribeiro, Professor Associado, Faculdade de Ciências e Tecnologia, Universidade NOVA de Lisboa, FCT/UNL

Júri:

Presidente: Prof. Doutor Paulo Manuel Assis Loureiro Limão-Vieira

Arguente(s): Doutor Antero José Pena Afonso de Abrunhosa

Doutora Susana Ferreira de Oliveira Silva

Vogais: Prof. Doutora Maria Alice Santos Pereira

Prof. Doutor André João Maurício Leitão do Valle Wemans

Doutora Quirina Alexandra Tavares Ferreira

Prof. Doutora Susana Isabel dos Santos Silva Sério Venceslau

FACULDADE DE CIÊNCIAS E TECNOLOGIA
UNIVERSIDADE NOVA DE LISBOA

Março, 2021

Sara Raquel Gemelgo Pereira

Mestre em Engenharia Biomédica

Study of the Effects of Cold Atmospheric Plasmas on Skin Cancer Cells

Dissertação para obtenção do Grau de Doutor em

Biofísica e Bioquímica da Radiação:
Especialização em Biofísica

Orientador: Susana Isabel dos Santos Silva Sério Venceslau, Professor Auxiliar, Faculdade de Ciências e Tecnologia, Universidade NOVA de Lisboa, FCT/UNL

Co-orientador: Paulo António Martins Ferreira Ribeiro, Professor Associado, Faculdade de Ciências e Tecnologia, Universidade NOVA de Lisboa, FCT/UNL

Júri:

Presidente:	Prof. Doutor Paulo Manuel Assis Loureiro Limão-Vieira
Arguente(s):	Doutor Antero José Pena Afonso de Abrunhosa
	Doutora Susana Ferreira de Oliveira Silva
Vogais:	Prof. Doutora Maria Alice Santos Pereira
	Prof. Doutor André João Maurício Leitão do Valle Wemans
	Doutora Quirina Alexandra Tavares Ferreira
	Prof. Doutora Susana Isabel dos Santos Silva Sério Venceslau

FACULDADE DE CIÊNCIAS E TECNOLOGIA
UNIVERSIDADE NOVA DE LISBOA

Março, 2021

[Study of the Effects of Cold Atmospheric Plasmas on Skin Cancer Cells]

"Success consists of going from failure to failure

without loss of enthusiasm."

Winston Churchill

To my parents.

Acknowledgments

First, I would like to thank my supervisor Prof. Dr. Susana Sério for all the support, encouragement, friendship and guidance throughout these last four years. I also want to express my gratitude to Prof. Dr. Paulo Ribeiro, for all the patience, the good mood, and all the jokes. I will never forget the conversations that the three of us had. I really want to acknowledge them for the excellent experience I lived during the past years, which was far easier with their help and friendship.

To Prof. Dr. Fátima Raposo for all her kindness, valuable conversations, and advices.

I also would like to acknowledge Prof. Dr. Jorge Silva for the opportunity to carry out *in vitro* experiments in his laboratory facilities, and for all the good advices he shared with me.

To Prof. Dr. Paula Videira and Prof. Dr. Zélia Silva, from UCIBIO – Applied Molecular Biosciences, for all the help and collaboration with the flow cytometry assays.

To Prof. Dr. Cecília Roque from UCIBIO, REQUIMTE, for the opportunity to use the fluorescence plate reader.

To Prof. Dr. Paulo Limão-Vieira, who as coordinator of the Radiation and Biophysics Doctoral Training Programme allowed me to pursue my PhD.

To Doctor Kristian Wende, and all the people I had the opportunity to meet and work with at INP during the three months I spent in Greifswald. Thank you for the warm reception, for helping me every time I needed, and for all the knowledge we had the opportunity to share. I will never forget this experience.

To the Department of Physics of NOVA University of Lisbon and CEFITEC through UID/FIS/00068/2019. To the financial support from the Portuguese National Funding Agency FCT-MCTES through PD/BD/114444/2016 (S. Pereira) scholarship. This work was also supported by Radiation Biology and Biophysics

Doctoral Training Programme (Rabbit, PD/00193/2012); Applied Molecular Biosciences Unit – UCIBIO UID/Multi/04378/2020 (UCIBIO) and CEFITEC UID/FIS/00068/2020 unit.

Beyond these direct actors in this work, others had a great importance in my PhD experience. Namely, I would like to thank to Ana Cruz and Afonso Moutinho for all the good conversations and supportive words. To Faustino for helping me whenever I ask for technical support. To "*Sr.*" Eduardo for all the friendliness, the smiles, and for all his positiveness.

To Érica Pinto and Tiago Cunha, no doubts the best work colleagues I could have in this journey. Thank you a lot my dear friends for all the patient, the coffee breaks, the breaks for no reason, the long conversations, the confidences and all the laughs. Thank you for turning stressful situations into funny situations. We definitely had good times. To Liliana Teixeira, for being such a good friend. Without you, these four years would have been very different. To Jorge Barreto, for his friendship, the conversations, the morning coffees, for all the times I have decided to appear in his laboratory without previous advice.

I also want to acknowledge to Diogo Miguel. Thank you for entering in my life, for open my eyes and of course thank you for showing me that there is time for everything. Thank you for all the hugs, for your smile, and your patient. Things are easier with you by my side.

To my grandparents who I love so much, and especially to my parents, whom despite the long physical distance that separates us always remained present. Thank you for your unconditional support during all my life, for all the "colinho", the good night message that you never forget; it is not the same that a good night kiss, but it feels so good. Thank you for always be by my side. There are no words that allow me to express all the gratitude and love that I have for both of you. Thank you.

Resumo

Os plasmas frios à pressão atmosférica (CAPs) são um caso particular de plasmas não-térmicos compostos principalmente por espécies reactivas de oxigénio e azoto (ROS e RNS, respectivamente), radiação ultravioleta (UV) e partículas carregadas. Nos últimos anos, tem-se vindo a investigar o tratamento indirecto de líquidos com CAPs tendo em vista a sua utilização no campo da oncologia. Estes tratamentos indirectos têm sido alvo de grande atenção, uma vez, que demonstraram possuir uma capacidade de destruir as células cancerígenas com uma efectividade semelhante à irradiação directa por CAPs. Além disso, têm a vantagem de evitar os efeitos da radiação UV e os campos electromagnéticos presentes nos plasmas, estando os seus efeitos apenas relacionados com a quantidade de espécies reactivas que são originadas em meios tratados por CAPs.

Para um melhor entendimento dos mecanismos envolvidos nas interacções entre os meios tratados, os CAPs e as células, procedeu-se, neste trabalho, ao desenvolvimento de um dispositivo de jacto (*Jet*) de plasma frio, para posterior estudo da vulnerabilidade de quatro linhas celulares humanas (SCC-15, Met-1, HGF-1 e HaCaT) a meio de cultura previamente exposto a CAPs. Foram também caracterizados os meios expostos ao plasma em termos de quantificação das concentrações de peróxido de hidrogénio (H_2O_2), nitrato e nitrito, com base em

métodos colorimétricos e cromatografia iónica, respectivamente. De modo a comprovar que os efeitos da exposição a CAPs são dependentes do dispositivo utilizado para a sua produção, realizaram-se estudos de espectrometria de massa, para comparar os espectros do dispositivo desenvolvido com o da kINPen09. Com base neste estudo, foi possível investigar a oxidação dos grupos tiol numa solução de cisteína. A cisteína foi escolhida por se tratar de um aminoácido que actua como biomarcador dos danos oxidativos. Com o intuito de completar estes resultados, realizou-se ainda o estudo da degradação do fenol e da adição de *scavengers* aos meios tratados. De acordo com os resultados obtidos, pode-se observar que as linhas celulares cancerígenas (SCC-15 e Met-1) são mais vulneráveis aos líquidos expostos a CAPs do que as linhagens não-cancerígenas (HGF-1 e HaCaT). Os efeitos dos CAPs aquando da utilização do dispositivo desenvolvido no âmbito deste trabalho, pareceram estar essencialmente relacionados com os mecanismos induzidos pelas espécies RNS, enquanto que no caso de tratamentos realizados com a kINPen09, se verificou uma maior taxa de oxidação, dada a elevada concentração de ROS presente, principalmente H_2O_2.

Palavras-chave: Plasma em medicina; CAPs; espécies reactivas de oxigénio (ROS) e azoto (RNS)

Abstract

Cold atmospheric plasmas (CAPs) are a specific type of non-thermal plasmas mainly composed of reactive oxygen and nitrogen species (ROS and RNS, respectively), UV radiation and charged particles. In the last years, liquids treated by CAPs (indirect CAPs treatments) have attracted attention in oncology due to its ability to destroy cancer cells with an effectiveness similar to direct irradiation of cells by CAPs. Moreover, these indirect treatments offer the advantage of avoiding the effects of UV radiation and of the electrical fields present in plasmas being their effects mainly dependent on the reactive species produced in CAPs treated medium.

To better understand the mechanisms behind the interaction between CAPs, treated medium and cells, in this work, a plasma jet device was engineered for study the vulnerability of four human cell lines (SCC-15, Met-1, HaCat, and HGF-1) to the culture medium previously exposed to CAPs. Besides that, also the characterization of the liquids exposed to plasma was done, by quantification of the concentration of H_2O_2, nitrate, and nitrite, using colorimetric assays and ion chromatography, respectively. To prove that the effects of exposure to CAPs are dependent on the used device, mass spectrometry studies were carried out in order to compare the spectra obtained using the developed device with that of the kINPen09. Based on this study, it was possible to investigate the oxidation of

thiol groups of a cysteine solution. Cysteine was chosen since it is an amino acid that acts as a biomarker of oxidative damage. To complete these results, the study of phenol degradation and the addition of scavengers to the treated medium were also evaluated. According to the obtained results it could be observed that the cancer cell lines (SCC-15 and Met-1) in study are more sensitive to the liquids treated by CAPs than the non-cancer ones (HGF-1 and HaCat). The CAPs effects, in the case of the developed jet, seem to be mainly related to the mechanisms induced by RNS species, while in treatments performed using kINPen09, a higher oxidation rate was observed, due to the high concentration of ROS species, mainly H_2O_2.

Keywords: Plasma Medicine; CAPs; jet devices; skin cancer; ROS; RNS.

Contents

List of Figures

List of Tables

List of Acronyms and Symbols

7AAD – 7-Aminoactinomycin D

A – Saturation ionization in the gas
AC – Alternating current
ADJ – Adjustment
AnnexinV – APC AnnexinV
ArN – Argon-Nitrogen
ArNO – Argon-Nitrogen-Oxygen
ArO – Argon-Oxygen
ATCC – American Type Culture Collection

B **–** Excitation and ionization gas energies
Bcl-2 - B-cell lymphoma 2

C – Equivalent capacitance of the capacitors
C_1 and **C_2 –** Capacitors
CAPs – Cold Atmospheric Plasmas

d **–** distance
D_1 and **D_2 –** Diodes
D_3 and **D_4 –** Zener diodes
DBD – Dielectric Barrier Discharge
DC – Direct Current
DMEM – Dulbecco's Modified Eagle's Medium
DMEM-F12 – Dulbecco's Modified Eagle's Medium: nutrient mixture F-12
DNA - Deoxyribonucleic acid

ERK – Extracellular Regulated Kinases

FBS – Fetal Bovine Serum

G – Metal Oxide Semiconductor Field Effect Transistor Gate

HPLC – High Performance Liquid Chromatography
HRP – Horseradish Peroxidase

I_L(min) –Minimum load current
I_o (max) – Maximum output current
IC – Ion Chromatography
INP – Input

JNK – c-Jun N-terminal kinase

L – Inductance of the central
L_1 – Central coil

MAK165 – Fluorometric Hydrogen Peroxide assay
MAPKs – Mitogen-Activated Protein kinases
MOSFET – Metal Oxide Semiconductor Field Effect Transistor
MS – Mass Spectrometry
MS/MS – fragmentation spectra

NADPH + H^+ – Nicotinamide Adenine Dinucleotide Phosphate
NMDA – *N*-methyl-D-aspartate receptor
NMSC – Non-melanoma skin cancer

OES – Optical Emission Spectroscopy
·OH – Hydroxyl radical
OUT – Output

***p* –** Gas pressure
PBS – Phosphate Buffered Saline
Pen/Strep – Penicillin-Streptomycin
PLA – Polylactic acid

R_1 – Variable resistance
R_2 – Fixed resistance
Resazurin – 7-Hydroxy-3H-phenoxaxin-3-one 10-oxide
Resorufin – 7-Hydroxy-3H-phenoxazin-3-one
RF – Radio Frequency
RNS – Reactive Nitrogen Species
RNOS or RONS – Reactive Nitrogen and Oxygen Species

ROS – Reactive Oxygen Species

SCC – Squamous Cell Carcinoma
slm – Standard liter per minute
SOD – Superoxide dismutase

Tj – Operating junction temperature range
TOF – Time-of-flight
TOF-MS – Time-of-flight Mass Spectrometers

US FDA – Food and Drug Administration
UV – Ultraviolet

V **–** voltage
$\mathbf{V_B}$ **–** Applied voltage
$\mathbf{V_{out}}$ **–** Output voltage range
$\mathbf{V_{out}}$**-** $\mathbf{V_{out}}$ **–** Voltage differential
$\mathbf{V_{ref}}$ **–** Voltage difference between the output pin and the adjustment pin
VUV – Vacuum Ultraviolet

ZVS – Zero Voltage Switching

λ_{em} **–** Emission wavelength
λ_{exc} **–** Excitation wavelength

γ_{se} **–** Secondary-electron emission coefficient

1

General Introduction

Nowadays, mainly due to the change of behaviour of the population favoring a greater and inadequate exposure to solar radiation, an increase in the incidence of skin cancer has been registered. According to statistics of the World Health Organization, one in each three diagnosed cancers corresponds to skin cancer. The most common types of skin cancer can be separated into melanoma and non-melanoma skin cancer (NMSC), the last representing the most common form of cancer in Caucasians. Depending on the type of skin cells from which the cancer cells are originated, NMSC can be divided in Basal Cell Carcinoma and Squamous Cell Carcinoma (SCC). The SCC arises from dysplastic epidermal keratinocytes and represents 20-30% of the reported cases of NMSC, and when compared to malignant melanoma they have an incidence about 20 times higher. The risk of developing SCC through life is about 15% for light-skinned individuals, which are more conducive to the onset of sunburn and it is twice more common in men than in women. It is also more likely in individuals who have received an implant (immunosuppressed), particularly kidneys, compared to control individuals of the same age[1–4]. With the increase of the average life expectancy, an increase in the incidence rates of SCC is expected, since in 2050 approximately 32% of the population will be over 60 years[5].

Given the high complexity of cancer, it is difficult to find treatments that successfully induce the killing of cancer cells, without damage to the

surrounding healthy tissue. This fact, coupled to the possibility of tumors develop drug resistance during chemotherapy treatments, highlights the need to discover more effective, accurate and minimally invasive treatment procedures. It was in this context that cold atmospheric pressure plasmas (CAPs) have started to be investigated as a possible complement and/or alternative to common cancer therapies. CAPs are a near-room temperature plasma, generally produced in laboratory conditions, by applying an external source of energy to a neutral gas up to a critical point, at which electrons dissociate from atoms. The resulting ionized gas will be mainly composed of a mixture of reactive oxygen and nitrogen species (ROS and RNS), ultraviolet (UV), visible and infrared light, electromagnetic fields, electrons, and ions. It is important to note that, since these plasmas are laboratory-generated, their properties, such as their energy and charged particles density, will be dependent on the features of the used set-up: applied power and its type, and of the feeding gas.

While the first established electro-surgical techniques using plasmas in medicine, such as plasma coagulation, were mainly based on their bio-destructible effects, over the past decade, CAPs have emerged worldwide as an independent field of high relevance in biomedical sciences and in medicine, since they can be directly applied to living cells and tissues offering the possibility of a minimally invasive surgery. CAPs are the only plasma sources that may be applied to living cells since biological applications require that the discharge occurs at atmospheric pressure[6–8]. It was demonstrated in the literature that CAPs lead to selective eradication of cancer cells *in vitro* and to the reduction of tumor size *in vivo*. Also, ROS metabolism and oxidative stress-responsive gene deregulation have been detected after CAPs treatments[9]. However, the full mechanism of action between CAPs and living cells or tissues remains not completely understood, the reason why further studies must be carried out to establish CAPs as a solid treatment on medicine fields. There are already some CAPs devices approved for use in medical applications, specifically in dermatology. It is thought that the CAPs effects on living cells are mainly related with the reactive oxygen and nitrogen (RONS) species produced in the gas phase

of the produced plasma. These species will interact with the surrounding ambient air, in a multitude of reactions that will result in the production of more reactive species, such as hydroxyl radicals, and long-lived species as hydrogen peroxide (H_2O_2).

Although conventionally CAPs have been directly applied to cancer cells and tissues over the last years, many investigation studies have emerged using CAPs irradiated medium (indirect CAPs treatment) as a possible method of anti-cancer therapy, instead of direct irradiation by CAPs. These indirect treatments have demonstrated similar effects to direct treatments with the advantage that the treated medium can be injected into the body and therefore can reach tissues inaccessible through direct irradiation. Additionally, indirect treatments also have the advantage of avoiding the electrical fields and UV radiation present in CAPs.

Considering this, the main goals of this work were the development and optimization of a CAPs jet device, and the study of the interactions between the produced CAPs and living cells, particularly skin cancer and non-cancer cells. Additionally, the interactions between CAPs and aqueous media were investigated with the special focus on hydrogen peroxide, nitrite, and nitrate production. Since it is known that ROS and RNS can induce oxidation and nitrosation, respectively, the chemistry of the plasma produced by the developed jet was also studied and compared with the chemistry of kINPen09, a well-characterized plasma jet device with CE approval for medical use.

1.1. Dissertation structure

The present dissertation is divided in eight chapters.

Chapter 1: General introduction

The present chapter intends to give a general framework of the work developed along this dissertation, as well as the summary of the main goals and an overview of the dissertation structure.

Chapter 2: Theoretical Fundamentals

This chapter aims to provide the theoretical concepts necessary to understand the themes addressed in this dissertation.

Chapter 3: Experimental concepts and methodology

In this chapter, the fundamentals of the instrumental techniques used to perform this work are described. The chapter is divided into three sub-chapters. In the first one, the technique Optical emission spectroscopy (OES) used for plasma characterization, i.e., for the evaluation of the species generated in the gas phase of the produced CAPs is explained. Then, in the second sub-chapter, the cytotoxic assay (Resazurin assay) used for the study of cellular viability after exposure to CAPs and CAPs treated liquids is presented, as well, as the flow cytometry principles, since this technique was employed to investigate the mechanisms of cell death induced by CAPs. Finally, in the last sub-chapter the fundamentals of the techniques used to examine the reactive species that are formed in liquids due to plasma exposure, namely, colorimetric assays for H_2O_2 detection, mass spectrometry, and ion chromatography, are exposed.

Chapter 4: Development and Characterization of the plasma jet device

Here, the developed CAPs jet device is depicted as well as the characteristics of the custom-made power supply. The characterization of the produced gas-phase plasma, by OES, is also presented in this chapter.

Chapter 5: Plasma treatment conditions affect cell viability

This chapter summarizes the most important results regarding the *in vitro* susceptibility of different skin cancer and non-cancer cells to liquids treated by CAPs. It also presents the cell lines that were used during this work, as well as the procedures carried out during cell culture experiments, and the way how plasma treatments were performed. The procedures followed for cytotoxicity

and flow cytometry studies are also shown in this chapter, just like the obtained results. A small discussion of the obtained results after all the performed *in vitro* assays, and the influence of using different working parameters during plasma treatments is also done in this chapter.

Chapter 6: Liquid characterization

This chapter addresses the characterization of liquids after plasma exposure. In this sense, the procedures followed for the determination of temperature and pH changes after CAPs exposure, and for identification and quantification of the species produced due to CAPs treatments are presented and discussed. Moreover, the addition of scavengers after CAPs treatment is also investigated in order to have a better idea of which species are the main responsible for plasma-liquid-cell interactions. The main conclusions and results of this part of the work are summarized in the last section of the chapter.

Chapter 7: Comparison between the developed plasma jet device and the well characterized kINPen09

Here, the cysteine amino acid and the phenol compound are used to investigate the plasma-derived liquid chemistry induced using two different set-ups: the developed jet, named *Jet*, and the kINPen09, in order to evaluate if with this model a fingerprint of the used devices can be obtained. The evaluation of the biological effectiveness of *in vitro* treatments done with both set-ups is also performed, and the influence of using different gas compositions is analysed. The quantification of the long-lived species deposition is also presented in this chapter, with the followed procedures and the obtained results being presented and discussed. Once again, a summary of the main conclusions about the work described in this chapter is done.

Chapter 8: Conclusions and future work

In this section, the main conclusions of the thesis are presented, together with a discussion regarding the future work perspectives. Additionally, the publications resulting from the developed work are presented.

2

Theoretical Fundamentals

2.1. Plasma

The term plasma comes from an ancient Greek word meaning "something molded". In physics, it was first identified in a Crookes tube, in 1879, and described by Sir William Crooke, who at the time called it radiant matter[10]. The term plasma as we know it was coined to Irving Langmuir in 1928, when he was investigating the electron transport from thermionic filaments, and developed the plasma sheaths theory in analogy to the liquid portion of blood (blood plasma), which serves as a medium of transport for delivering nutrients to the cells of the different parts of the body[11].

Nowadays, plasma is considered the fourth state of matter[12]. As the temperature increases, molecules become more energetic and transform the states of matter in the sequence: solid, liquid, gas and plasma. Plasmas can be found in nature (e.g. plasmas created in stars, polar aurora, lightning), and can be generated in laboratory conditions by applying an external source of energy to a neutral gas up to a critical point, at which electrons dissociate from atoms. The resulting ionized gas will be mainly composed of ions, electrons, UV photons and highly reactive chemical species, such as reactive oxygen and nitrogen species (RONS), ozone (O_3), visible and infrared light and electromagnetic fields, all of them moving in random directions as Figure 2.1 depicts. Therefore, the

overall ratio between positive and negative particles is such that the produced plasma is considered electrically neutral[13–17].

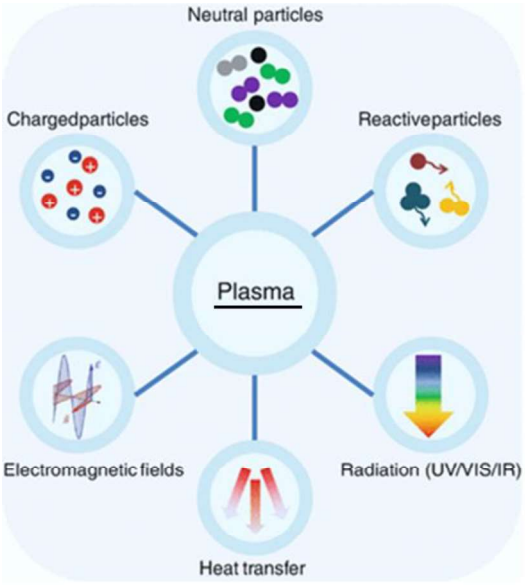

Figure 2.1 Schematic representation of the plasma composition adapted from[18].

In a general way, plasmas can be divided into two major categories: thermal and non-thermal plasmas[19]. Thermal plasmas are those in which ions and electrons are in thermodynamic equilibrium, meaning that all the present particles have the same temperature. To note, that as in any gas, the temperature of the plasma reflects mostly, that of the ions, heavy particles or neutral molecules, and not that of the electrons. Thus, since the mass of an electron is much lower than the mass of a heavy particle, many collisions are needed to achieve a state of thermal equilibrium, which implies quite long discharge times. Contrariwise, non-thermal plasmas, also known as cold plasmas, are characterized for having electrons at a higher temperature than the ions and neutrals, which are close to room temperature[20,21]. These two types of plasmas can be found not only in the laboratory but also in nature. An example of non-thermal plasma in nature is the solar aurora, while the solar plasma is an example of thermal plasma in nature.

Within the non-thermal plasmas, there is the specific case of Cold Atmospheric Pressure Plasmas (CAPs), which have gained interest in terms of

biomedical applications since they can operate stably under open atmospheric conditions and have successfully shown its potential in wound healing, medical sterilization, dermatology, and cancer treatments[19,22,23].

2.1.1. Generation of Cold Atmospheric Plasmas[a]

In direct current discharge systems, gas breakdown starts in a stationary electric field created between two different electrodes. In the absence of an electrical field, the total charge of the electrons and protons, atoms or molecules in gases is equal. However, when an external field is applied, a difference of potential between the cathode and the anode is created, and as consequence a very weak current is produced, and the voltage starts to increase[24,25]. As a result, energy is imparted to the electrons, which can gain enough kinetic energy to produce secondary electrons, through collisions with the electrodes and the neutral gas atoms, in a process known as the avalanche breakdown or *Townsend* mechanism. In the case of low pressures, the electron mean free path is high and the avalanche process is observed until the plasma extends across the entire region between the electrodes[26,27].

To facilitate the understanding of the *Townsend* mechanism, a direct current system of two parallel electrodes[28], separated by a distance d to which a V voltage is applied, providing an electric field E is considered (Eq 2.1)[29]:

$$E = \frac{V}{d} \tag{2.1}$$

According to Townsend discharge model, each primary electron produced near the cathode drifts to the anode generating positive ions by collision with the species supplied to the system, that are moving in the opposite direction as depicted in Figure 2.2. These, in turn, will contribute to the extraction of the electrons from the cathode due to the emission of secondary electrons.

[a]This sub-chapter is based on a chapter of the book CIBB 2018: Pereira S., Pinto É., Ribeiro P.A., Sério S. (2020) Non-thermal Atmospheric Pressure Plasmas: Generation, Sources and Applications. In: Raposo M., Ribeiro P., Sério S., Staiano A., Ciaramella A. (eds) Computational Intelligence Methods for Bioinformatics and Biostatistics. CIBB 2018. Lecture Notes in Computer Science, vol 11925. Springer, Cham.

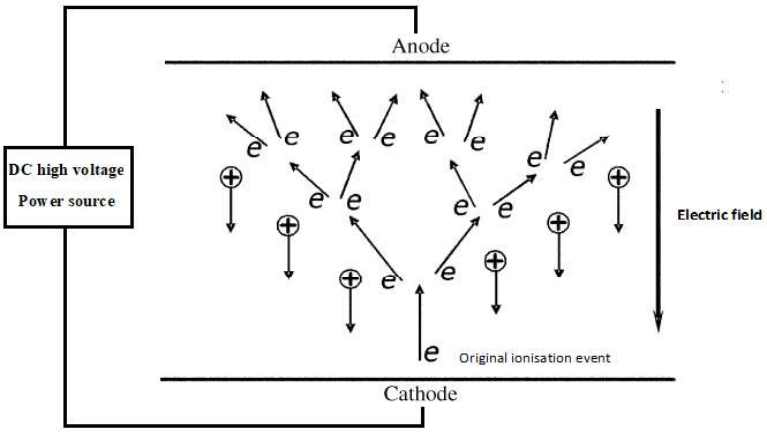

Figure 2.2 Representation of the electron avalanche mechanism, adapted from[30].

Although Townsend was the first researcher to develop a model to explain the breakdown of gas molecules in the presence of an electrical field, it was F. Paschen who first studied the breakdown conditions at different gas pressures. The main outcome of the Paschen studies is the well-known experimental Paschen curve, that relates the applied voltage V_B with the product of gas pressure and electrode separation (pd)[27,31]. The experimental Paschen curve for different gases is represented in Figure 2.3, where all curves present a minimum voltage point, corresponding to the most favorable breakdown condition.

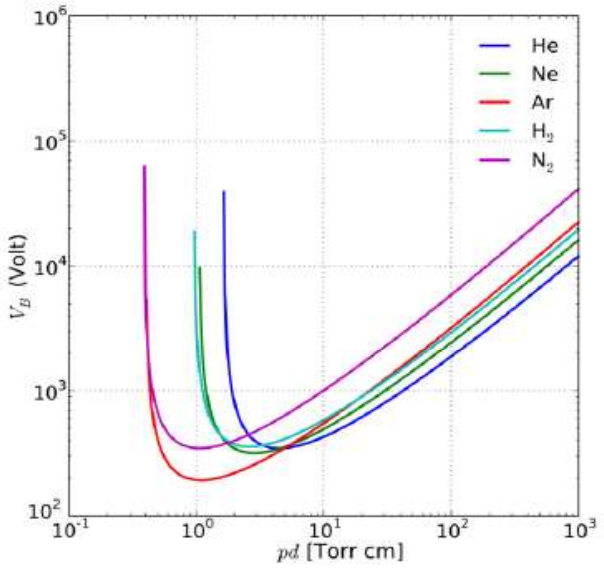

Figure 2.3 The experimental Paschen curve , reprinted with permission from[32].

This relationship between the applied voltage (V_B) and the product between the gas pressure and electrode separation (pd) can be expressed by equation 2.2:

$$V_B = \frac{C_1(pd)}{C_2 + \ln(pd)} \tag{2.2}$$

where C_1 and C_2 are constants that depend on the used gas.

According to this, to the left of the Paschen minimum, at low *pd* values, the electrons mean free path is high and the frequency of ionizing collisions is small. Consequently, a higher voltage is needed to produce ions in number and with energy enough to regenerate, over the cathode, the electron flow that generated these ions. On the other hand, for small distances between electrodes (small *d*), the extension of the ionizing trajectories will be limited to *d*. Together, this means that decreasing the frequency of ionizing collisions and the extension of the electronic trajectories, a higher voltage is needed to initiate a self-sustained discharge. At higher *pd* values (right side of Paschen curve), the electron mean free path is smaller and the frequency of the collisions is higher. However, as *d* is also higher, the increase in electron energy between collisions is lower due to the decrease of the electric field. The excitation collisions dissipate energy, compete with the ones of ionization, and consequently, a higher voltage is needed, to generate a number of ions able to produce enough electrons over the cathode. Still in this situation, at higher pressures, the mean free path is lower, and the ions lose energy in the gas due to inelastic collisions and resonant charge-exchange. Consequently, to provide more energy to the ions higher voltage is needed.

2.1.2. Cold atmospheric plasma sources for biomedical and plasma medicine applications

Since the first dielectric barrier discharge (DBD) reactor was designed in the 19th century by W. von Siemens, several different sources for CAPs production have been developed. Nowadays, in the field of plasma medicine research, two different configurations are being widely used for CAPs production: the DBD and the non-equilibrium atmospheric pressure plasma jets (jets). The typical

layout of a typical DBD reactor is shown in Figure 2.4[6,20,23,33,34]. Plasma jets are generally composed of two different electrodes and a nozzle through which the gas flows. The two electrodes, usually a sharp point and a hollow cylindrical, are normally mounted in a coaxial arrangement. The plasma, formed inside the tube, is transported to the outside through the gas flow[35]. Different power driving methods can be used, including DC, RF and microwave power. The DBD uses plate electrodes covered by a dielectric (such a glass). The plasma is generated in the space between the electrodes by application of a high sinusoidal voltage. When compared to DBDs, plasma jets have the advantage of allowing more localized treatments, since the plasma can be conveniently transported to the target at a more remote location and away from the main plasma generation area[22,33,34]. Moreover, jets present greater inherent stability once the gas flow can be controlled more readily[19]. The DBDs, on another hand, allow the treatment of larger areas and often do not require a gas source, once most of these devices can work using only atmospheric air. However, in this last situation, the stability of the DBDs will depend not only on factors such as the distance between the electrodes and the conductivity of the tissue to be treated but also on the ambient air humidity[33,35,36].

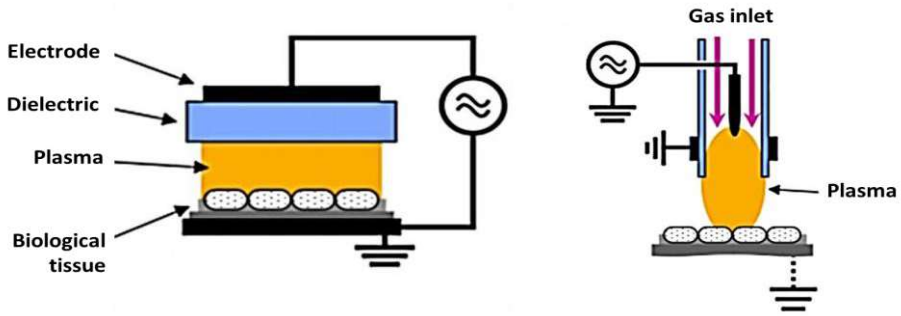

Figure 2.4 Schematic representation of a DBD and a plasma jet device adapted from[22].

2.1.2.1. The atmospheric pressure argon plasma jet kINPen09

In this section, special attention will be given to the kINPen09, since nowadays it is one of the most used devices in plasma medicine research, and it was used in a part of the work of this thesis.

The kINPen is a commercially available atmospheric pressure plasma jet, Figure 2.5, developed in Leibniz-Institute for Plasma Science and Technology, INP Greifswald, Germany. It has the CE mark which certifies that the product meets EU consumer safety, health, and environmental requirements. The device consists of a pin-type powered electrode in a dielectric ceramic tube with a grounded outer electrode, being operated using a power supply and a gas supply unit. The centered driven electrode has a diameter of 1 mm and is sharpened to a tip. The distance from the tip to the nozzle exit is about 3.5 mm. The inner and outer diameter of the ceramic capillary are 1.6 mm and 2 mm, respectively. The kINPen can be operated with noble gases (especially argon), with (up to 2%) or without molecular admixtures, such as oxygen and nitrogen. The gas flow typically lies in a range from 3 to 5 standard liters per minute (slm). The plasma is generated by applying a sinusoidal voltage (2-6 kV_{pp}) with a frequency of 1.0-1.1 MHz applied to the central electrode. Power dissipation inside the plasma of 0.3-3.5 W has been reported at these operating conditions. Depending on the used parameters, the plasma effluent displays a length of 7 to 15 mm, with approximately 1 mm of diameter[37]. The plasma is generated from the top of the central electrode and expands to the surrounding air outside the nozzle. The physical and chemical aspects of kINPen09 have been already extensively investigated. High spatial and optical resolution have shown that the produced plasma propagates in a bullet-like manner[38]. Typical reactive species generate by kINPen include ions, electrons, RONS, electric and magnetic fields, UV, visible and infrared light and neutral particles. It is estimated that hundreds of different reactions take place in the plasma gas phase[19,39,40]. It is known that kINPen09 does not produce significant amounts of nitric oxide (NO) but produces significant amounts of ozone[38,41].

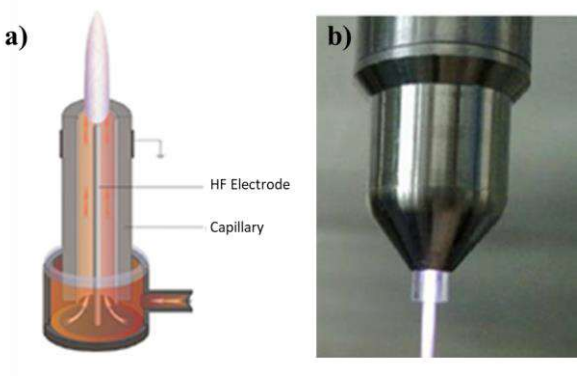

Figure 2.5 a) Schematic representation and b) image of the kINPen09 adapted from[42].

2.1.3. Plasma medicine: state of art

Plasma medicine is a relatively new scientific field that grew from the research of the application of CAPs in bioengineering. In the mid of the 1990s, the first experiments involving the use of plasma in the biomedical field were conducted showing that these plasmas can be successfully used to inactivate bacteria[43]. At the time, these results were widely disseminated in literature and conferences attracting attention to the possible application of CAPs in different areas of biomedical engineering and even medicine.

The first application of plasmas in medicine relied essentially on its thermal effects for the purpose of tissue removal, sterilization of medical devices and cauterization. Although, since these thermal plasmas have temperatures above the 40ºC, their application is limited given the possibility that when in contact with living tissues may cause adverse effects such as skin irritation and burns.

In the early 2000s, due to the increased knowledge about non-thermal plasmas, and specifically about CAPs, this field of research was extended for application of CAPs on eukaryotic cells. These studies revealed that CAPs are able to increase phagocytosis, accelerate fibroblasts proliferation, allow cell death detachment without necrosis, and induce apoptosis. The first CAPs sources approved for medical use appeared in the late 2000s. In 2008 the US FDA approved the Rhytec Portrait®, a plasma jet, for use in dermatology. In 2013, in Germany, the medical device certification class IIa was given to the kINPen®, also a plasma jet, being the first CAPs device getting authorization for clinical trial for

wound healing, and to the PlasmaDerm® device (a DBD device). Today, there are other CAPs devices with authorization for use in medical applications as it is the case of the Bovie J-Plasma®, the Canady Helios Cold Plasma, and the Hybrid Plasma™ Scapel[39,44]. Nowadays, the kINPen is probably the most used plasma device in plasma medicine.

The field of plasma medicine is constantly increasing, with investigations regarding the application of CAPs being performed in areas as different as sterilization, disinfection, decontamination, wound-healing, dentistry, cancer (plasma oncology), pharmacology and treatment of implants for enhancement of its biocompatibility. Igor Alexeff and Mounir Laroussi[23] were some of the first researchers to employ CAPs for sterilization, while Eva Stoffels[8] can be considered the pioneer of the direct application of CAPs discharges in cells.

2.1.3.1. Plasma interaction with eukaryotic cells

The effects of CAPs on eukaryotic cells after treatment have been studied in different cell types, including, fibroblasts, keratinocytes, and different tumor cell lines. Two clinical applications are in focus in plasma medicine: wound healing and plasma oncology.

Regarding wound-healing studies, Arjunan *et al.*[45] have shown that CAPs treatment induces a stimulating effect in endothelial cells by promoting angiogenesis through reactive oxygen species, while Ngo M. H. T *et al.*[46] observed that CAPs treatments enhanced fibroblasts proliferation rate, by increasing the release of growth factors. Besides the *in vitro* studies, also some *in vivo* and *ex vivo* animal studies (conducted in pigs, rats, mice, dogs, and cats) showed the potential of CAPs in wound treatments, with no histological skin damage being observed after the treatments, while at the same time the wound healing improved[47–52]. Also, Keidar *et al.*[53] have demonstrated that the heat that is dissipated by CAPs can lead to an increase in skin temperature only up to 2ºC, which is not enough to cause thermal damage.

In the field of plasma oncology, the studies of Arndt *et al.*[54] showed that it is possible to induce pro-apoptotic changes in melanoma cells, such as

phosphorylation of the p53 tumor suppressor gene, and the cytochrome c through exposure to cold plasmas. These changes mainly block the cell cycle at checkpoint G2/M as represented in Figure 2.6, with higher selectivity to cancer cells. Yan *et al.*[55] determined that the plasma generated reactive species, oxygen (O_2) and hydrogen peroxide (H_2O_2), were the main responsible for apoptosis induction in tumor cell lines after CAPs treatments. Many other studies demonstrating that the CAPs treatments induce apoptosis were performed, showing that generally, apoptotic signaling events involve the p53, but also the extracellular regulated kinases (ERK), the c-Jun N-terminal kinase (JNK), and/or the p38 mitogen-activated protein kinases (MAPKs)[56–58]. Volotska *et al.*[59] have demonstrated that the results obtained after CAPs treatment depends not only on the treatment duration and the chemical composition of the plasma effluent (helium-plasmas was used on this experiment) but also of the number of cells that are in the S-phase of the cell cycle at the moment of the treatment. The S-phase is that in which Deoxyribonucleic acid (DNA) replication occurs[60]. The fact that the cancer cells are mostly on this phase (about 40-50% of them, and only 10-15% of the non-cancer cells) due to the high proliferation rate that they present, makes them more susceptible to CAPs treatment than the non-cancer ones[61,62]. Other *in vitro* studies using U87 gliomas and cutaneous melanoma were also successfully treated with CAPs[63–65].

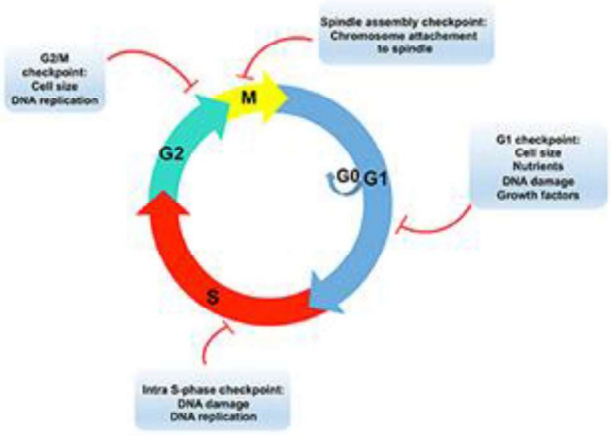

Figure 2.6 Schematic representation of the eukaryotic cell cycle and its regulation adapted from[66].

A small number of clinical studies in humans have also been carried out. The results of these studies demonstrated that CAPs significantly improved the healing in 40 patients subjected to skin transplantation[67] and of the bacteria decontamination of hair follicles[68].

2.2. Molecular events in cell biology

As referred before, CAPs are a specific type of cold plasmas that are generated at atmospheric pressure and when in contact with the ambient air a large amount of Reactive Oxygen Species (ROS) and Reactive Nitrogen Species (RNS) are produced. These reactive species are known for having a key role in altering cell biochemistry, inducing mechanisms like oxidative stress, cell death, and DNA damage. As one of the goals of this work is to explore the mechanisms of interaction between cold plasmas and cells, a brief introduction to the mechanisms underlying the cellular behavior is done in this sub-chapter.

2.2.1. Oxidative stress

The concept of oxidative stress was first formulated in 1985 at the introductory chapter of the book entitled Oxidative Stress and was defined as a "*disturbance in the prooxidant-antioxidant balance in favor of the former*". This imbalance between the free radicals (ROS and RNS) and its neutralization by antioxidant[b] mechanisms may conduce to disturbances in the normal redox state of cells. This causes toxic effects through the production of peroxides and free radicals that damage all cell components, including proteins, lipids, and DNA[69,70].

Reactive nitrogen and oxygen species (RNOS) are well recognized for playing a dual role as deleterious and beneficial species[71,72]. They are harmful if in excess but up to some point they are necessary for important cellular functions,

[b] Antioxidants are molecules that can donate an electron to a free radical without turning themselves unstable. This causes the free radical to stabilize and becomes less reactive.

being involved in a variety of different cellular processes ranging from apoptosis and necrosis to cell proliferation and carcinogenesis. Molecular events, such as induction of cell proliferation, decreased apoptosis and oxidative DNA damage have been proposed to be involved in carcinogenesis[73]. ROS can modify several intracellular signaling pathways including protein phosphatases, protein kinases, and transcription factors[72,74,75]. Therefore, suggests that the effects of ROS are caused by their action in signaling pathways instead via non-specific damage of macromolecules[76–79]. However, how oxidative stress promotes tumor formation is still under investigation.

In cases of small perturbations, a cell can overcome the imbalance between ROS and antioxidants and regain its original state, with the RNOS species being required for cellular process as wound healing, angiogenesis, and cell signaling[80–83]. In a balance cell state, intracellular reactive species are produced as a byproduct of cellular metabolism in the respiratory chain. In a general way, as more adenosine triphosphate (ATP) a cell requires, more oxygen is metabolized, and more ROS are formed by accident[84,85]. In normal conditions, the superoxide dismutase (SOD), dismutates the superoxide radical (0_2^-) to hydrogen peroxide (H_2O_2), which later is converted to water (H_2O) by glutathione peroxidase, that also detoxifies lipid hydroperoxide products[86–88]. Besides, SOD and glutathione peroxidase, also catalase, present in mitochondria, acts as a cellular antioxidant by scavenging the produced H_2O_2[70,89,90]. Likewise, the endogenous sources of ROS, cells are also exposed to a large variety of ROS from exogenous sources like UV radiation, food, drugs, pollutants, and electrophysical phenomena including non-thermal plasma and photodynamic therapy[91]. This can lead, to a very high ratio between the RNOS and antioxidants, and consequently, the cells are unable to inactivate the effects of the excess of RNOS, with damage being caused[69,70,92]. If this damage is irreparable, then injury, mutagenesis, carcinogenesis, accelerated senescence, and cell death can occur[73,90]. In humans, oxidative stress is being linked, for example, to diseases as Parkinson's, Alzheimer's, atherosclerosis, autism, depression, sickle-cell disease, myocardial infarction, and allergic and inflammatory skin diseases[93–95].

Thus, since cancer cells have a lower antioxidant capacity than non-cancer ones, exogenous RNOS produced by CAPs can be used to selectively induce oxidative damage and cell death (by apoptosis or necrosis) in cancer cells.

2.2.2. Cell death

Cell death can occur essentially by two mechanisms: necrosis and apoptosis. Necrosis is primarily provoked by an external stimulus such as trauma or infection. It is morphologically characterized by loss of mitochondrial, peroxisomal and lysosomal membranes integrity, leading to swelling of organelles, dilatation of the nuclear membrane and increased cell volume. This culminates in the eventual rupture of the plasma membrane and consequent release of the intracellular content into the extracellular space[96–99]. The released cell contents are often toxic to the adjacent cells or can act as an alarm, preparing the injured tissue to fight infection by inducing a strong inflammatory response[76,100].

In turn, apoptosis is a sequence of molecular events that lead to the controlled breakdown of the cell in a "suicide" mechanism, involving the degradation of cellular constituents by a group of cysteine proteases (caspases)[101]. Apoptosis is characterized by morphological changes, like membrane bleeding, nuclear fragmentation, chromatin condensation, and chromosomal DNA fragmentation[102]. It can be activated through intrinsic or extrinsic pathways. The intrinsic apoptotic pathway is characterized by loss of mitochondrial membrane, potential leading to its permeabilization and consequent release of pro-apoptotic proteins in the cytoplasm as, cytochrome c which activates caspase 9[103–105]. The extrinsic pathway is triggered by the binding of death-signals to dead receptors, leading to the activation of caspase 8[106,107]. The activated caspase 8 then activates the caspase 3, which induces the mitochondrial release of apoptotic factors[108,109]. Several studies have shown that apoptosis can be induced by oxidative stress, while antioxidants and thiol reductants, such as N-acetylcysteine, and the endogenously produced protein B-cell lymphoma 2 (Bcl-2), can block or delay it by antioxidative mechanisms[110,111]. The use of CAPs, for example, induces

extracellular signals that converge in the mitochondria, increasing its membrane potential and conducing to a state of oxidative stress, with consequent release of pro-apoptotic factors and caspase activation.

2.2.3. DNA damage

Although DNA is a stable, well-protected molecule, DNA damage is a continuous process that happens as a result of different factors such as intracellular metabolism, DNA replication, and exposure to genotoxic agents, such as ionizing radiation[112,113]. Metabolism releases RONS species, reactive carbonyl species, lipid peroxidation, and alkylating agents, that are responsible for inducing natural DNA oxidative damage[86,113], which in humans arise at least 10 000 times per cell per day[114]. Oxidative DNA damage can produce more than 50 different types of modified purine and pyrimidine base modifications, including the addition of hydroxyl groups, and ring-opening, that can lead to DNA single breaks or base deletion[115]. To note, that not all ROS can cause DNA damage, with the hydroxyl radical being the main responsible for oxidative DNA damage, since it can easily modify the nucleobases of DNA. It must be noted, that although H_2O_2 and superoxide do not lead to damage in their biological concentrations, they may lead to the production of more hydroxyl radicals, via the Haber-Weiss reaction[116,117]. Additionally, superoxide can react with nitric oxide, which is a gaseous signaling molecule that plays an important role as a biological messenger, leading to the formation of peroxynitrite that can easily cause DNA damage similar to the one caused by the hydroxyl radical[117–119].

DNA damage via exogenous factors occurs both directly by ionization of the nucleotides or indirectly by increasing the ROS concentration and/or through the formation of DNA crosslinks. Ionizing radiation, as CAPs[120], might induce DNA double and single-strand breaks and oxidize purines and pyrimidines[113]. The most of DNA damage, approximately 80%, resulting from ionizing radiation is thought to be caused by radiolysis of water molecules. This process results in an increase on the concentration of ROS, by formation of hydroxyl radicals, due to the splitting of ionized water molecules, and possible reactions with hydrated

electrons formed by ionized radiation, that can reduce the hydroxyl radicals into superoxide. These hydroxyl radicals can, then, be dismutated to hydrogen peroxide with possible extra production of hydroxyl radicals[121,122].

2.3. Squamous cell carcinoma (SCC)

Cancer is a disease that corresponds to an abnormal cell growth with the potential to invade or spread to other parts of the body. In a non-disease situation, cells are able to multiply and later dye by apoptosis (a mechanism of programmed cell death), in a process of constant cell renewal. However, in cases of cancer, this process of cell renewal does not happen as consequence of genetic mutations that greatly increase the rate of cell division.

The squamous cell carcinoma, also known as epidermoid carcinoma, comprises many different types of cancer that result from an abnormal growth of squamous cells. These cells are responsible for the protection of what lies beneath them, reason why they can be found in all parts of the human body[123–125].

In the skin, this cancer is usually not life-threatening and tends to grow slowly. However, it may have different manifestations and may range from superficial tumors, which are relatively easy to treat, to deep/infiltrating tumors that easily metastasize. In this last situation, the cancer can injure nerves, blood vessels and anything else in its path becoming life-threatening. It can vary in its appearance, but usually, it begins as a scaly or crusty patch of skin, with a dome-shaped bump, red inflamed base, that can easily bleed if scraped.

The most common cause for the onset of skin SCC is an inadequate exposition to ultraviolet (UV) radiation that will increase the production of ROS, which change the chemical structure of DNA, start lipid peroxidation and can cause unrepaired abnormalities in the cellular metabolism. SCC can also develop in skin damaged by a burn, persistent chronic ulcers, wounds and old scars. The diagnosis is always performed by biopsy[1,123,126].

2.3.1. Treatment

Nowadays, there are different treatment possibilities regarding the disease progression, size and location of the tumor, associated risk or recurrence and the existence or not of metastasis. For example, in superficial cases, ablative solutions, like electrodissection and CO_2 laser can be efficiently used, but in invasive situations, techniques that allow greater depth of treatment, as well as histological control of the tumor margins, are needed. In this case, if detected in an early stage, SCC of skin can be completely removed through excision without major complications. One of the most used excision techniques is the micrographic Mohs surgery, which consists in cutting out the cancer spot and some healthy skin around it, with the posterior inspection of the excised skin in a microscope, aiming the reduction of the amount of healthy tissue that is removed[127–129].

Other alternative treatments include curettage and electrocoagulation, cryosurgery, photodynamic therapy, and radiotherapy[1,124]. Curettage and electrocoagulation is a repeated and phased procedure in which a part of the tumor is removed and an electrical scalpel is used to cauterize the tumor zone. This phased procedure is employed in order to destroy any possible residual tumor cells and control the bleeding, having success rates close to the ones of the excision[130]. In cryosurgery, the tumor tissue is destroyed by freezing it with liquid nitrogen. It is a non-invasive and non-bleeding procedure that may need to be repeated a few times during the same session to ensure that all tumor has been destroyed. Cryosurgery is an inexpensive technique; however, it has successful rates much lower than the other surgical techniques[131]. Photodynamic therapy is a form of phototherapy involving light and a photosensitizing chemical substance that is applied to the skin being then activated by exposure to a specific light, or even daylight, or sometimes with intense pulsed light[132–134]. Radiotherapy is a process in which X-rays are directed to the tumor. The biggest disadvantage of this technique is that it does not provide precise control over the removal of the tumor cells affecting simultaneous cancer and non-cancer cells[108,135,136].

All these possibilities have disadvantages either in terms of success rates and consequent tumor eradication, or because they carry side effects or even because they are invasive, painful and expensive. All these factors contribute to the increase necessity of a new technique for cancer treatment able to combine high success rates with high selectivity for cancer cells. On this sense, CAPs are emerging as a potential alternative to the aforementioned common anti-cancer therapies, since *in vitro* and *in vivo* experiments have successfully showed their ability to selectively kill cancer cells in a non-invasive way, without harming normal surrounding tissue[7,13,14,19,22,23,137,138] and without causing thermal damage[53].

3

Experimental concepts and methodology

Different diagnostic and characterization techniques have been used during this work. This chapter describes the general concepts behind the techniques used for the characterization of the plasma plume and of the treated liquids, as well as for the evaluation of the cell cytotoxicity and the mechanisms of cell death. It is worth to mention that the detailed description of the used devices and procedures (details about concentrations, distances, and time of plasma exposure, among others) only was done in the respective chapter in order to avoid information repetition.

3.1. Plasma plume characterization

Cold atmospheric plasma applications are mainly based on their enhanced plasma chemistry[139]. Chemically active plasma is a multi-component system that is highly reactive due to a large concentration of charged particles, excited atoms, molecules, radicals, and UV photons[140]. Investigation of the species generated by the plasma expanding into the ambient air is of great importance in biological and medical applications, since it allows the understanding of the mechanisms behind the interactions between these plasmas, liquids and living cells[26].

Due to the high reactivity of these plasmas, optical emission spectroscopy which can be performed without physical contact with the plasma has become a very popular tool for the diagnosis of the reactive species present in plasmas.

3.1.1. Optical emission spectroscopy (OES)

OES is a relatively simple and non-invasive technique widely used for plasma diagnostics, to get an overview of plasma characteristics even if its information value is restricted to excited and radiant species[6]. Optical emission spectra can be observed when transitions of the outer energy level electrons occur within an atom. Notwithstanding an electron in an atom has a definite amount of energy, when energy is applied, electrons are transferred from low energy to high energy levels as depicted in Figure 3.1. After a short time interval, the electrons in the high-energy levels undergo transitions into states of lower energy, being the resulted energy difference emitted in the form of electromagnetic radiation[141,142].

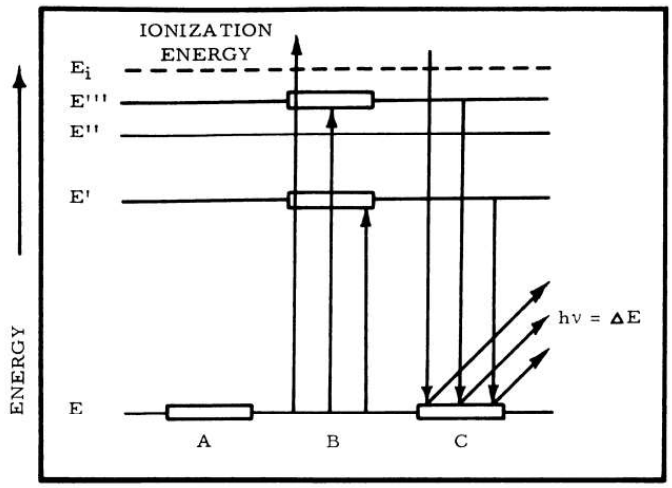

Figure 3.1 Energy-level diagram showing electronic transitions. (A) Ground-state conditions. (B) Excitation. (C) Emission, adapted from[141].

In the case of atmospheric plasmas, when electrical energy is supplied to a CAPs jet device, a cold plasma is generated at the central electrode and driven to the outside of the jet by a gas flow. The plasma plume will then interact with the ambient air species generating high amounts of reactive oxygen and nitrogen species, by electron impact. In this case, emission spectroscopy exploits the fact

that plasma emits light, examining the wavelength of the photons emitted by the formed reactive species (atoms, molecules, ions) during their transition from the excited state to the lower energy level. The wavelength of the emitted photon, Figure 3.2, is given by the energy difference between these two levels. Since the energy of a transition is characteristic of a particle, by the observation of the central wavelength of the emission lines present in the emission spectrum, unambiguous identification of the species existent in plasma can be done[142,143].

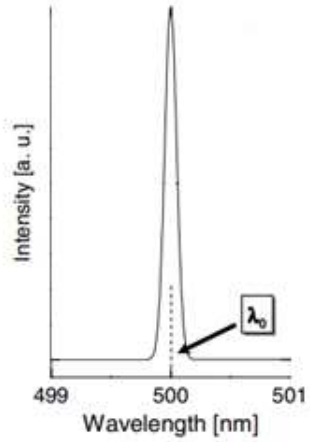

Figure 3.2 Representation of an obtained peak and the correspondent wavelength of the emitted photon, adapted from[143].

3.2. Characterization of plasma-treated cells

3.2.1. *In vitro* cytotoxic assays

Cytotoxic assays are the basis of several *in vitro* studies, being the cytotoxicity one of the most important indicators for the evaluation of a cell population's response to external factors. One of the most common ways to measure cell viability of eukaryotic cells, through cytotoxicity assays, is assessing cell membrane integrity, since compounds that are toxic to the cells can compromise the cell membrane integrity[144,145].

The resazurin assay, also known as Alamar Blue assay, is a widely used colorimetric assay to monitor the reducing environment of a living cell, using resazurin (7-Hydroxy-3H-phenoxaxin-3-one 10-oxide) as the active ingredient. Resazurin is a water-soluble compound, stable in the cell culture medium, non-toxic and permeable through cell membranes[146,147].

This assay is based on the ability of metabolically active cells non-reversely reduce resazurin into a highly fluorescent pink resorufin (7-Hydroxy-3H-phenoxazin-3-one) product, that is freely released from cells[148,149]. This irreversible reduction process is associated with the mitochondrial metabolic activity via mitochondrial reductase[150], but may also be mediated by intracellular diaphorase enzymes[148], which are probably responsible for the transference of electrons from the reduced form of nicotinamide adenine dinucleotide phosphate ($NADPH + H^+$) to resazurin[146,147,151,152], according to the reaction depicted in Figure 3.3. The amount of resorufin produced can be monitored by measuring fluorescence or absorbance, and correlated with the number of viable cells in the sample[149,151]. Background contributions of wells containing medium with resazurin alone must be subtracted from all samples. The incubation time needed to generate an adequate signal is usually between 1 and 4 hours, in dark, at 37°C in a humidified atmosphere of 5% CO_2, and it is dependent on the cell line, cell concentration, and the concentration of the used solution. Assays should be carried out at an uniform temperature to ensure reproducibility of all wells and between plates.

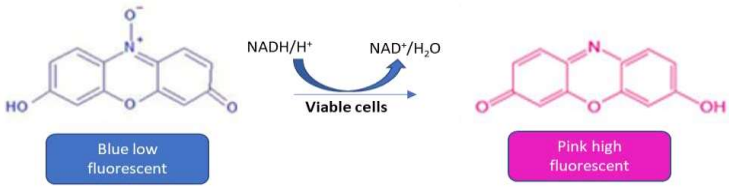

Figure 3.3 Reduction of resazurin to resorufin.

Compared with other viability assays, specifically with tetrazolium reduction assays, resazurin, has the advantage of being slightly more sensitive, non-toxic to cells at low concentrations, and needs shorter incubation periods

[149,153,154]. Moreover, resazurin can be dissolved into physiological buffers and in the cell culture medium, reason why it can be directly added to the cells[147,149,155].

3.2.2. Investigation of cell death mechanisms by flow cytometry

Flow cytometry is a powerful technique widely used to characterize single particles or cells as they move in a liquid stream across a laser/light beam through a sensing area[156]. Its significance can be summarized as the measure (-metry) of the optical properties of cells (cyto-) transported by a liquid sheath (flow) to a light source excitation (usually a laser)[157].

Once inside the device, the liquid is focused in a way that ideally the cells flow one after the other in the sample stream, which passes through different lasers subsequently mounted in modern cytometers. As the cells pass through the lasers, light is scattered in all directions, being the light scattered proportional to the size of the cell or particle in study[156]. Moreover, the light may enter the cell and be refracted by the nucleus or other cell components, being the 90º light scattering (side scattering) considered proportional to the cell granularity. It must be noted that some of the emitted light is not scattered light but fluorescence, since several cells (and particles in general) have natural background (auto-) fluorescence, that can be detected by the cytometer[158].

Particles with and without auto-fluorescence are often labeled with antibodies conjugated with specific fluorochromes or stained with fluorescent dyes[156,159], to make non-fluorescent compounds visible to the cytometer. A fluorescent dye is characterized for absorbing light of a specific color, losing energy before emitting light of a different color. This is based on vibrational states, being energy and light inversely correlated, and therefore, the emitted light is usually of a longer wavelength than the absorbed one (Stoke's shift)[158]. The scattered and the fluorescent light are then collected by appropriately positioned lenses. A combination of optical mirrors and filters steers the scattered and the fluorescent light to the appropriate detector based on the different wavelength bands, and the emission intensities are recorded by photomultiplier

tubes that amplify photon signals via electron dissipation[159,160]. Finally, an analog-to-digital converter allows the signal to be displayed, analyzed and compared.

It must be noted, that the use of fluorescent dyes used for staining cells need to be appropriate to the cytometer, requiring knowledge about the wavelength of the illuminating light, the wavelength specificities of the filters in front of the instrument's photodetectors, and of the absorption and emission characteristics of the dyes themselves[158].

One of the major advantages of using flow cytometry is its ability to integrate hundreds of thousands of events into one single analysis, which allows separating populations by defining their boundaries of distribution using *gates*. The use of gates allows the analysis of subsets of cells within a mixed population[158], permitting for example, to differentiate between live, early and late apoptotic cells. All these aspects make flow cytometry a powerful technique to characterize different cell types, and therefore, the key method used in this work to study the mechanisms of cell death following plasma treatment.

3.3. Identification and quantification of reactive species in liquids

Low-temperature plasmas are sources of high concentrations of energetic and chemically active species. At ambient conditions, humidity can influence the resulting species chemistry forming hydroxyl radical (·OH), which interacts with air ambient species generating further reactive species[39]. Many of these species have short lifetimes (e.g. O, N, H) and in case of plasma treatment of liquids may not efficiently diffuse/dissolve into the liquids[161]. The resulted long-lived species usually include hydrogen peroxide, nitric acid (HNO_3) and nitrous acid (HNO_2)[39].

When treating liquids, these species together with molecular species (e.g. OH, NO, HO_2, NO_2) will interact between them and with the species present in the liquid phase, and consequently, ·OH radicals, H_2O_2, superoxide anions radicals, nitrate, and nitrite, are some of the species that can be detected in the treated liquid[39].

3.3.1. Quantification of hydrogen peroxide (H_2O_2)

Among the reactive species produced in CAPs, H_2O_2 is the most stable and has the particularity of being able to efficiently diffuse into the liquid medium and hence more easily to be measured[161,162]. It is an oxygen-dependent killing agent, with a well-known role in both intra and extracellular toxicity, since it contributes to the oxidation of proteins, lipid membranes and DNA through the peroxide ions[140,151,161].

In this work, the H_2O_2 quantification was done according to the manufacturer's instructions using the *Fluorometric Hydrogen Peroxide assay* (MAK 165, Sigma-Aldrich) kit and the Pierce Quantitative Peroxide assay (Pierce™ Quantitative Peroxide Assay kit, Thermo Scientific, Rockford, USA).

The Fluorometric Hydrogen Peroxide assay kit provides a simple and reproducible colorimetric method to quantify H_2O_2 levels, using horseradish peroxidase (HRP) to catalyze the reaction. Most of the oxidation reactions catalyzed by HRP can be described through the following reactions 3.1 to 3.3,

$$E + H_2O_2 \rightarrow E_I + H_2O \quad (3.1)$$

$$E_I + AH_2 \rightarrow E_{II} + AH\cdot \quad (3.2)$$

$$E_{II} + AH_2 \rightarrow E + AH\cdot + H_2O \quad (3.3)$$

where AH_2 and $AH\cdot$ represent a kind of reducing substrate and its free-radical product, respectively, E the original enzyme (HRP), E_I and E_{II} are its intermediates[163,164].

The kit also uses a red peroxidase substrate, which is a specific probe for H_2O_2 but not for superoxide. In the presence of HRP, this substrate reacts with H_2O_2 to produce a red fluorescent oxidation product (resorufin, λ_{exc} = 570 nm, λ_{em} = 590 nm) that can easily be measured. The produced fluorescent product is highly stable and presents a H_2O_2 dose linear response. However, for high H_2O_2 concentrations (> 100 μM)[39], this linear response is lost, and the fluorescent product is converted again into a non-fluorescent compound[162]. This fall in

fluorescence also occurs with time and usually indicates that the H_2O_2 release is beginning to exceed the substrate concentration[162]. Thus, precise control of the incubation time must be done, and to ensure reproducibility all the measurements must be performed after the same incubation time.

In its turn, the Pierce Quantitative Peroxide assay is an aqueous-compatible peroxide kit that detects peroxides based on the oxidation of ferrous to ferric iron in the presence of xylenol orange dye. The kit's formulation also includes sorbitol, which provides sensitivity enhancement. The biggest advantage of this kit is that most proteins do not interfere with the assay reactions, however, some metal chelators may require the use of a blank (i.e. control) to mitigate possible side effects.

3.3.2. Mass spectrometry

Mass spectrometry (MS) is an analytical technique used to quantify different atoms and molecules constituents of a sample by converting them into ions, to identify unknown compounds within a sample and to elucidate the structure and chemical properties of the different molecules.

Spectrometry had its origin in 1898 when Wilhelm Wien demonstrated that a positive ion beam could be deflected using electric and magnetic fields. In 1912 Sir Joseph J. Thomson verified the existence of two neon isotopes using a simple magnetic deflection instrument, being credited as the precursor of mass spectrometry. In the 1940s mass spectrometry was a highly developed technology as it played a very important role in the Manhattan project and in the oil industry[160,165].

Mass spectrometric analysis is based on the principle that gas-phase ions of a compound in study can be produced and posteriorly fragmented, being all the formed ions separated in the mass spectrometer according to their mass-to-charge ratio (m/z), and detected in proportion to their abundance[160,166,167].

There are different types of mass spectrometers, all of them composed of three essential components: an ignition source, a mass analyzer, and a detector.

The mass spectrometer must also be connected to a computer system to process and record the data, and to a vacuum pump to control the pressure within the mass spectrometer[168]. In the ignition source, also known as ionizer, a neutral atom or molecule is electrically charged, with a portion of the sample being converted into ions.[168,169]. Ions are used in MS since unlikely to neutral species, they are easy to experimentally manipulate and detect. Atoms may be positively or negatively charged, but when negatively charged only a few atoms may accept more than one electron. On the contrary, any number of electrons can be removed. The most common ionizer types include electron impact ionization, chemical and thermal ionization, and must be chosen according to the desired degree of ionization and fragmentation, and with the properties of the sample[167,168,170].

After ionization, the resulted ion beam is focused and directed into the mass analyzer, where the ions are separated into their characteristic mass components according to their mass-to-charge ratios The most common mass analyzers are the quadrupole, the ion trap, the time-of-flight (TOF) and the Fourier transform-ion cyclotron resonance analyzer[168]. In the case of this work, a time-of-flight instrument was used. TOF analyzer uses an electric field to accelerate the ions through the same potential and then measures the time they need to reach the detector. If the particles have the same charge, their kinetic energy will be the same, and their velocities will only depend on their masses. Consequently, the lighter ions of the same charge in the same potential field, will reach the detector first[167,171]. A mass spectrum of the molecule is then produced, displaying the obtained result in the form of a plot of ion abundance in function of the mass-to-charge ratio (m/z). However, even particles with the same m/z can arrive at different times if they have different initial velocities. This broadens the peaks depicted in the obtained mass spectra, but generally does not change the central location of the peaks, since the average initial velocity of ions relative to the other analyzed ions is usually centered at zero[170]. In order to fix this problem, delayed extraction systems are coupled to TOF-MS (TOF mass spectrometers). This results in a mass resolution improvement due to the correlation between velocity and position of the ions. Ions with higher initial velocity, during the delay time,

move closer to the extraction electrode before the accelerating voltage is applied across the target, while the slower ions stay closer to the target when the accelerating voltage is applied. Therefore, the slower ions start to be accelerated at a greater potential compared to the ions farther away from the target (the faster ones). So, with the proper delay time, the slower ions will receive extra potential energy to catch the faster ones after flying some distance from the acceleration system, and consequently, ions of the same m/z will this way drift through the TOF at same time[172–174].

3.3.3. Ion chromatography

Ion chromatography (IC), also known as ion-exchange chromatography, is an analytical technique that separates ions and polar molecules based on their affinity to the ion exchanger[175,176]. Several ion equilibrium mechanisms use different solid stationary phases and mobile phases (eluent), which allows the analysis of almost any kind of molecules, including large proteins, amino acids, peptides, and small nucleotides[177,178].

The most widely used IC method combines high-performance liquid chromatography (HPLC) technology with ion exchange capabilities[179]. In Figure 3.4, a diagram of a typical IC instrument is presented.

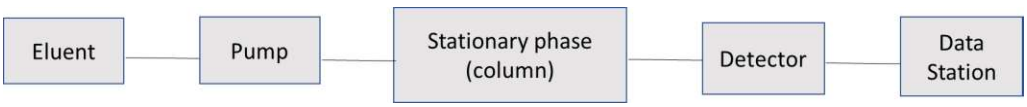

Figure 3.4 Diagram of a common IC instrument.

There are two different types of IC, the anion-exchange and the cation-exchange. Anion-exchange chromatography is used when the molecule of interest is negatively charged. The molecule is negatively charged because the pH for IC is higher than the isoelectric point[c] (pI). In this type of chromatography,

[c] Isoelectric point (PI) is the pH at which a molecule carries no net electrical charge or is electrically neutral in the statistical mean.

the stationary phase is positively charged and the negatively charged molecules are loaded to be attracted to it. On the contrary, in cation-exchange chromatography, the molecule of interest is positively charged (pH for IC is lower than the pI), while the stationary phase is negatively charged[176,179]. In both IC types, the charged molecules undergo electrostatic interactions with opposite charges, forming ionic bonds with the insoluble stationary phase, which is an ion-exchange column, consisting of ionizable functional groups. In addition to these interactions, other types of binding can occur, but these effects are very small and mainly due to van der Waals forces and nonpolar interactions[176,179–181].

In general, the basic process of IC using ion-exchange can be described in five main steps. The first step is the equilibration of the stationary phase (column) to the desired initial conditions. When in equilibrium all stationary charged groups are bound with exchangeable counter ions (present in the eluent in order to achieve electroneutrality). The pH and the ionic strength of the initial eluent must be chosen to ensure that when the sample is loaded the molecules of interest will bind to the ionic functional groups of the column, while the present impurities do not bind. Then, a defined volume of sample is injected onto the column, being there separated in its components (analyte ions). These analyte ions bind to the ionic groups on the column surface of opposite charge, becoming concentrate. Uncharged molecules, or those with the same charge as the ionic group, pass through the column at the same speed as the eluent, eluting during or just after sample application. After all the sample is loaded, the column is washed with the initial eluent, and the bound molecules are eluted. This can occur by increasing the ionic strength of the eluent (salt concentration) or by changing the pH. As ionic strength increases the salt ions compete with the bound molecules for charges in the column surface[176,179,180].

The competition for charged sites on the column (S) between the eluent ion (counter ion, H) and the analyte ion (A) can be expressed by reaction 3.4, which represents the equilibrium for an ion exchange process involving a cation exchange:

$$S^{-}H^{+} + A^{+} \leftrightarrow S^{-}A^{+} + H^{+} \quad (3.4)$$

According to this, ions present in higher concentration will take greater portion of the ion exchange sites. The molecules with the lowest net charge will be the first ones to be eluted from the column. The separated sample components flow then through the detector, and data is collected on a data station, where the quantification of the analyte is performed and stored[176].

Several methods of detection are available for IC. In this work, the conductivity method, which has the major advantage that all ions are conductive, was used. Two different modes of conductivity can be used in IC: direct and indirect, being direct detection the most common approach. In a general way, direct detection is used when the limiting ionic conductance of the analyte is much higher than the one of the eluent and an increase in conductance is observed when the analyte passes through the detector. Indirect detection requires a high conductive eluent, with a decrease in its conductivity being observed when the analyte is detected[182].

4

Development and Characterization of the plasma jet device

In this chapter, the developed argon jet device and the custom-made high voltage power supply are described. The characterization of the cold atmospheric plasma (CAPs) produced by the developed jet is also presented. Regarding the power supply, the used circuit diagrams are shown, as well as a brief explanation of its operation parameters and of the results obtained after its construction. With respect to the CAPs device itself, the different configurations that were tested until the final set-up was reached are reported here.

Since this research project was mostly based on the development and optimization of the plasma jet device, special attention was given to its design, in order to allow the user to point precisely the jet on a specific area.

4.1. High-voltage power supply and its components

For proper sizing and implementation of the power supply, it was necessary to define the minimum operating requirements. To determine the minimum output voltage to be implemented, it was necessary to use the Paschen Law, which relates the disruption voltage (V_B) of a gas with the product of gas pressure, p, and electrode separation, d (pd)[27,183]. According to Paschen Law, the disruption

voltage can be calculated by equation 4.1, resulting in the Paschen curve represented in Figure 2.3 (see chapter 2), with the minimum voltage point of each curve representing the most favorable breakdown condition:

$$V_B = \frac{B\,p\,d}{\ln(A\,p\,d) - \ln\left[\ln\left(1 - \frac{1}{\gamma_{se}}\right)\right]} \tag{4.1}$$

where, V_B is the breakdown voltage in volts (V), B is related to the excitation and ionization gas energies, p is the pressure in pascal, d is the distance between the electrodes in meters (m), A refers to the saturation ionization in the gas at a particular $\frac{E}{P}$ (electric field/pressure), and γ_{se} is the secondary-electron-emission coefficient.

For example, at the atmospheric pressure and with an electrode separation of 1 mm, the breakdown voltage of argon (the gas used in this work) is approximately 3 kV. Although, the electrode separation of the developed argon plasma jet device is higher than 1 mm it was decided to develop a DC power supply up to 20 kV and able to support a current of 20 mA, allowing it to work in a wide range of conditions.

The developed DC high-voltage power supply is based in a variable amplitude oscillator circuit, also known as ZVS – Zero Voltage Switching, connected to a flyback transformer. The electrical scheme is shown in Figure 4.1.

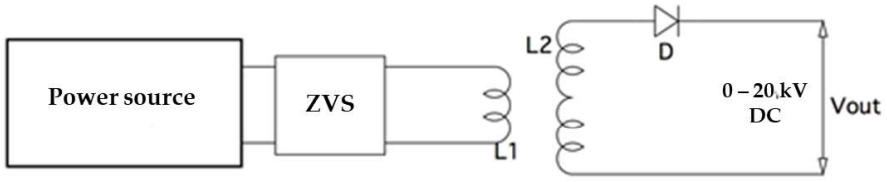

Figure 4.1 Schematic representation of the developed DC high voltage power supply. It consists of a variable DC power supply, connected and producing a variable continuous output voltage. This source powers the ZVS oscillator circuit that is coupled to the primary winding of a line transformer (flyback), L1. On the right, it is represented the secondary winding of the flyback, L2, which is connected to the rectifier, responsible for converting the alternated output voltage of the flyback into a continuous voltage (DC).

The ZVS oscillator is powered by a variable power supply, based on the integrated circuit LM317, according with the scheme of Figure 4.2. The integrated

circuit LM317 device is an adjustable three-terminal positive-linear voltage regulator able to provide an output-voltage range between 1.25 and 37 V DC and adapted to ensure a maximum current of 15 A. The three terminals are: input (INP), output (OUT) and adjustment (ADJ). The variation of the output voltage of the LM317 is done through a fixed-resistance and a potentiometer, as indicated in Figure 4.3. The specifications of the LM317 are summarized in Table 4-1.

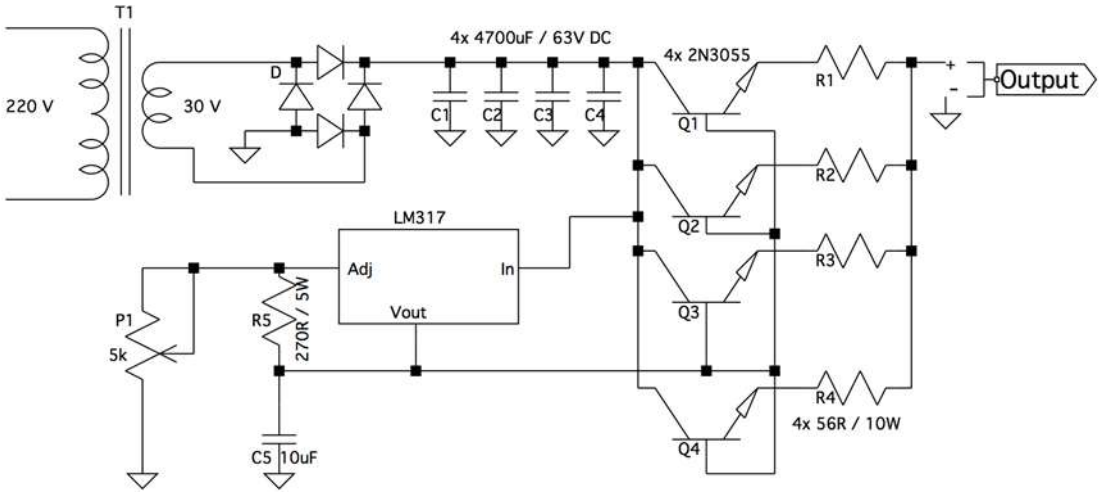

Figure 4.2 Diagram of the built high voltage DC power supply. The power supply aims to produce a variable DC voltage that supplies the ZVS oscillator and the flyback transformer to produce the high voltage.

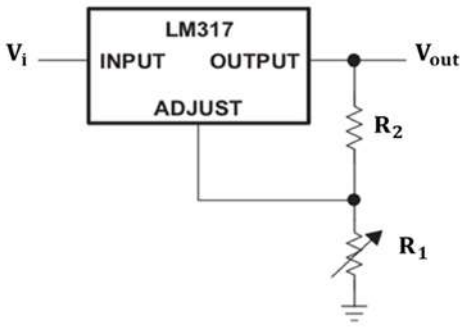

Figure 4.3 LM317 circuit for voltage regulation. The circuit has three pins: adjacent (adjust), the input (Vi) and the output (V_{out}) pin. R_1 and R_2 are responsible for regulating the output voltage. Adapted from166.

Table 4-1 LM317 specifications.

Symbol	Parameter	Value	Unit
V_{out}	Output voltage range	1.25 – 37	V
V_{out} - V_{out}	Voltage differential	3 – 40	V
Tj	Operating junction temperature range	0 – 125	C
I_o (max)	Maximum output current	1.5	A
I_L (min)	Minimum load current	3.5 mA typical, 12 mA maximum	mA

In the case of the developed power supply, the adjustment pin was connected to the ground, and consequently the output pin delivers a regulated voltage according with (Equation 4.2):

$$V_{out} = V_{ref}\left(1 + \frac{R_1}{R_2}\right) \tag{4.2}$$

where V_{ref} corresponds to the voltage difference between the OUT pin and the ADJ pin, being typically 1.25 V; and R_1 and R_2 to the variable and fixed resistances, respectively, being chosen according to the desired output voltage range, Equation 4.2.

It was used, R_1 = 5 kΩ and R_2 = 270 Ω, resulting in an integrated circuit output voltage between 1.25 and 24 V.

It must be noted that the dimensioning of the DC voltage source, regulated by the LM317 was made for 24 V instead of 20 V, to count with the losses that inevitably happen along the circuit, and considering that when tested in "no-load" it provides higher output values than when the load is added (in this case the oscillator and the flyback transformer will be added).

4.1.1. Amplitude oscillator circuit (ZVS) and flyback transformer

The ZVS circuit is responsible for "driving" the flyback. Its function is to provide the flyback with a high-frequency pulsed input signal, allowing it to work. The schematic of the oscillator circuit used is shown in Figure 4.4.

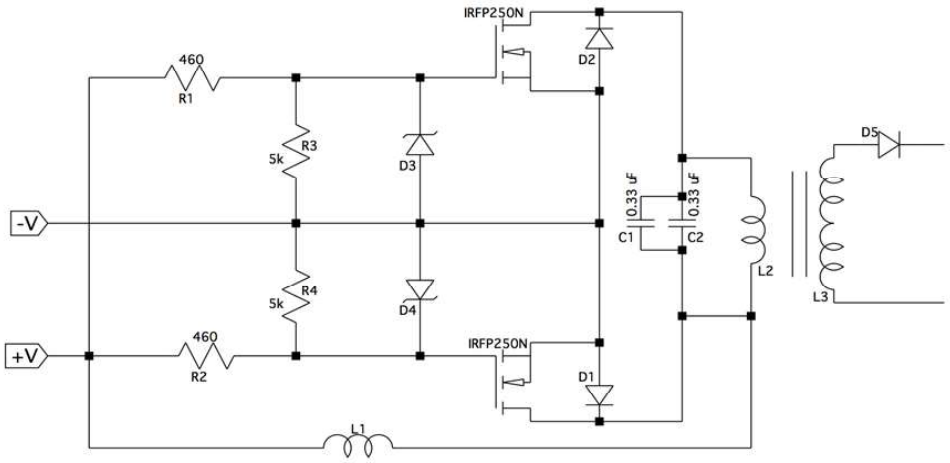

Figure 4.4 Oscillator circuit and flyback diagram (represented by L2 and L3). The oscillator circuit is directly connected to the flyback and is responsible for its operation.

In general, when a voltage is applied at +V terminal, current starts to flow through the 470 Ω resistances to the MOSFETs (Metal Oxide Semiconductor Field Effect Transistor, IRFP250 N) gates activating them. These 470 Ω resistances limit the MOSFETs gate (G) current preventing them from being damaged. However, since two MOSFETs are never perfectly alike, one of the MOSFETs is activated first allowing more current to flow through it. Consequently, current flowing through the non-active MOSFET gate is consumed by the activated MOSFET with the diode (D_1 or D_2) blocking the gate of the non-activated one.

As can be observed in Figure 4.4, the circuit has capacitors (C_1 and C_2) in parallel with the coil L_2, resulting in a resonant circuit responsible to do the drain (D) of the inactive MOSFET reach 0 V. These capacitors are responsible for sinusoidally changing the voltage, preventing the current from constantly rising until it saturates and damage the MOSFETs. When the voltage of 0 V is reached, the active MOSFET starts to discharge through the diode (D_1 or D_2) connected to the drain of the opposite MOSFET, turning off the active one. When the first activated MOSFET is turned off the other MOSFET is activated, and so on.

The Zener diodes (D_3 and D_4) in this circuit act as protection systems for MOSFETs ensuring that the gate voltage never exceeds 12 V (voltage of the used

diodes). The central coil (L_1) serves to protect the circuit from possible current surges that could damage it.

Since the circuit is a resonant oscillator, its oscillation frequency is determined by the capacitors (C_1 + C_2, since they are in parallel) and by the inductance of the central coil (L_1) being given by (Equation 4.3):

$$f = \frac{1}{2\pi\sqrt{LC}} \tag{4.3}$$

where L represents the inductance of the central coil L_1, and C the equivalent capacitance of the capacitors. For a L = 47 μH and C = 0.66 μF, an oscillation frequency of approximately 25 kHz was obtained.

The flyback primary winding has 6 turns on each side, Figure 4.5, resulting in an output voltage of the secondary winding 10^3 times higher than the one at the input. Moreover, the flyback embodies a diode which rectifies, the AC voltage supplied by the ZVS into a DC voltage.

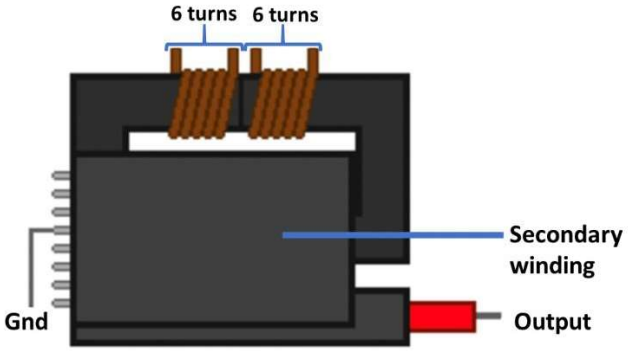

Figure 4.5 Schematic representation of the line transformer. Illustration of the ground and output pins (HV, high voltage) and the primary winding made with 6 turns per side.

Once all the parts of the power supply were connected, values between 1.5 and 20 V were obtained at the output of the ZVS DC power supply, resulting in a variable DC output voltage up to 20 kV. In Figure 4.6, it is possible to observe the values that were obtained at the flyback output, when the voltage of the power supply was changed. Through the analysis of this figure, it is possible to confirm the existence of linearity between the obtained input and output signals and the 1:1000 ratio between the primary and the secondary windings of the

flyback. Moreover, it could be observed that the ZVS only is activated for input voltages around 5 V. The final scheme of the custom-made DC high voltage power supply can be found in Figure A.1 of Appendix.

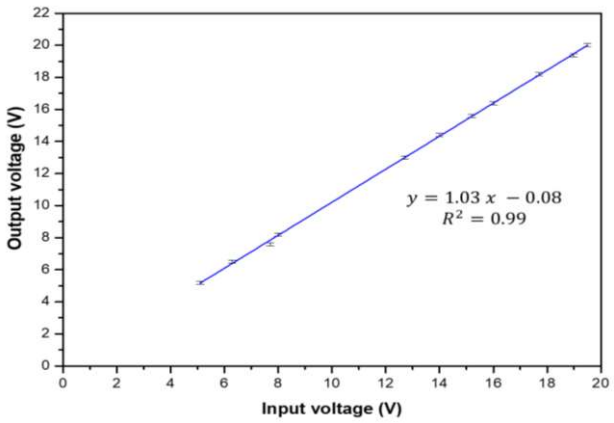

Figure 4.6 Representation of the obtained DC output voltage as function of the voltage supplied by the DC power supply, which can be modified by regulation of the potentiometer.

4.2. Plasma jet device

The developed cold atmospheric plasma (CAPs) jet consists of a hand-held unit composed by a borosilicate capillary with an outer diameter of 6.93 mm and an inner diameter of 3.76 mm, with two metal electrodes, and a gas supply inlet as shown in the scheme of Figure 4.7. Borosilicate was used since it is resistant to both, heat and chemicals, and has a low expansion coefficient. The jet operates at an argon (99% purity, Air Liquide) flow rate of 3 slm (standard liters per minute) controlled by a flowmeter (Dynamal Argon 0-15 L(min, Air Liquid), which ensures a vigorous mixing of the medium during the plasma treatments and drives the plasma stream from the top of the pin-type electrode to the surrounding air, outside the borosilicate tube.

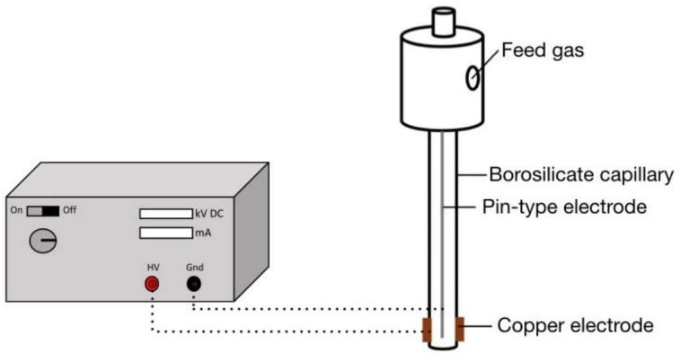

Figure 4.7 Schematic representation of the developed CAPs jet device connected to the custom-made DC high voltage power supply.

The electrode on the inside of the capillary is a stainless-steel needle with 2 mm diameter, while for the outer electrode (connected to the DC high voltage power supply) three different configurations were tested: a copper ring, a titanium ring and one made from enameled copper wire, Figure 4.8. In order to choose the electrode that produces a more stable and less energetic plasma, spectroscopic analysis of the plasma plume obtained using each one of the referred electrodes was performed. According to the obtained results, presented in section 4.2, it was chosen to develop the jet using the configuration of a coiled copper wire around the capillary (Figure 4.8 (c)). The copper wire coil used has 1 mm of thickness and 7 mm of high, corresponding to seven turns.

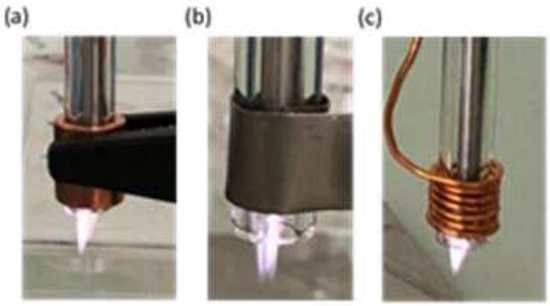

Figure 4.8 Tested electrodes: (a) copper ring, (b) titanium ring, and (c) copper wire.

Two different configurations of the borosilicate tube were also tested, to identify if its configuration has influence on the species generated in the plasma.

The jet was tested with a cylindrical and with a tapered tube at the lower end as shown in Figure 4.9. However, no plasma formation could be achieved using the tapered tube, reason why this option was discarded, and the normal cylindrical tube was used.

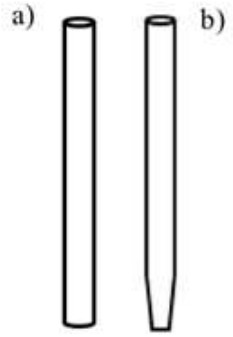

Figure 4.9 Scheme of tested borosilicate tube configurations: a) cylindrical lower end; b) tapered tube at lower end.

Once the optimal configuration in terms of stability was achieved, the device was coated in order to facilitate safe handling and system automation, Figure 4.10. The covering was designed in Autodesk® Tinkercad® online software. When sizing, it was necessary to dimension and print a piece that would allow the device to be coupled to the positioner. This part is shown in Figure 4.11. The material used to print both pieces was Polylactic acid, (PLA) which is used in some medical devices due to its high rigidity, strength and melting temperature between 150 and 160 ºC.

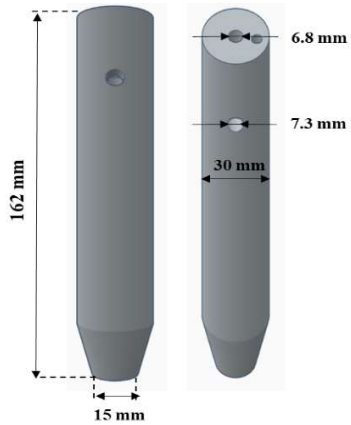

Figure 4.10 Layout and dimensions of the device-sized enclosure.

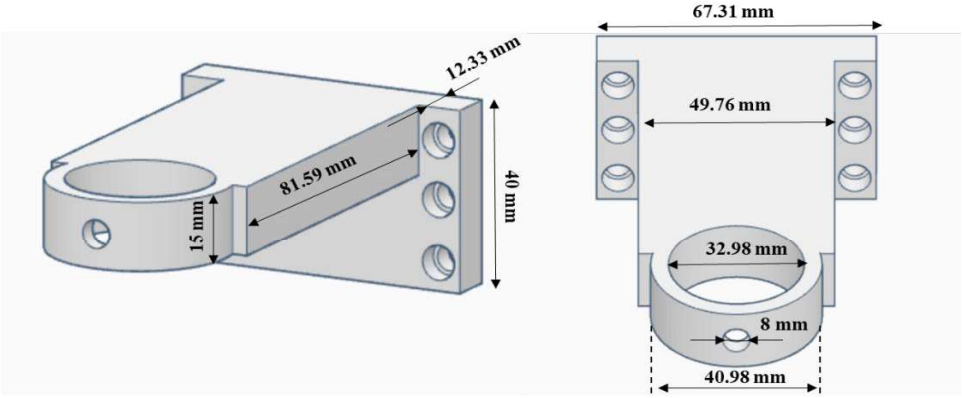

Figure 4.11 Scheme and dimensions of the extender sized to attach the device to the positioner.

A digital caliper was incorporated into the positioner and the aluminum plate to allow the precise set position of the jet probe. The probe layout is shown in Figure 4.12. To determine precisely the distance between the jet device and the wells at the time of treatment, the caliper was set as zero when the bottom of the borosilicate tube touched the upper edge of the well where the treatment was performed. This way, any subsequent displacement made by the vertical positioner will be indicated by the caliper, always with reference to the defined zero position, allowing to know the exact distance between the jet and the well.

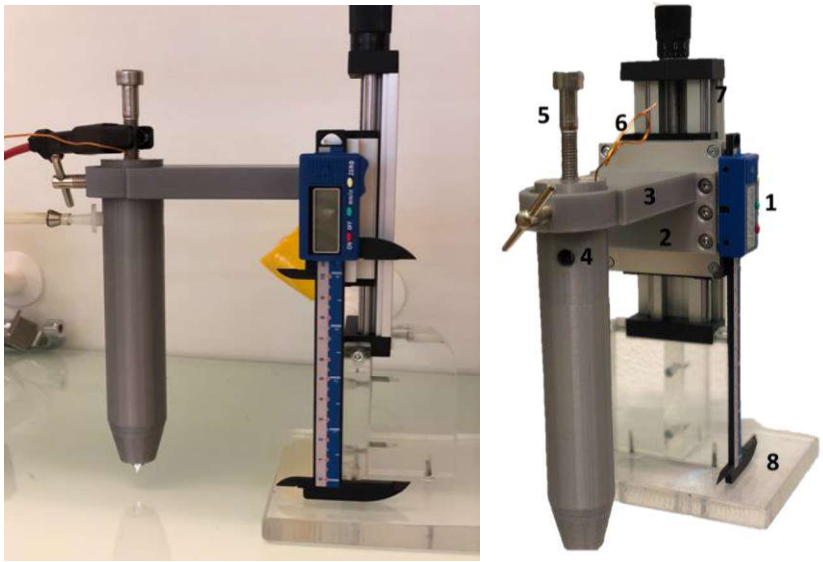

Figure 4.12 Final device configuration, where: 1) digital caliper; 2) Aluminum plate; 3) Extender; 4) Argon input; 5) Inner electrode; 6) Outer electrode; 7) Vertical positioner; and 8) Acrylic holder.

The device is attached to the extender by an M8 thread, having on its side the argon inlet and on the top the connections for the two electrodes. The central thread corresponds to the stainless-steel electrode (inner electrode), which is connected to the ground, while the wire corresponds to the copper electrode (outer electrode), where the high voltage output of the DC high voltage power supply is connected.

The plasma plume begins to be obtained at voltages around 7 kV, being used throughout all this work a voltage of around 8 kV. As expected, when the argon disruption occurs and the plasma starts to be produced, the voltage decreases considerably to values around 2 kV. This demonstrates that once the breakdown voltage is reached, the produced plasma will trigger a series of interactions with the surrounding ambient air, as well in case of liquid treatments, with the liquid being treated. During the assays performed in this work, a voltage around 2 kV was used during the plasma treatments resulting in a plasma plume with a length of approximately 7 mm.

4.2.1. Characterization of the plasma plume by OES

The emission of UV radiation by CAPs is a well-known phenomenon. The UV radiation can be divided into UV-A, UV-B, UV-C, and vacuum UV (VUV). They decrease in wavelength from A to VUV but increase in energy. VUV photons have energy enough for breaking the chemical bonds in biological cells. UV-C photons possess a larger penetration depth and have sufficient energy to cause lethal damage to organic tissues, being able to induce mutagenesis and photochemical oxidation processes in cells[184].

Spectral characteristics of plasma generated UV radiation can be affected by several factors, as for example, the feeding gas used and its purity, the addition of different gases, and the electrodes used[185]. To investigate which species are being generated by the plasma expanding into the ambient air, and whether the plasma produced using the three different outer electrodes tested (copper ring,

titanium ring, and copper wire) would have the same composition, the emission spectrum of the plasma effluent was recorded using an optic fiber (FC-UV600-2, Avantes) spectrometer (SPEC STD, Sarspec's). The size of the spectrometric quartz glass lens covered the whole length of the effluent and was kept at approximately 5 mm perpendicular to the plasma plume. The instrument has a resolution of 1.7 mm and emission intensities on the range 180-1100 nm were recorded[186]. Addition of molecular gases was done using a mass flow controller, and peak intensities were obtained as an average of ten consecutive measurements.

The optical emission spectrum of the Ar plasma discharge (3 slm), in the wavelength range from 200 to 900 nm, for the three tested outer electrodes is shown in Figure 4.13. Although no changes in composition could be observed between the emission profiles obtained for the three referred electrodes, some small differences were found regarding the relative intensities of the obtained emission peaks. Specifically, for the copper wire, comparing the peaks corresponding to the radical (·OH) and to the nitrogen, higher intensities were registered for nitrogen, with the opposite being observed when using the copper and the titanium rings.

Regarding the composition, all the obtained emission spectra show an emission peak belonging to reactive hydroxyl radical in the UV-B region at 308 nm and some emission peaks between 330 and 400 nm corresponding to the nitrogen (N_2) emission, in UV-A range. Since neither oxygen nor nitrogen are present in the working gas used, the appearance of these emission bands can be attributed to the interactions between the generated plasma and the species present in the surrounding ambient air[6,185]. According to Lukes et al.[187], the ·OH radical in the gas phase discharge appears as a consequence of the electron impact of H_2O molecules in the water vapor above and near the liquid surface. The near-infrared (700-900 nm) emission peaks mainly represent excited molecules of argon. No detectable emission peaks were found in UV-C range meaning that possible biological damages due to UV-C irradiation can be excluded.

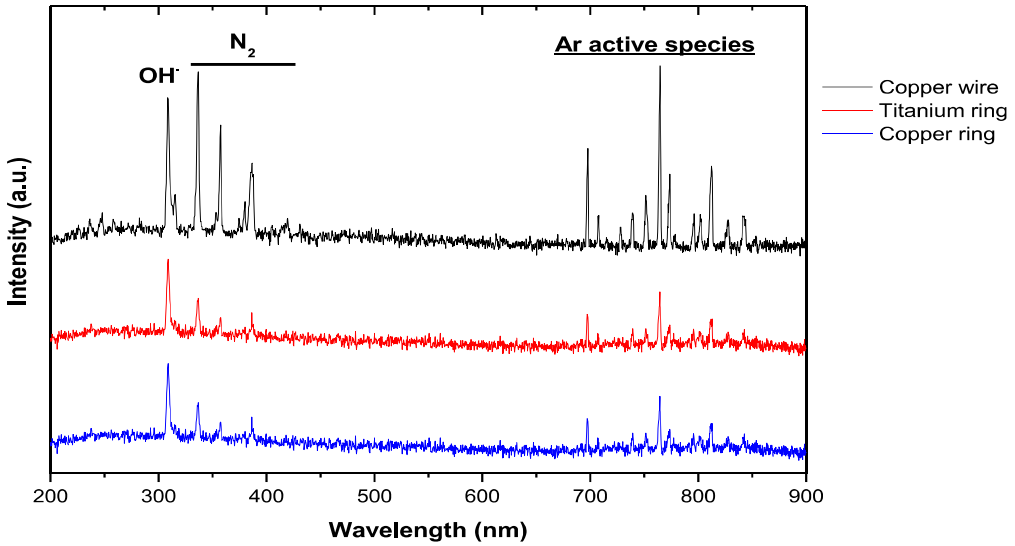

Figure 4.13 Optical emission spectrum of the plasma plume for three different electrodes, obtained using an Argon flow of 3 slm.

It is known that the plasma plume emission profile is dependent on the working gas used. To evaluate the influence of the gas used, admixtures of oxygen (O_2), nitrogen (N_2), and nitrogen-oxygen (N_2O_2) to pure argon were performed and the emission profiles were recorded. The obtained spectra are shown in Figures 4.14 to 4.16. The study of the influence of the gas admixture was only performed using the copper wire as the outer electrode.

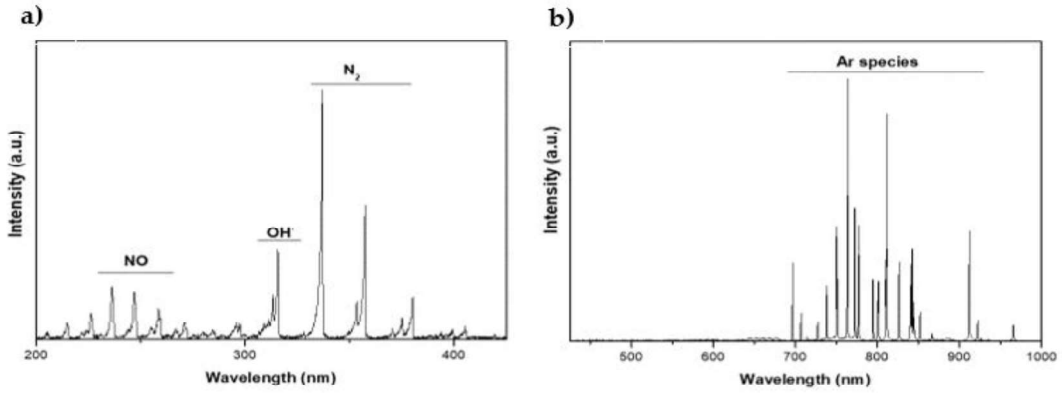

Figure 4.14 OES spectrum obtained after addition of 0.5% O_2 to the working gas (Ar), for wavelengths from a) 200 to 420 nm, b) 420 to 1000 nm.

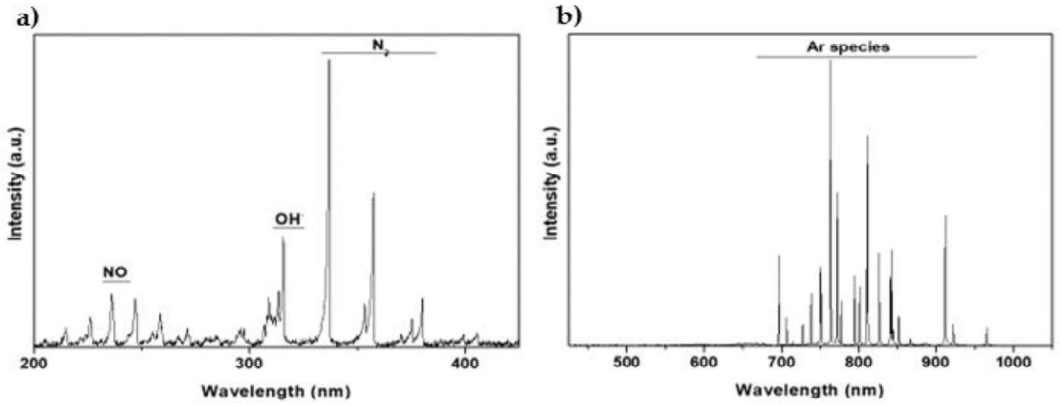

Figure 4.15 OES spectrum obtained after addition of 0.5% N_2 to the working gas (Ar), for wavelengths from a) 200 to 420 nm, b) 420 to 1000 nm.

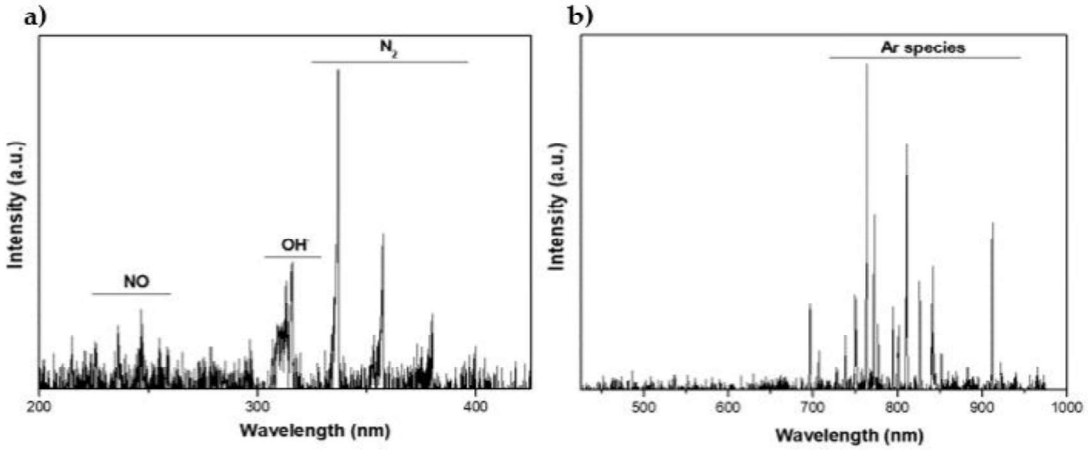

Figure 4.16 OES spectrum obtained after addition of 0.5% N_2O_2, for wavelengths from a) 200 to 420 nm, b) 420 to 1000 nm.

As can be observed by analysis of Figures 4.14 to 4.16, differently to what happens when using pure Argon, the addition of O_2 and N_2 to the working gas produces some nitric oxide (NO) in the UV-C region (from 200-280 nm). The NO production is attributed to the electron-impact dissociation of the O_2 and N_2, with oxygen and nitrogen working as $NO^{\cdot}$precursors[41]. Despite the NO production could sometimes be explained by ozone (O_3) absorption, in the case of the developed jet, this hypothesis can be excluded. For this jet, the admixtures of O_2 and N_2 to Ar flow, lead to a significant increase of the NO emission, but almost no differences were found between the intensity of the different NO bands

indicating that O_3 absorption is not the main factor explaining the NO excited level enhancement.

4.3. Summary

CAPs are a near-room temperature plasmas, usually produced in laboratory by applying an external source of energy to a neutral gas up to a critical value, in which electrons dissociate from atoms[6,30] On last decade, they have gained great interest in terms of biomedical applications, including cancer therapies because they can stably operate under open atmospheric conditions and have low working temperatures[13,14]. However, the properties of the produced plasma will depend on the applied power and its type and the feeding gas used. For this reason, it was decided to develop a dedicated cold plasma jet device and investigate the mechanisms behind cold plasmas and living cells, specifically skin cells.

The CAPs jet device developed in this research work was designed and entirely constructed in our laboratory (Plasma and Applications laboratory, CEFITEC, Portugal). It consists of a hand-held unit composed of a borosilicate capillary and two different electrodes. The jet is coupled to a custom-made high voltage power supply able to work up to 20 kV through a copper wire electrode. Copper was used since it has good strength and is a very good electricity conductor.

The jet operates at a gas flow of 3 slm, which was chosen based on previous studies that will not be shown in this thesis. Here, different gas admixtures were tested. It was observed that when O_2 and N_2 were added to Ar, NO starts to be produced. NO is a gaseous signaling molecule present in several physiological and pathological processes, having also roles as a neurotransmitter, and vasodilator agent, among others. It is a member of both reactive nitrogen species and reactive oxygen species. Attention must be given to the fact that NO is formed in the gaseous phase of plasma, being able to rapidly react with the oxygen to yield NO_2. For this reason, and once the final goal of this project is to

study the killing specificity of CAPs for cancer cells, the addition of O_2 and N_2 to argon feed gas needs to be evaluated in terms of cell cytotoxicity. This allows to confirm if its addition will not increase the toxicity of the developed jet device to levels also toxic to non-skin cancer cells.

5

Plasma treatment conditions affect cell viability[d]

The final goal of this work was to prove that plasma treatments induce a selective response in cancer cells compared to non-cancerous ones. So, one of the main questions regarding this work was: how is plasma affecting skin cells viability? To answer this question two different approaches of plasma treatments *in vitro* were tested: direct and indirect. In direct treatments, cells were directly exposed to the cold atmospheric pressure plasma (CAP), while in indirect treatments, first the liquid was irradiated by CAP, and only after that, the treated liquid was transferred to cells.

It must be noted that *in vitro* assays are used to decrease the number of *in vivo* studies, once they allow a more detailed analysis that cannot be done in *in vivo* due to the high complexity of the living organisms, being used as a first approach to collect information about the biological mechanisms of action and the variables in study. The *in vitro* assays must be done according to the 3R's principle: replacement, reduction, and refinement, which was proposed

[d] This chapter is based on the article: Pereira, S., Pinto, E., Ribeiro, P. A. & Sério, S. Study of a Cold Atmospheric Pressure Plasma jet device for indirect treatment of Squamous Cell Carcinoma. *Clin. Plasma Med.* **13**, 9–14 (2019)

by Russel and Burch in 1959, in their book "The Principle of Humane Experimental Technique"[188]. This principle is increasingly being incorporated into legislations, guidelines for toxicity testing, such as the guidelines developed by the Organization for Economic Co-operation and Development, and into test guidelines applicable for safety assessments/toxicity evaluations. Briefly, replacement refers to the substitution of living animals for insentient material; reduction to any strategy that will result in a lower number of animals being used to obtain enough data to answer the research question, or maximizing the information obtained per animal; and refinement refers to the modification of the animal experiments procedure, to minimize the pain and distress of animals used in science, since the time of it is birth until its death[188,189].

In the specific case of this work, *in vitro* assays were used to test the cytotoxicity of the developed plasma jet device and to help to optimize the parameters of plasma treatments. All the *in vitro* procedures regarding cell manipulation were carried out in certified cell culture laboratories, in dedicated laminar flow chambers in sterile conditions.

5.1. Materials and methods

Plasma properties depend on the applied power and its type (e.g. AC, DC, RF, etc), the feeding gas used and on the working parameters[20]. For this reason, to investigate the effects behind the interactions between cold plasmas and living cells, the working parameters of the developed plasma device were systematically investigated.

5.1.1. Cell lines and cell cultures

Since one of the main goals of this work was to study the effects of CAPs, and CAPs treated liquids into Squamous Cell Carcinoma (SCC), three different cell lines were used during this study. One non-cancerous cell line, namely, HGF-1,

and two cancer cell lines, SCC-15 and Met-1 cells. The non-cancerous cell line was used to prove that the killing effects of plasma are more effective when applied to cancerous cells.

Met-1[e] is a keratinocyte cell line, that has been derived from a primary and invasive SCC excised from the back of the hand. This cell line was purchased from Ximbio (153539, London), and was maintained in complete DMEM [(*Dulbecco's Modified Eagle's Medium*, Sigma, D5030), supplemented with 1.0 g/L D-glucose (Gibco, 15023-021), 3.7 g/L sodium bicarbonate (Sigma-Aldrich, S5761), 1% GlutaMAX™ (L-alanyl-L-glutamine dipeptide, Life Technologies, 35050-038), 1% sodium pyruvate (Gibco, 11360039), penicillin (100U/mL) and streptomycin (100 μg/mL) (Invitrogen, 15140122), and 10% FBS (Fetal Bovine Serum, Invitrogen, 10270106)].

SCC-15[f] is also a squamous cell carcinoma line, but it was derived from the tissue of a human tongue, and purchased from American Type Culture Collection (ATCC, LGC standards, Barcelona). It was maintained in DMEM-F12 (Dulbecco's Modified Eagle's Medium: nutrient mixture F-12; ATCC® 30 2006™) supplemented with 10% fetal bovine serum (FBS, Sigma, 102710), 1% antibiotic Penicillin/Streptomycin (Pen/Strep, Sigma, A5955) and 400 ng/mL of hydrocortisone (Sigma, H0888).

HGF-1[g] cells are a class of well-characterized fibroblast cells obtained from a human gingival biopsy, purchased from ATCC, and maintained in complete DMEM as Met-1 cells.

All the used cell lines are adherent and were cultured in 75 cm^2 filter cap cell culture flasks (43061U, Corning), at 37°C in a humidified atmosphere 5% CO_2 (standard conditions), and passaged by an enzymatic method, twice a week. For that, cells were incubated at standard conditions with 5 mL of Tryple™

[e]Additional information regarding Met-1 cells can be found in https://ximbio.com/reagent/153539/met1-scc-cell-line

[f]Additional information regarding SCC-15 cells can be found in: https://www.lgcstandards-atcc.org/products/all/CRL1623.aspx?geo_country=pt#documentation

[g] Additional information regarding HGF-1 cells can be found in https://www.lgcstandards-atcc.org/products/all/CRL-2014.aspx?geo_country=pt#

(12604021, Gibco), or 3-4 mL of Trypsin 0.25% solution (T4049, Sigma-Aldrich), during the necessary time to become detached from the bottom of the flask. About 2 mL of culture medium was then added to the flask to inactivate the enzymatic solution. The cellular suspension was collected to a sterile 15 mL falcon (62.554.001, Sarstedt) and centrifuged for 10 minutes at 1100 rpm and 4ºC. The supernatant was then discarded, and the pellet resuspended in the corresponding cell culture medium.

5.1.2. Plasma treatments

To determine how plasma treatments, affect cell viability and which factors influence cell-plasma interactions, plasma treatments were performed under several conditions and cell viability was assessed by the resazurin assay.

Two different approaches of plasma treatment were tested: direct and indirect plasma treatments. In direct plasma treatments, cells cultured with a confluence of 5×10^4 cells/mL were directly exposed to plasma. On the other hand, in indirect treatments, the plasma jet device was used to vertically irradiate the medium in different wells of a 12-well plate, and only then the treated medium was transferred to the previously cultured cells. In both cases, cells had to be cultured in the day before the plasma treatments, and incubated at 37ºC, with 5% of CO_2.

As can be observed in Figures 5.1 a) and b), the results obtained in this part of the study demonstrated that although after direct plasma exposure the cell viability reduction was slightly higher, no significant differences were found, meaning that cells react in a similar way to both types of plasma exposure.

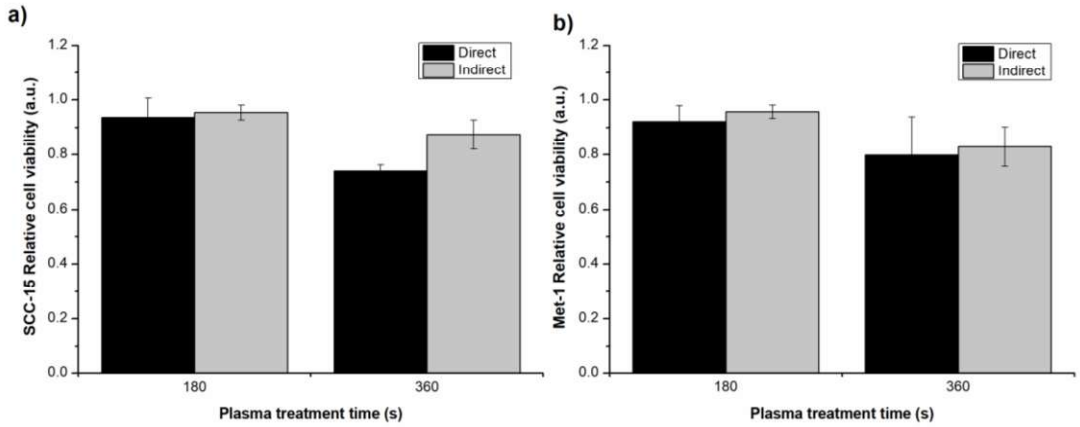

Figure 5.1 Relative cell viability of: a) SCC-15 and b) Met-1 cells, after direct and indirect plasma treatments.

In this context, this work was based only on the study of the effects of indirect plasma treatments and their parameters. Another reason for the exclusion of direct treatments was the fact that indirect plasma treatments have the advantage of avoiding the effects of UV radiation and of the electric discharges present in CAPs[190–192]. Moreover, liquids treated by plasma can easily be combined with other cancer therapies and be injected into the body reaching tissues inaccessible through direct irradiation[193,194].

As referred before, for indirect plasma treatments, the plasma jet was placed vertically to a 12-well microplate at a fixed distance of the upper edge of the wells containing the medium to be treated and it was kept at this position until the end of the treatment as schematized in Figure 5.2. The treated liquid was mixed by a gas flow of 3 standard liters per minute (slm) controlled by a flowmeter (Dynamal Argon 0-15 L/min, Air Liquide). Since, CAPs cytotoxicity is dependent on the concentration of the reactive species produced during liquid irradiation (mainly from reactive nitrogen and oxygen species, RNS and ROS respectively), it is important to understand how treatment parameters, such as the distance between the end of the plasma device and the upper edge of the well where the treatment was performed (gap), the cell concentration, the volume of medium and the working gas used, influence the cell viability.

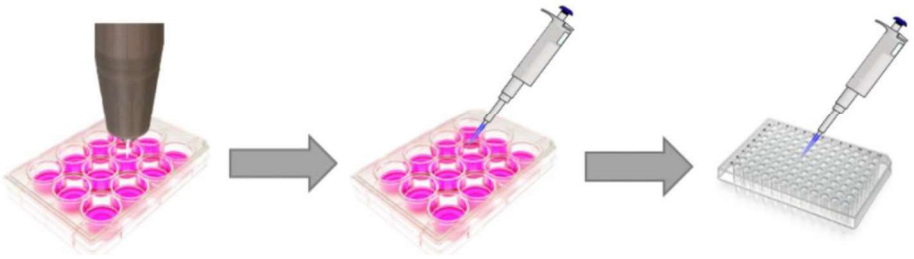

Figure 5.2 Scheme of an indirect plasma treatment procedure. First, the liquid is exposed to plasma in a 12-well plate during the desired time. Then, 100 or 150 μL of the plasma-treated liquid is transferred to different wells of a 96-well plate.

In this sense, in order to determine the conditions that allow the optimization of the indirect treatments performed with the developed jet device, the indirect plasma treatments were done alternating the following conditions: gap (2, 7 and 9 mm), time of exposure (between 2 and 9 minutes), cell concentration (2×10^4, 3.5×10^4 and 2×10^5 cell/mL), volume of medium to be treated (1 and 2 mL) and the volume of treated medium transferred to the cells (100 and 150 μL). It must be noted that all the tested cell concentrations, as well as the volume of treated medium, and the volume of medium transferred to the cells, were chosen according to the characteristics of the used microplates. At the end of the treatments, the treated medium was immediately transferred to the previously cultured cells, in sextuplicate. Before this step, the medium which has been used to culture the cells overnight was discarded and the cells were washed with 200 μL of Phosphate Buffered Saline (PBS) without calcium and magnesium. After that, the cells were incubated under standard conditions for further evaluation of the cell viability.

When performing indirect plasma treatments, the cells were cultured in 96-well plates on the day before the treatments. As mentioned in the previous section, the cells were washed with PBS, detached from the 75 cm^2 flask, and seeded in the 60 inner wells of a 96-well microplate in the desired cell concentration. A positive control of cells in untreated medium was used in all the realized experiments.

Of note, that not all the aforementioned parameters were tested for the three referred cell lines, since one of them (Met-1) was acquired later and at the time some conditions were already optimized. In table 5-1, are summarized the different conditions that were evaluated during the development of this study.

5.1.3. Cell cytotoxicity assay

As previously referred, after plasma treatments, the cells were incubated under standard conditions for further evaluation of cell viability by resazurin assay. These conditions allowed stabilizing the pH in carbonate-buffer solutions, as it is the case of the cell culture medium used in this work. The chosen incubation times were 48 and 72 hours. Tests longer than 72 hours were not performed because several toxic products of aerobic respiration are accumulated in the cell culture medium over incubation time, which can contribute to cell death and possibly influence the obtained results[195–197].

Table 5-1 Different working parameters tested during the development of this work.

Cell line	Confluence (cell/mL)	Gap (mm)	Volume of medium to be treated (mL)
SCC-15	2×10^4	9	1
	3.5×10^4	2	2
		7	2
		9	1
			2
	2×10^5	9	1
HGF-1	2×10^4	9	1
	3.5×10^4	2	2
		7	2
		9	1
			2
	2×10^5	9	1
Met-1	3.5×10^4	2	2
		7	2
		9	1
			2

After each incubation period, the medium in the wells was discarded, 100 μL of resazurin (final concentration of 100 μM, Alfar Aesar, USA) was added,

and the plates were incubated. As mentioned in Chapter 3, resazurin can freely penetrate the cell membranes being reduced to its fluorescent product, resorufin, by metabolically active cells. Four hours after incubation, the absorbance was measured in a microplate reader (BioTec, ELX800), using a wavelength of 570 nm and a reference wavelength of 600 nm. Background fluorescence of wells containing medium with resazurin alone (without cells) was subtracted from all samples.

5.1.4. Flow cytometry

First, the medium used to previously culture the cells was collected for a 15 mL falcon. After this, the wells were washed with PBS, and the used PBS was collected for the same 15 mL falcon. Subsequently, Tryple™, an animal origin-free recombinant enzyme used for dissociating adherent mammalian cells, was added to all the wells, only during the necessary time to observe cell detachment. Then, cell culture medium was added to all wells to stop the Tryple™ reaction and all the content was collected to the same 15 mL falcon. The falcon was centrifuged at 1500 rpm for 10 minutes. The supernatant was discarded, and the cells were resuspended in 185 μL of PBS with calcium. 5 μL of APC AnnexinV and 10 μL of 7-Aminoactinomycin D (7AAD) were added, and the cells were incubated in the dark for 10-15 minutes. At the end of these steps, the results were read on the cytometer.

5.1.5. Statistics

Statistical analysis was performed with Excel. All data are expressed as mean $\pm$ standard deviation of at least three independent experiments. The statistical significance of the differences was evaluated using the ANOVA and it was recognized as * $p < 0.05$, ** $p < 0.01$ and *** $p < 0.005$. To better illustrate the influence of plasma treatment parameters on cell viability, all the results have been normalized, i.e., the data from experimental groups were divided by the data corresponding to the control group and relative values were obtained.

5.2. Results

5.2.1. Influence of plasma treatment conditions on cell viability

To understand the relationship between plasma treatments and cytotoxicity, the treatment conditions were modified. This included the change of the distance between the plasma jet device and the upper edge of the well where the treatment was performed (gap), the cell confluence, the treated volume, and the time of plasma exposure. The addition of molecular gases (O_2 and/or N_2) to argon was also investigated. For the assays, it was decided to use only DMEM without sodium pyruvate, since some authors claim that sodium pyruvate could act as a scavenger for hydrogen peroxide, which is considered one of the main agents responsible for the effects of CAPs on cells[198,199]. Indeed, such scavenging effect was also experimentally observed in some preliminary investigations performed with this jet device (data shown in Chapter 6).

First, distinct cell confluences were tested, namely, $2 \times 10^4, 3.5 \times 10^4$ and 2×10^5 cells/mL for SCC-15 and 2×10^4 and 2×10^5 cells/mL for HGF-1 cells. In both cases, indirect plasma treatments were performed under the same conditions (gap=9mm, 1 mL of DMEM w/o sodium pyruvate) during 3, 6 and 9 minutes. From the obtained results of Figure 5.3 a) and b), it was clear that cell viability decreases as the treatment time increases, and for the same treatment time increases as the cell seeding confluence increases. These findings are in accordance with the studies of Dayun *et al*.[200], who observed that the anti-cancer capacity of plasma treatments is determined by the dose of plasma acting on a unit cell instead of the whole treatment dose[55,200–202].

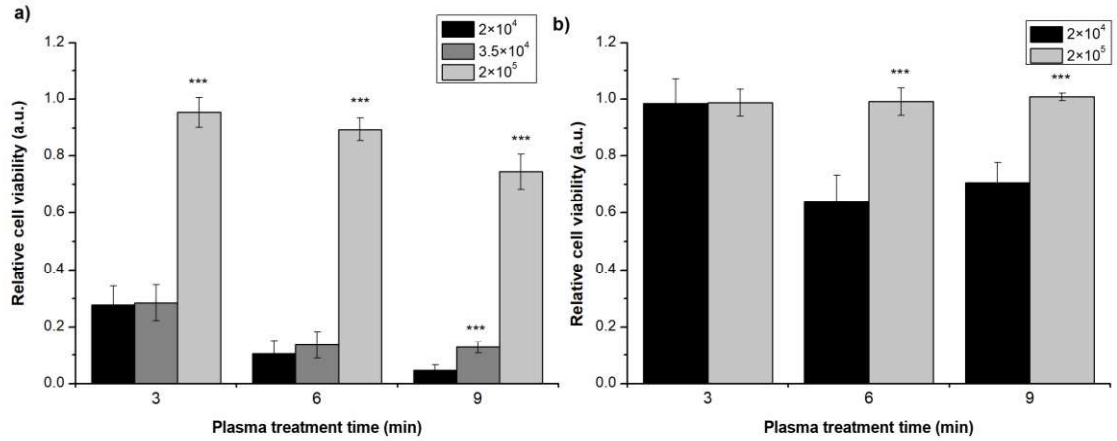

Figure 5.3 Influence of the cell seeding confluence on cell viability results after indirect plasma treatments: a) for SCC-15 and b) HGF-1 cells. Results are presented as mean±SD of three independent experiments performed in sextuplicate. The significance compared to the first bar (for each time, cell confluence of 2×10^5 cells/mL) is indicated as * p<0.05, ** p<0.01 and ***p<0.001.

By analyzing Figures 5.3 a) and b), it can also be detected that SCC-15 cells are more sensitive to indirect CAPs treatments than HGF-1 cells. For example, after 3 minutes of plasma exposure using a cell confluence of 2×10^4 cells/mL the relative cell viability[h] of HGF-1 cells remains almost unaffected (≈ 0.98), while the one of SCC-15 cells decreases for approximately 0.28. These differences in the relative cell viability between SCC-15 and HGF-1 cells remain significant for longer treatment times and different cell confluences. This seems to prove the higher vulnerability of cancer cells to plasma treatment as well the ability of CAPs to kill cancer cells leaving the non-cancer ones almost unaffected. For the next assays, it was decided to work only with the cellular confluence of 3.5×10^4 cells/mL since it seems to be the one to conduce to a moderate response to plasma treatments.

Then, to understand how the chosen gap can affect cell viability, for a cell confluence of 3.5×10^4 cells/mL, 2 mL of DMEM w/o sodium pyruvate were plasma treated for 2 and 3 minutes, using different gaps: 2, 7 and 9 mm. Results shown in Figures 5.4 a) and b), and in Figure 5.5 indicate that independently on

[h] Relative cell viability can be defined as the viability compared to the control group. It represents the number of living cells after the plasma treatments normalized to the control (untreated cells).

the plasma exposure time, and on the used cell line, the viability of the cell lines increases as the distance from the plasma jet increases. This means that the proximity of the jet enhances its killing capacity, and for this reason, the gap used to perform the treatments must be carefully chosen.

By the analysis of the significances indicated in Figures 5.4 a) and b), it was found that the differences in cell viability decrease for longer treatment times. This could mean that the influence of the gap as a parameter of plasma treatments is related to the possibility or not of the produced plasma interact with the surrounding ambient air.

For example, since many of the active species produced by plasma have a short life span, for shorter treatment times, if the used gap is to small the plasma will directly interact with the cell culture medium, and almost no interactions between the plasma and the species present in the ambient air will occur. In this case, the active species may immediately interact with the medium components, like amino acids and proteins, leading to the production of long-lived reactive hydroperoxides, that may induce lipid peroxidation and cell membrane damage, and/or may bind to cell membrane receptors activating intracellular signaling pathways[203–206]. As can be observed in Figure 5.5, the gap also influences the viability of non-cancerous cell lines. Therefore, to assure that the treated liquid is not too toxic and at the same time that the effects on cell viability will not be strongly influenced by the surrounding ambient air, a compromise between the used gap and the time of plasma exposure must be achieved.

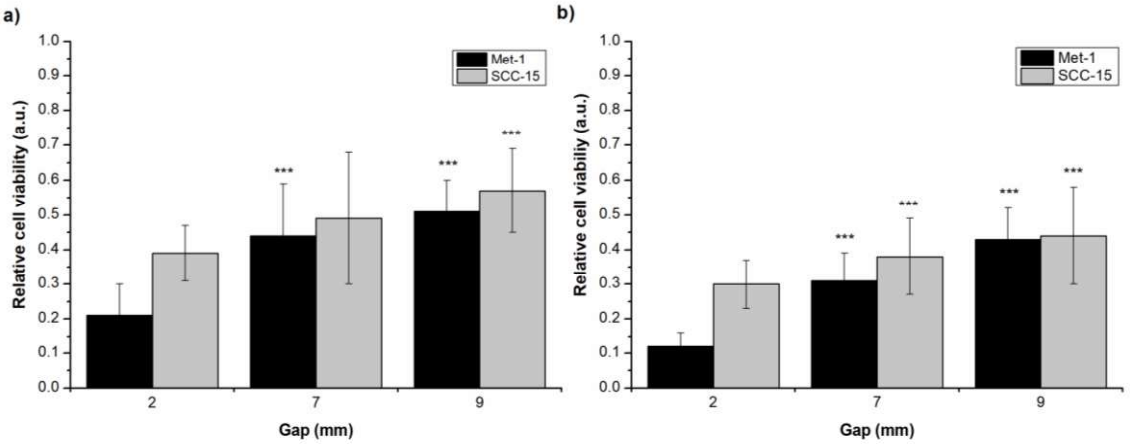

Figure 5.4 Gap influence on Met-1 and SCC-15 cells viability, after a) 2 minutes, and b) 3 minutes of plasma exposure. Results of three independent experiments, presented as mean±SD. The significance compared to the first bar (gap of 2 mm) is indicated as * p<0.05, ** p<0.01 and ***p<0.005.

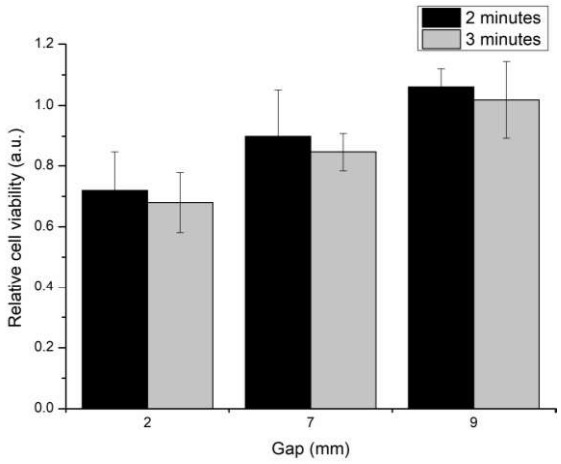

Figure 5.5 Gap influence on relative viability of HGF-1 cells, after 2 and 3 minutes of plasma exposure. Results of three independent experiments, presented as mean±SD.

Regarding the volume of the medium to be treated, to understand if the killing capacity of treated liquids is volume dependent the influence of using 1 or 2 mL of DMEM w/o sodium pyruvate for the CAP treatment was investigated. For that, SCC-15, Met-1, and HGF-1 cells were seeded with a confluence of 3.5×10^4 cells/mL in different wells of a 96-well microplate and cultured as previously referred. 1 and 2 mL of DMEM w/o sodium pyruvate were vertically irradiated in wells of a 12-well plate for 2 and/or 3 minutes, using a gap of 9 mm. After that, the cells were cultured in 100 μL of treated medium and incubated

under standard conditions for 48 hours. By the analysis of Figures 5.6 a), b), and c), it can be seen that independently on the cell type and time of plasma exposure, the killing capacity of plasma-treated medium decreases when larger volumes of medium were treated. According to the literature, such results can be explained by the dilution of the reactive species[200,207,208] (ROS and RNS) that are generated during the CAPs treatments in either gaseous and/or aqueous phase, when primary plasma species (ions, electrons, and other dissociated molecules) interact with the ambient air and the liquids being treated[20].

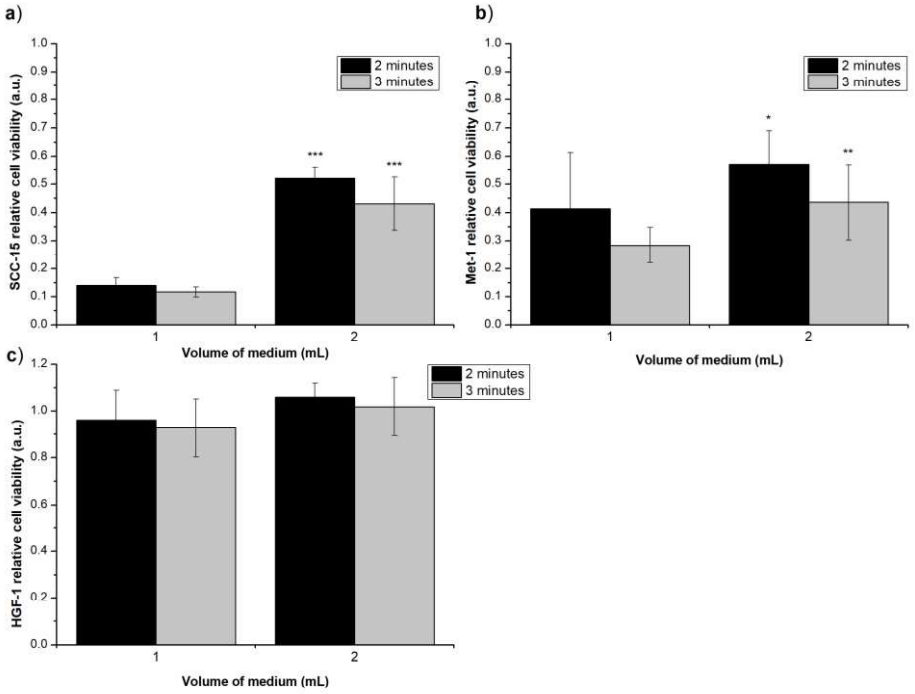

Figure 5.6 CAPs anti-cancer capacity dependence with the volume of medium. Results of three independent experiments, presented as mean±SD, performed using: a) SCC-15, b) Met-1, and c) HGF-1 cells. The significance compared to the volume of 1 mL is indicated as * $p<0.05$, ** $p<0.01$ and *** $p<0.005$.

Besides this, also the influence of transfer 100 or 150 μL of treated medium to the cultured cells has been investigated (for SCC-15 and Met-1 cells). Concerning this study, the killing capacity of CAPs treated medium was found to be higher when cells were cultured in 100 μL of the treated medium. According to this finding, the optimized anti-cancer capacity of CAPs indirect treatment can be achieved when cells are surrounded by a few medium as it can be inferred from Figure 5.7.

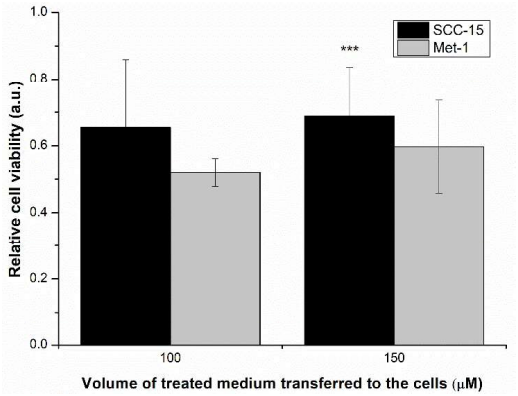

Figure 5.7 CAPs anti-cancer capacity dependence with the volume of treated medium transferred to the cells. Results of three independent experiments, presented as mean±SD, performed using SCC-15 and Met-1. The significance compared to the volume of 100 μL is indicated as * $p<0.05$, ** $p<0.01$ and *** $p<0.005$.

To confirm the time dependence of plasma treatments, for Met-1, HGF-1, and SCC-15, using a gap of 7 mm, and a cell confluence of 3.5×10^4 cells/mL, a volume of 2 mL of DMEM w/o sodium pyruvate was plasma treated for 15, 60, 120 and 180 seconds. These conditions were chosen, based on the previously presented results, since they seem to be the ones that induce a reduction of approximately 50% on the viability of the studied cancer cells. As can be observed in Figure 5.8, for all the tested cell lines, the relative cell viability decreases as the time of exposure of the liquid (plasma treatment time) increases.

For SCC-15 and Met-1 cells after 120 seconds of plasma exposure, the cell viability was already reduced to less than half of the control group (0.49, 0.44, respectively). When analyzing the results obtained for HGF-1 cells, differently to what happens with SCC-15 and Met-1 cells in neither of the tested treatment times, the relative cell viability showed a reduction near 50%.

Hence, it can be concluded that CAPs effectiveness is very dependent on treatment time, being much more effective in killing SCC-15 and Met-1 cells than HGF-1 (only a small percentage of these cells is affected). Accordingly, to the literature[193,200,209], this occurs due to the increase of the concentration of H_2O_2, nitrites and nitrate present on the treated medium as the treatment time increases. This assumption will be investigated in the next chapter.

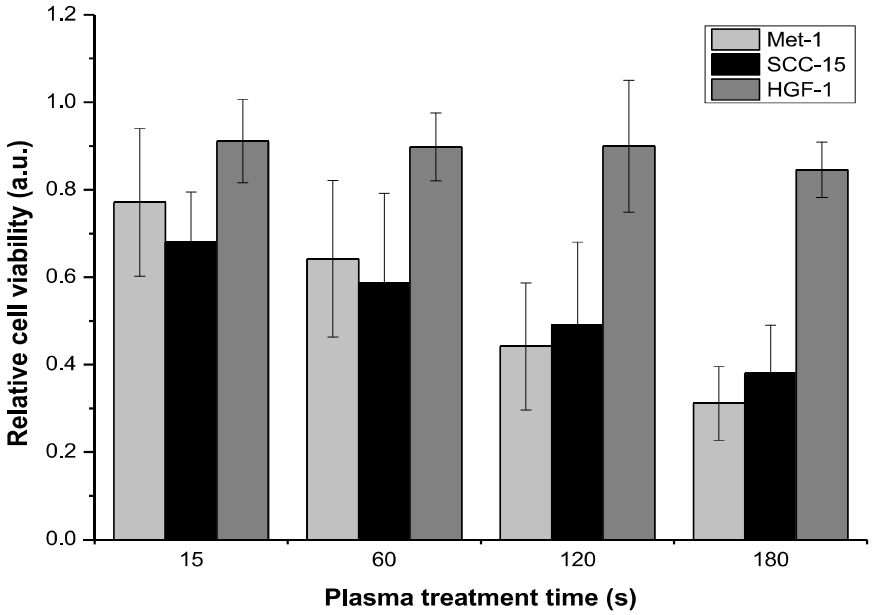

Figure 5.8 CAPs anti-cancer capacity dependence with time of plasma exposure. Results of three independent experiments, presented as mean±SD.

Until now, the obtained relative cell viability results for all the tested parameters (cell number, gap, medium volume, treatment time) were obtained 48 hours after plasma treatments, and all of them have evidenced that indirect plasma treatments can be a good alternative to common anti-cancer treatments for skin cancer, such as conventional laser surgery, which is mainly based on thermal interactions and therefore often leads to accidental cell death[6,23].

5.2.2. Effects of CAPs on cell viability after an incubation period of 48- and 72-hours after plasma treatment

In this work, it was also decided to study how long plasma-treated liquids can influence cell viability. Therefore, 2 mL of DMEM w/o sodium pyruvate was CAPs irradiated by 15, 20, 120 and 180 seconds, with a gap of 7 mm.

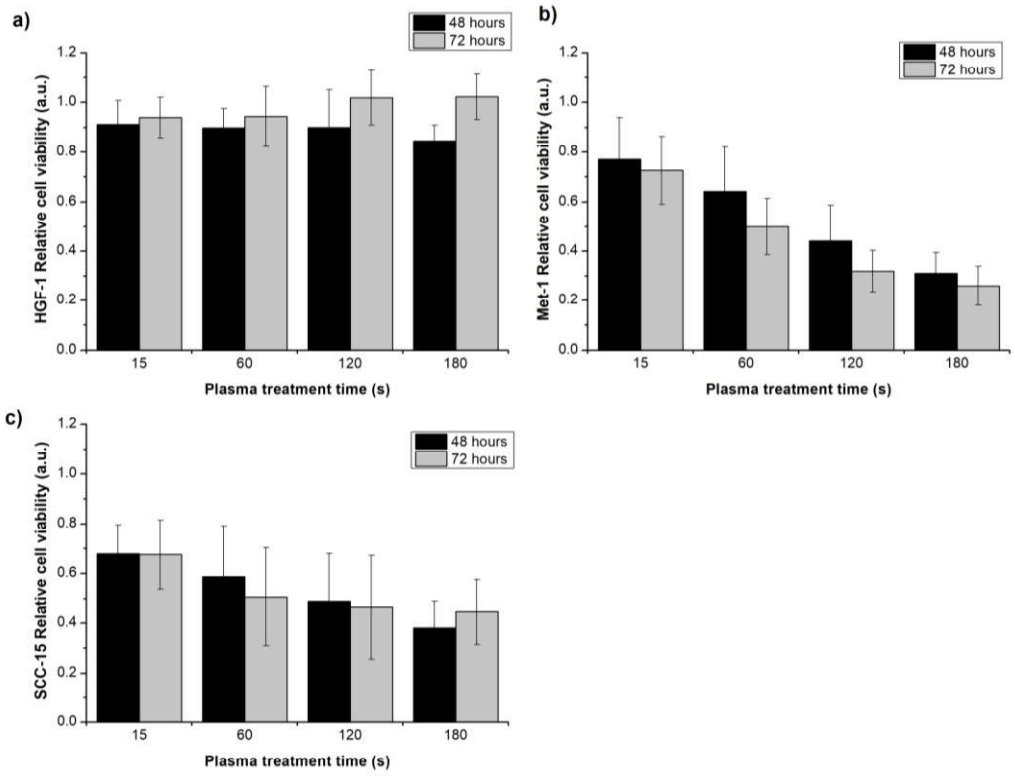

Figure 5.9 Relative cell viability of: a) HGF-1, b) Met-1, and c) SCC-15 cells, after 48 and 72 hours of plasma exposure, using a cell confluence of 3.5×10^4cells/mL, a gap of 7 mm, 2 mL of medium, and 100 μL of treated medium.

According to the results depicted in Figure 5.9, the relative cell viability of the cancer cell lines (Met-1 and SCC-15 cells) in study continues to decrease 72 hours after plasma exposure. Interestingly, comparing the results obtained for 48 and 72 hours for HGF-1 cells, an increase in cell viability was registered for all the tested exposure times for the longest incubation time. This could mean that 72 hours after plasma treatment cancerous cells continue to be sensitive to liquids treated by plasma, while the non-cancerous ones seem to be able to adapt to the presence of the treated medium.

5.2.3. Influence of the working gas composition in cell viability after plasma treatments

To identify if the working gas composition influences the results of indirect plasma treatments, the addition of 0.5% oxygen, 0.5% nitrogen and 0.5% oxygen-nitrogen to argon gas were conducted. According to literature, an explanation

can be the electron attachment, quenching of argon metastable states and quenching of UV-C photons by the added nitrogen and oxygen[210]. It must be noted that when exposing cells to plasma-treated medium, the effects of radiation and short-lived species on cells must be excluded.

This study was performed for the three cell lines in the study, and all the plasma treatments were performed in the same conditions (3.5×10^4 cells/mL, 7 mm gap, 2 mL of DMEM w/o sodium pyruvate, incubated for 72 hours under standard conditions for further evaluation of relative cell viability).

It is expected that the addition of nitrogen to the working gas leads to an increase in the generation of RNS whereas the addition of oxygen leads to the production of more ROS species in the gas phase, which probably contributes for a rising in the free nitrogen and oxygen radicals in the liquid phase, respectively[211].

As can be observed in Figure 5.10, when operating in the open air, the admixture of nitrogen and oxygen has nearly no impact on the viability of all the tested cell lines. Comparing with the results obtained for treatments performed using Ar alone, significant differences were found only for SCC-15 cells in medium treated during 1 minute with ArN ($p<0.005$), as it can be inferred from Figure 5.10 a). In this case, the effects of plasma treatment were weaker than it was expected. Interestingly, SCC-15 and Met-1 cells have responded in the same way to oxygen, and nitrogen-oxygen admixtures. When in contact with medium treated by plasma for 1 minute, both cell lines have shown to be more vulnerable to treatments performed with 0.5% oxygen-nitrogen admixture, and less sensitive to 0.5% of nitrogen admixture, but the registered differences in cell viability were not significant. Contrary to the expected behavior, no significant decrease in cell viability due to the increase of free oxygen radicals when O_2 was present in the working gas was observed. This can be related to the fact that a high oxygen gas flow influences the generated plasma, contributing to a decrease in the number of radicals formed due to the electron attachment to oxygen inside the nozzle[57]. Although in an indirect way, these findings, confirm the interaction between the produced plasma and the surrounding ambient air.

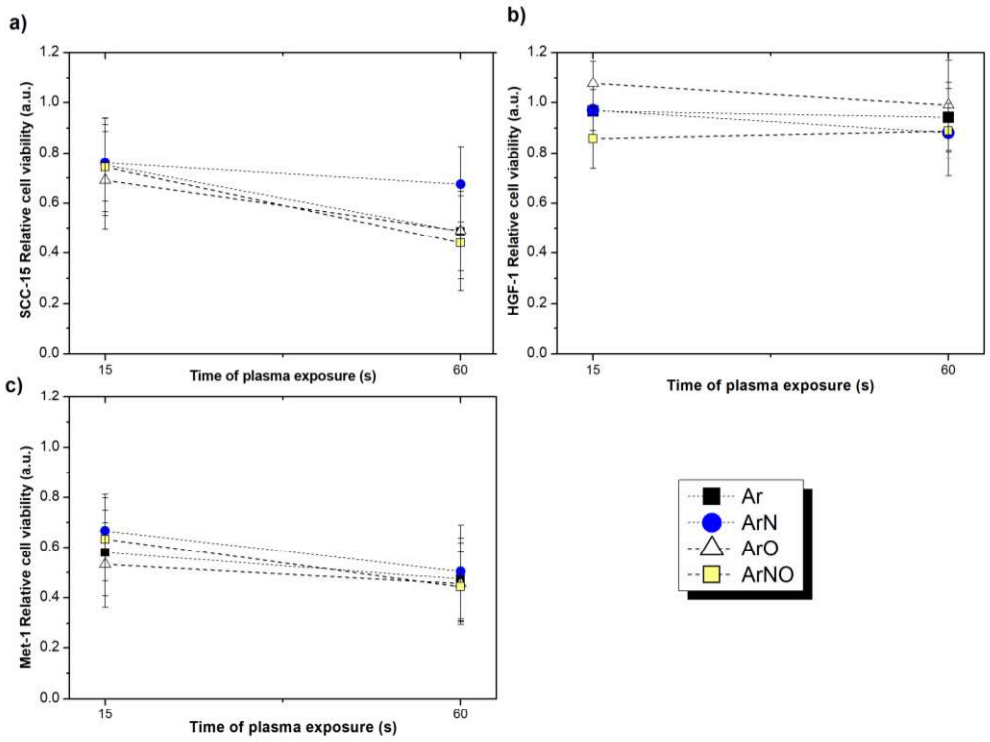

Figure 5.10 Influence of the working gas used on the relative cell viability of a) SCC-15, b) HGF-1, and c) Met-1 cells. To note that the dash lines are only represented to allow a better visualization of the obtained results and not as an indicator of a linear relationship.

5.2.4. Cell death mechanisms induced by CAPs in cancer cells

Since cell viability was compromised after plasma treatments, and one of the most relevant mechanisms of action of anti-cancer drugs is the apoptosis induction, it was decided to investigate whether after plasma treatments cells are dying through necrosis or apoptosis.

Apoptosis is a non-inflammatory type of cell death, characterized by specific changes in cell morphology, as membrane asymmetry (caused by translocation and exposure of phosphatidylserine on the external leaflet of the plasmatic membrane), nucleus and cytoplasm condensation and internuclear DNA cleavage[156,212]. It is defined as a mechanism of programmed cell death, in which cellular disintegration occurs as a regulated process, that can be signalized by external factors involving the activation of specific proteins (caspases) or by an internal mechanism initiated by the release of pro-apoptotic factors by mitochondria[7,213].

In contrast to apoptosis, necrosis is a mechanism of traumatic cell death resulting from acute cellular damage, being characterized by an immediate loss of membrane integrity following direct physical insult[214,215].

As shown in Chapter 3, flow cytometry is a technique that uses light scattered from cells for the identification of its physical properties. It is often used to study the mechanisms of cell death, with the cells being labeled with fluorescence markers so that light is first absorbed and then emitted in a range of wavelengths.

In this work, flow cytometry was used to investigate the mechanisms of cell death by combination of Annexin, a staining of phosphatidylserine, with the staining of DNA in the cell nucleus with 7-Aminoactinomycin D (7ADD), which does not readily pass through intact cell membranes. This double-staining allows to distinguish between early-, late-apoptotic and necrotic cells. Briefly, during the early phase of apoptosis, phosphatidylserine is exposed on the outside of the membrane with the cellular membrane remaining intact excluding nucleic acid-binding fluorescent dyes as 7AAD, but staining to Annexin-V. In later stages of apoptosis, the membrane starts to lose its integrity and cells stain positive for both AnnexinV and 7AAD, while necrotic cells only bind to 7AAD due to the complete loss of membrane integrity.

To identify which cell death mechanism is being induced by plasma treatments, first 7×10^4 cells/mL (SCC-15 and Met-1, separately) were cultured in a 12-well plate and incubated under standard conditions overnight. On the next day, the medium used to culture the cells was discarded and the cells were washed with PBS. 2 mL of DMEM w/o sodium pyruvate were plasma treated for different times (3, 6, and 9 min) and transferred to the cells. 24 hours after incubation with the treated medium cells were stained with AnnexinV and 7AAD and the flow cytometry results were evaluated.

According to Figure 5.11 a) and b), it can be seen that both cell lines in the study, SCC-15, and Met-1 cells stained positive for apoptosis after plasma treatments, with the percentage of apoptotic cells increasing as the treatment time increases. To facilitate the comparison and the understanding of the results,

the number of live and dead cells is presented as a percentage of the total (100%). For example, 24 hours after incubation of SCC-15 cells with medium exposed to CAPs for 3 minutes (see Figure 5.11 b)), only 13.44% of the treated cells have died, meaning that 86.56% of the cells treated under these conditions remain alive. Among the dead cells, 0.88% of them died by necrosis, 1.67% by late apoptosis and 10.89% by early apoptosis.

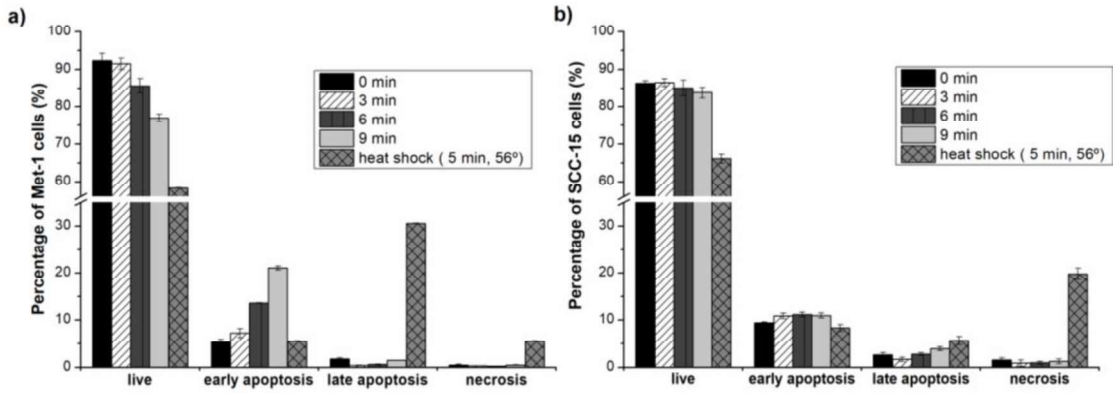

Figure 5.11 Flow cytometry results. Percentage of live and death cells detected 24 hours after plasma treatments of a) Met-1 and b) SCC-15 cells.

In accordance with the previously performed cytotoxicity assays, the percentage of dead cells increases as the plasma treatment time increases. Both, the percentage of early-apoptotic and late-apoptotic cells increase, as well as a slight increase in the percentage of necrotic cells also occurs. Despite the rise observed on the number of necrotic cells, no significant differences compared to the control group (untreated cells) were found for any of the evaluated treatment times, as well as between the tested times. This way, necrosis induction after plasma exposure (in the tested conditions) can be considered negligible for both cell lines. Heat shock was used as the positive control, to confirm that cells are staining for 7AAD, with statistically significant differences being found when compared with all the evaluated treatment times.

These results show that plasma exposure induces programmed cell death in cells (apoptosis) probably through changes in cell cycle due to oxidative and/or nitrosative stress. They further evidence that when the time of plasma exposure is not adequately chosen, with the cells being exposed to plasma treated liquids

for very long periods, there is the possibility that the liquid will become too toxic for the cells. This can induce necrosis due to the high concentration of RNOS species in the liquid phase, which may contribute to DNA strand breaks[213,216–218].

Additionally, through the analysis of flow cytometry results, it was also found that the autofluorescence of Met-1 cells changes due to plasma exposure. When neither AnnexinV nor 7ADD was added to the cells (only cells), comparing graphs of fluorescence obtained for the untreated cells (negative control) with the ones obtained for cells with treated medium, the appearance of a new peak can be observed. Moreover, the intensity of this peak increases as the time of plasma exposure increases, see Figure 5.12. This can be due to the activation of an adaptative response increasing cell robustness to severe stress, as reported by Surre J. et al.[219] . Eukaryotic cells usually respond to stress situations, by increasing the production of energy, through the increase of their respiratory activity, leading to an enhance of adenosine triphosphate (ATP) and also of the ROS production. Consequently, the expression of the genes encoding flavoproteins, which is a fluorescent cellular structural component involved in energy production and ROS detoxification, will increase, leading to the autofluorescence rise.

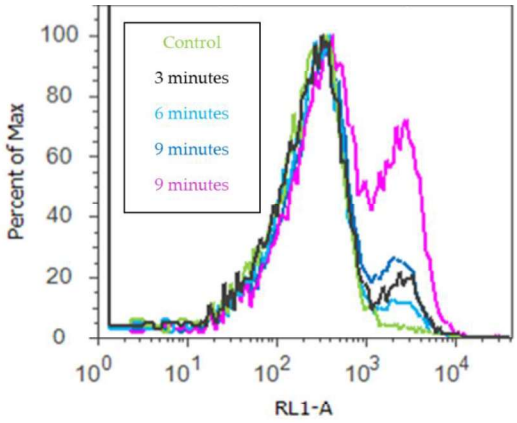

Figure 5.12 Autofluorescence of Met-1 cells as a function of the plasma exposure.

5.3. Summary

The applicability of cold plasma treatments has evolved rapidly in the fields of plasma medicine. These plasmas show huge potential in several medicine areas as sterilization, wound healing and cancer treatment. In this work, its applicability to skin cancer cells was investigated not to try to find a *de novo* treatment for skin cancer, but to try to understand how plasmas interact and influence human skin cells.

Here, two different plasma treatment approaches were tested: direct and indirect, and a similar behavior between them was found. This evidenced that the direct contribution of UV radiation, local heating, and electrical fields, to plasma cytotoxicity, are very unlikely. Moreover, when considering direct plasma treatments special attention must be given to the gas flows, since high gas flows can lead to cell detachment, especially of cancer cell lines. These cells, have smaller and fewer adhesion complexes compared to non-cancer cells[220–223], making them more sensitive to direct CAPs treatments, which can mask the results of cell viability after plasma treatments. Based on this, it was decided to proceed only with indirect treatments, since they offer the advantage that treated liquids can be directly injected into the tissues or integrated into drug delivery systems in order to prevent tumor growth and reaching tissues which would be inaccessible by another way.

To find the conditions that allow an optimization of the anti-tumor capacity of the plasma-treated medium, in this study, the influence of different working parameters used to perform the *in vitro* CAPs indirect treatments was evaluated. In summary, an adequate gap and a smaller volume of the medium being treated seem to induce few toxic effects, leading to a stronger killing capacity of CAPs treated medium. Skin cancer cells, specifically SCC-15 and Met-1 cells have shown to be more vulnerable to indirect plasma treatments than the non-cancer cell lines used in this study (HGF-1).

It was also shown that plasma treatments are time-dependent, with its killing ability increasing as the treatment time increases. Moreover, the

admixture of other molecular gases to argon seems to not induce significant differences in the interaction between the treated medium and cells. This is probably due to the fact that the plasma is being produced at open-air, and consequently, interactions between the atmospheric oxygen and the generated plasma are always occurring.

The mechanisms of cell death after plasma exposure were also investigated, being found that for longer treatment times the percentage of cells that died by late apoptosis and necrosis increases, suggesting that the cell membrane integrity is affected by plasma. By the analyses of the flow cytometry results, it was also found that the auto-fluorescence of Met-1 cells rises after plasma exposure probably due to a change in cell metabolism, as a response to the stress provoked by plasma, which can be related with the increased expression of the genes encoding flavoproteins. More studies are needed to better understand this relationship.

In short, the impact of plasma on cells will depend on the composition of the treated medium, the cell type, and concentration, as well as the parameters chosen to perform the treatment. So, a compromise among all the involved factors must be found. It is important to point out that high treatment times could promote several reactions between the plasma, the ambient air and the liquid being treated, and consequently the treated medium could become toxic also to non-cancerous cells.

6

Liquid characterization

Since *in vivo* cells are surrounded by a liquid environment it was an early idea, in the fields of plasma medicine research, to investigate the role of liquid phase for the transmission of the biological effects of plasma to the cells.

As shown in Chapter 5, plasma-treated medium has an anti-cancer ability so effective as direct plasma irradiation. These treated liquids have the advantage of avoiding the effects of UV/Vis radiation and electric fields present in plasmas. Consequently, its biological effects seem to be mainly connected with the reactive oxygen and nitrogen species (ROS and RNS, respectively) generated in or transferred into the liquid phase, being the concentration of these species directly related to its effectiveness on killing cancer cells.

However, know what species are active in plasma-treated liquids remains a challenge, since the results will depend on the atmospheric pressure plasma device and the working gas (e.g. argon, helium or gas mixtures containing oxygen and/or nitrogen) used, and also on the composition of the treated liquid.

In this chapter, the characterization of the indirect plasma-treated cell culture medium (DMEM w/o sodium pyruvate) used in this work, is presented and the obtained results discussed. To the understanding of plasma-treated

liquid-cell interactions, must be noticed that cell culture medium is an aqueous solution containing in its composition several salts, proteins, glucose, and amino acids, among other components, that can react with plasma (via reactive species) being transformed in their oxidized state. So, in this work, the temperature and pH of the used cell culture medium were measured before and after treatments, as a standard procedure for liquid analysis. The concentration of H_2O_2, NO_2^- and NO_3^- produced was investigated, and the addition of scavengers to the treated medium was tested, to verify if other reactive species than those mentioned above, influence the results of plasma treatments.

6.1. Materials and methods

6.1.1. Cell lines and cell cultures

In the last part of the work, besides the three cell lines in study, the HaCaT cell line, a non-cancerous cell line, was also investigated. HaCaT is a spontaneously transformed aneuploidy immortal keratinocyte cell line from adult human skin that was kindly given by Dr. Kristian Wende from ZIK plasmatis group, Leibniz Institute for Plasma Science and Technology, INP Greifswald, Germany.

To carried out the assays, MET-1, HGF-1 and HaCaT were cultured in 75 cm^2 flasks (Corning®, 4314640) with complete DMEM [(*Dulbecco's Modified Eagle's Medium*, Sigma, D5030), supplemented with 1.0 g/L D-glucose (Gibco, 15023-021), 3.7 g/L sodium bicarbonate (Sigma-Aldrich, S5761), 1% GlutaMAX™ (L-alanyl-L-glutamine dipeptide, Life Technologies, 35050-038), 1% sodium pyruvate (Gibco, 11360039), penicillin (100U/mL) and streptomycin (100 μg/mL) (Invitrogen, 15140122), 10% FBS (Fetal Bovine Serum, Invitrogen, 10270106)]. SCC-15 cells were maintained in DMEM-F12 (Dulbecco's Modified Eagle's Medium: nutrient mixture F-12; ATCC® 30 2006™) supplemented with 10% fetal bovine serum (FBS, Sigma, 102710), 1% antibiotic Penicillin/Streptomycin

(Pen/Strep, Sigma, A5955) and 400 ng/mL of hydrocortisone (Sigma, H0888). When reaching confluence, the cells had to be transferred into new flasks by an enzymatic method. The four cell lines are adherent cell lines that have to be maintained under 37°C in a humidified atmosphere of 5% CO_2 (standard conditions).

6.1.2. Temperature and pH measurements

2 mL of DMEM w/o sodium pyruvate were plasma treated as described in Chapter 5. Immediately after the treatment the pH of the treated medium was measured using a pH-meter (SevenEasy, Mettler-Toledo, Switzerland), and the change in temperature was estimated using a multimeter associated with a k type thermocouple[i] (123-1938, RS, Portugal).

6.1.3. H_2O_2 quantification and H_2O_2 rich medium preparation

The quantification of H_2O_2 was done according to the manufacturer's instructions using a *Fluorometric Hydrogen Peroxide Assay kit* (Sigma-Aldrich, MAK165). The samples were plasma treated and transferred in triplicate to wells of a black 96-well microplate (50 µL/well). As control, 50 µL of non-treated sample was also added in triplicate to wells of the same plate. 50 µL of a previously prepared master mix (assay reaction solution) was added to all the wells in study (samples, standards, and controls). The plate was then incubated at room temperature for 30 minutes protected from light and the fluorescence intensity was measured at $\lambda_{excitation}$=540 nm and $\lambda_{emission}$=590 nm using a fluorescence plate reader (Tecan infinite 200). Final concentrations were calculated using a H_2O_2 standard curve.

For the study of the effects of H_2O_2 rich medium, H_2O_2 solutions of different concentrations were prepared by mixing a 30% w/w H_2O_2 solution (Sigma) into complete DMEM without sodium pyruvate. The prepared H_2O_2 rich medium was then transferred to the previously cultured cells (3.5×10^4 cells/mL, SCC-

[i] The k type thermocouple is a nickel-chromium/nickel-alumel thermocouple available in a wide variety of probes (-270 to 1260 °C) with a sensitivity of approximately 41µV/°C.

15, HaCaT, HGF-1, and Met-1, in a transparent flat-bottom 96-well microplate) in sextuplicate. Before this step, the medium that has been used to culture the cells overnight was discarded and the cells were washed with PBS. The cells were incubated for 48 hours under standard conditions, and only then the cellular viability was assessed. A positive control of the cells in untreated DMEM w/o sodium pyruvate and without H_2O_2 was used in all the realized experiments.

6.1.4. Scavengers addition

2 mL of DMEM w/o sodium pyruvate were plasma treated as indicated in section 5.1.2. Immediately after plasma exposure, the desired concentration of the scavenger was added to the treated medium. The tested scavengers and the respective concentrations are summarized in Table 6.1.

Table 6-1 Tested scavengers.

Scavengers	Concentration	Reference
D-mannitol	100 μM	M9647, Sigma
Superoxide dismutase	20 U/mL	S9697, Sigma
Sodium azide	10 mM	S8032, Sigma
Catalase	10 U/mL	C1345, Sigma
Uric acid	100 μM	A13346, Alfa Aesar

6.1.5. Ion chromatography (IC)

Ion chromatography (ICS-5000, Dionex Corp., Sunnyvale, USA) was used to detect nitrite (NO_2^-) and nitrate (NO_3^-) ions. An IonPac® AS23 pre-column (2 × 50mm, Thermo Fisher Scientific Inc., Waltham, USA) coupled to an IonPac® AS23 anion exchange column (2 × 50mm, Thermo Fisher Scientific Inc., Waltham, USA) was used for separation in an isobaric mobile phase (4.5 mM Na_2CO_3 / $NaHCo_3$) regime with 250 μLmin^{-1} flow rate. The analytes were detected through

conductivity and UV detection (210 nm). IC principles were described in Chapter 3.

6.1.6. Statistics

Statistical analysis was performed with Excel. All data are expressed as mean ± standard deviation of at least three independent experiments. The statistical significance of the differences was evaluated using the ANOVA and it was recognized as * $p < 0.05$, ** $p < 0.01$ and *** $p < 0.005$. To better illustrate the influence of plasma treatment parameters on cell viability, all the results have been normalized, i.e, the data from experimental groups were divided by the data corresponding to the control group and relative values were obtained.

6.2. Results

6.2.1. Temperature and pH changes due to plasma treatments

Temperature and pH are essential parameters that must be considered for biomedical applications, to exclude possible thermal damages and poisoning due to the acidification of the treated medium.

Regarding the pH of the treated culture medium, a slight increase could be observed as the time of plasma exposure increases as shown in Figure 6.1. This increase can be explained by the degassing effect of the carbonate buffer sodium bicarbonate, present in the treated medium[224,225], due to the argon flow of the plasma jet. In chemistry, degassing is the name given to the procedure in which an inert gas, like argon, is bubbled through a liquid, leading to the removal of dissolved gases, such as oxygen and carbon dioxide. In the case of this work, the degassing effect resulted in the loss of carbon dioxide leading to the observed increase in pH.

The longest plasma exposure of 270 seconds yielded a pH value of 8.55 compared to a pH value of 8.16 of the untreated medium (0 seconds of exposure). Student t-test was performed, and the significance compared with the first bar (pH of untreated medium) being indicated as * for $p<0.05$, ** for $p<0.01$ and *** for $p<0.005$.

By the analysis of the obtained results, no significant differences were found between the pH value of the untreated medium and the one registered for the different tested exposure times, as indicated in Figure 6.1. Nevertheless, these small differences are not statistically significant, as demonstrated by Bundscherer et al.[225], an increase in extracellular pH can lead to a parallel rise in intracellular pH, and consequently to changes in signal transduction and cell death pathways due to the increase of alkaline stress. However, the registered change in pH is so reduced (0.39) that it can be concluded that it does not play a key role in plasma-induced apoptosis.

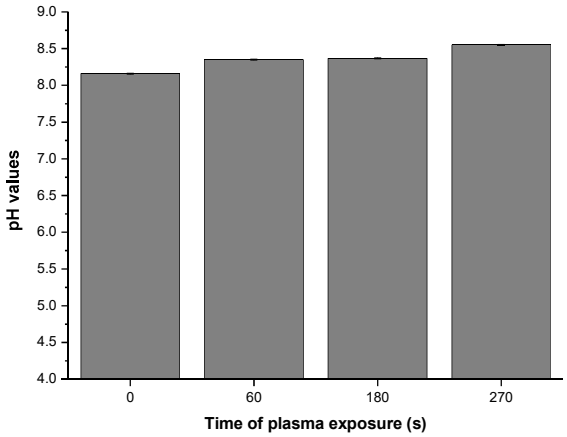

Figure 6.1: pH values as a function of time of plasma exposure. Results of 3 independent measurements of pH of the treated culture medium expressed in terms of mean ± std.

The change in pH was also measured for plasma-treated Milli-Q-water. In this case, the acidification of the treated liquid was observed. The initial registered pH value, corresponding to untreated Milli-Q-water was 5.93, but after a plasma treatment of 180 seconds, this value decreases to 4.37. This may indicate that significant amounts of excited nitrogen species and their end

products (NO_2^-, NO_3^-), as well as H_2O_2, which is a weak acid, and also singlet oxygen were produced during plasma exposure.

In terms of temperature, the longest plasma exposure of 270 seconds yielded a temperature of 31°C, Figure 6.2. The cellular tolerance without thermal damage is around 40°C, reason why it can be concluded that this increase in temperature is not enough to cause thermal damage on its own[53]. This evidences that the results obtained after the cellular assays are not a consequence of the thermal effects caused by plasma treatments, but rather due to the oxidative stress caused by the presence of some reactive species formed during the plasma treatment of liquids.

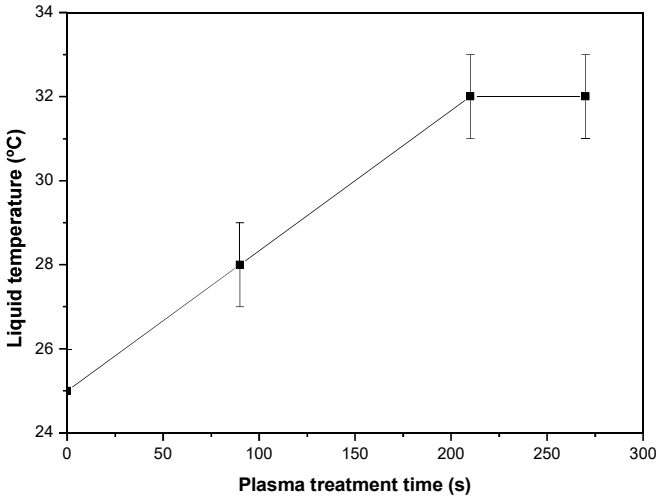

Figure 6.2 Temperature of DMEM w/o sodium pyruvate as a function of plasma treatment time. Results of three independent experiments presented in terms of mean±SD. To note that the solid line is only represented to allow a better visualization of the obtained results.

6.2.2. Hydrogen peroxide

Among the plasma generated ROS, hydrogen peroxide is being pointed as the main reactive species responsible for the selective effects of CAPs, due to its high stability and role in a variety of multiple cellular pathways[152,194,226].

H_2O_2 is a very important reactive oxygen species in plasma medicine, as it can be produced by exposure of liquids to cold plasmas, and it is also present on living cells. Hydrogen peroxide is a viscous liquid, that in concentrations from

10 to 100 μM is toxic to many cells, inducing senescence and apoptosis, while at lower concentrations it can promote the proliferation of certain cell types, and at higher levels induces necrotic cell death[227]. The H_2O_2 can react at the gas phase, at the liquid surface and in the bulk target solution with solute, since it is completely soluble in water and *in vivo* can readily cross through membrane water channels (aquaporins).

Three different mechanisms have been proposed to explain the H_2O_2 generation in plasma-treated liquids. The first points that H_2O_2 can be produced from the dismutation of superoxide anion; the second that it is produced through recombination of atomic oxygen with water molecules, and the third considers that H_2O_2 can be generated through recombination of water molecules with excited water molecules[39,228]. In all these processes, the H_2O_2 production is independent of the pH values in the range from 6 to 9[229]. Another, possible explanation for the detection of H_2O_2 in the liquid phase can be related to its relative high Henry's constant. This means, that for example, in the presence of a humidified feed gas, H_2O_2 can be mainly formed in the plasma/gas phase and then be dissolved in the liquid phase instead of being formed inside the liquid[230]. The main mechanism of H_2O_2 cytotoxicity involves penetration into cells and the generation of hydroxyl radicals through interactions of H_2O_2 with intracellular transition metals (Cu^+ and/or Fe^{2+}) by the Fenton's reaction, forming more damaging reactive species such as hydroxyl radicals (Equation 6.1):

$$H_2O_2 + Fe^{2+} \rightarrow OH^- + Fe^{3+} + \cdot \mathrm{OH} \qquad (6.1)$$

Despite ·OH accounts for almost all the damage done to DNA in H_2O_2 treated cells, H_2O_2 can also interact with haem proteins causing oxidative damage.

In this work, to investigate the importance of H_2O_2 in plasma treatments, the concentration of H_2O_2 produced during CAPs treatments, in DMEM w/o sodium pyruvate, was measured. Additionally, to investigate whether if it is the sole factor causing the cell death, it was decided to study the response of four cell lines (Met-1, SCC-15, HGF-1, and HaCaT) to H_2O_2 rich medium and compare the obtained results with the effects of plasma-treated medium.

6.2.2.1. Effectiveness of H_2O_2 produced in CAPs and H_2O_2 rich medium

Regarding the study of the effects of H_2O_2 rich medium, up to a H_2O_2 concentration of 2.34 μM, the growth of the four cell lines presents an alike concentration-dependent response to the H_2O_2 rich medium, as it can be observed in Figure 6.3. Moreover, similarly, to what happens with indirect plasma treatments, while the H_2O_2 concentration in DMEM w/o sodium pyruvate is relatively low (<9.38 μM) non-cancer cells show stronger resistance to H_2O_2 rich medium than the cancerous ones. For H_2O_2 concentrations higher than 9.38 μM, a reduction on HaCaT cells viability becomes also evident (see Figure 6.3) which is not surprising since high doses of H_2O_2 induce cell death[162,212,226,231,232]. Inquiringly, HGF-1 cells have shown to be almost unaffected by the H_2O_2 rich medium. In terms of values, an IC_{50}[j] = 11.2 μM and IC_{50} = 24.7 μM of H_2O_2 were calculated for Met-1 and SCC-15 cells, respectively, while an IC_{50} = 23 μM and IC_{50} = 184 μM of H_2O_2, were calculated for HaCaT and HGF-1, respectively. It is important to note that the real concentration of H_2O_2 rich medium is different than the one calculated for the preparation of the solutions (being lower) since H_2O_2 reacts with the proteins present in the medium, for example via Fenton's reaction[200]. When the H_2O_2 concentration in the referred culture medium is higher than 9.38 μM, HaCaT and SCC-15 cells share a similar response, which is proved by the obtained IC_{50} values. This behavior is quite different from the one observed for indirect plasma treatments, in which cancer cells (SCC-15 and Met-1) are more sensitive to plasma-treated medium, for all the tested exposure times.

On the case of indirect plasma treatments, an IC_{50} of approximately 8.25 μM of H_2O_2 was obtained for Met-1 cells and SCC-15, corresponding to 90 seconds of plasma exposure, and an IC_{50} of 56.97 μM of H_2O_2 was obtained for HGF-1 and an IC_{50} of 18.99 μM for HaCaT (medium treated by approximately 10 and 4 minutes, respectively).

According to these results (summarized in Table 6-2), it is clear that the response of the four cell lines under study to the CAPs medium is different from

[j] IC_{50} is defined as the concentration of a chemical which reduces cell viability to 50%.

the response to the H_2O_2 rich medium, with the four cell lines being more sensitive to the presence of CAPs medium instead of the H_2O_2 rich medium. For example, a reduction of 50% on SCC-15 cells viability was found in the presence of a H_2O_2 solution in DMEM w/o sodium pyruvate with a concentration of 24.7 μM of H_2O_2. However, when considering indirect plasma treatments, 90 seconds of plasma exposure of DMEM w/o sodium pyruvate, corresponding to a H_2O_2 concentration of 8.25 μM, is enough to cause the same reduction on cell viability.

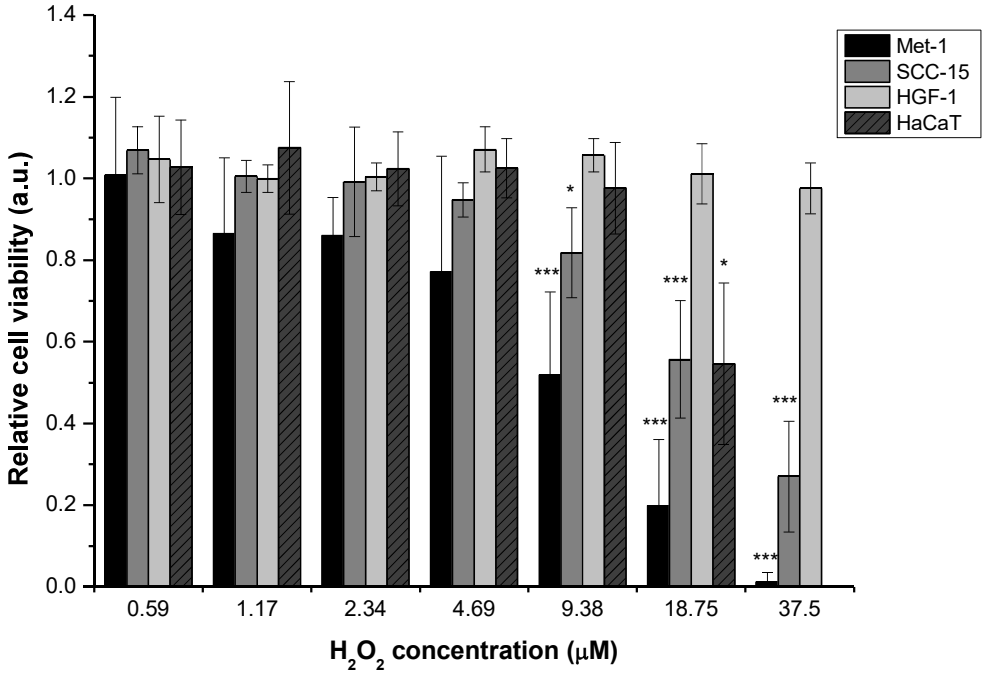

Figure 6.3 Vulnerability of Met-1, SCC-15, HGF-1 and HaCaT cells to H_2O_2 rich medium. Results are present as mean±SD, and the significance compared to the first bar (concentration of 0.59μM) is indicated as * $p<0.05$, ** $p<0.01$ and *** $p<0.005$.

Table 6-2 Summary of the H_2O_2 concentrations that conduce to a reduction of 50% in cell viability.

Cell line	[H_2O_2] in rich medium (μM)	[H_2O_2] in CAPs medium (μM)
HaCaT	23.00	18.99
HGF-1	184.00	56.97
Met-1	11.20	8.25
SCC-15	24.70	8.25

Additionally, observing the values obtained for the quantification of H_2O_2 produced in CAPs treated medium, it can be observed that H_2O_2 concentration increases as the time of plasma exposure increases, indicating a dose-dependent response.

All these results demonstrate that H_2O_2 has an important role in plasma-induced chemistry, and consequently in the interactions between treated medium and cells. However, the differences observed between H_2O_2 rich medium and the H_2O_2 concentrations measured in CAPs treated medium indicate that it is not the only reactive species responsible for the anti-cancer effects of CAPs treated medium, supporting the idea that other reactive species also have a key role in indirect plasma treatments.

6.2.3. Scavengers addition

The addition of scavengers can be used to non-quantitatively investigate the different reaction pathways occurring in plasma-treated liquids. This technique blocks certain chemical pathways, being useful to check different reaction mechanisms. In this work, different scavengers were added to the treated medium to facilitate the identification of the different reactive species created by the developed jet device (Jet) and to analyze its effects on Met-1, SCC-15, and HaCaT cells viability.

The addition of D-mannitol (100µM, M9647, Sigma) as a hydroxyl radical scavenger did not change the biological impact of plasma-treated medium (see Figure 6.4). Also, no effect on cell viability was observed after the addition of superoxide dismutase (20 Units, SOD, S9697, Sigma), which seems to indicate that the effect on cell viability is not dominated by the superoxide radical. The addition of sodium azide (10 mM, NaN_3, S8032, Sigma) as a singlet oxygen quencher was also tested. A significant change in cell viability after plasma treatment was observed by its addition when compared with the positive control (1 min of plasma exposure). However, this difference was based on a decrease in cell viability and not in an increase as it was expected. This could mean that maybe sodium azide has a synergetic effect with the plasma-treated medium

instead of working as a scavenger. It should be noted that the use of scavengers is not always specific. This is the case of sodium azide which could be used not only as an $^1O_2$ scavenger but also, as referred by Wende *et al.*[207] to scavenge possibly present NO_2^- according to the reactions indicated in 6.2 and 6.3:

$$NO_2^- + H_2O_2 + H^+ \rightarrow NO_3^- + H_2O + H^+ \quad (6.2)$$

$$3NO^- + NO_2^- + 4H^+ \rightarrow 5N_2 + 2H_2O \quad (6.3)$$

The addition of catalase (10U/mL, C1345, Sigma), which is expected to react with H_2O_2 to form water and molecular oxygen was also evaluated. Despite, no significant difference was found, a slight increase in cell viability was observed by its addition. This seems to be in accordance with the results presented in the previous section, indicating that H_2O_2 is active in treated medium, but it is not acting alone, otherwise, a complete rescue in cell viability would be observed.

As can be observed in Figure 6.4, a significant increase in cell viability was achieved by the addition of uric acid (100µM, A13346, Alfa Aesar). Uric acid is a scavenger for peroxynitrite anion ($ONOO^-$), which can be produced by (i) the reaction of nitric oxide and superoxide anion radicals (reaction 6.4); (ii) the reaction of the nitrite anion with hydrogen peroxide (reaction 6.5); and (iii) the reaction of $NO_2^{\cdot}$ with an ·OH radical (reaction 6.6)[207,233]:

$$O_2^{-\cdot} + NO \rightarrow ONO_2^- \quad (6.4)$$

$$NO_2^- + H_2O_2 \rightarrow O = NOO^- + H_2O \quad (6.5)$$

$$\cdot OH + NO_2^{\cdot} \rightarrow O = NOO^- + H^+ \quad (6.6)$$

Special attention should be given to the second mechanism since it is known that a significant amount of H_2O_2, nitrites, and nitrates are produced in gas-liquid plasma interactions. The first reaction is more likely to occur in cancer cells, since they have shown to be more responsive to plasma-mediated NO production than non-cancer cells[234]. In this work, the scavengers' study was done using DMEM w/o pyruvate as the liquid phase, in alkaline conditions (pH>7). In these conditions, peroxynitrite formed in the liquids during plasma exposure can react with the lipids present in the membranes of living cells contributing to the

oxidative stress, and consequently causing cell wall damage[233]. Moreover, peroxynitrite as the ability to diffuse through several cell diameters and cell membranes entering in the cells, where the pH is around 7, and the $ONOO^-$ reacts with the CO_2 present inside of them[235] via reaction 6.7:

$$ONOO^- + CO_2 \rightarrow ONOOCO_2^- \quad (6.7)$$

which has a lifetime of only 1 μs and spontaneously decomposes into nitrogen dioxide (NO_2) (reaction 6.8):

$$ONOOCO_2^- \rightarrow CO_3^- + NO_2 \quad (6.8)$$

It is important to note, that peroxynitrite has a very short lifetime (around 1 s under alkaline conditions) and the radicals produced as the result of the $ONOO^-$ reactions inside the cells recombine almost immediately forming nitrate and carbon dioxide, with only a small part being able to react with other molecules. For this reason, the role of $ONOO^-$ in plasma treatments can be mostly related to its ability to generate nitrate, as an end product of the reactions inside the cells.

The influence of all the referred scavengers on cell viability is represented in Figure 6.4.

Additionally, the addition of sodium pyruvate, which is also considered a scavenger for hydrogen peroxide, to the cell culture medium was also investigated. This study was only performed for SCC-15 cells and as expected different results were obtained in its presence. While DMEM w/o sodium pyruvate treated for 3 minutes results in a reduction of SCC-15 cells viability for 0.50±0.19 (a.u.), treating DMEM with sodium pyruvate during the same time of exposure and in the same conditions only reduces SCC-15 cells viability for 0.91±0.18 (a.u.). These results confirm the scavenging effect of sodium pyruvate.

Concluding from the scavenger study, H_2O_2, nitrate, and peroxynitrite seem to be the main active species and/or the precursors that cause a reduction in viability principally of cancer cells in the case of the developed plasma jet device.

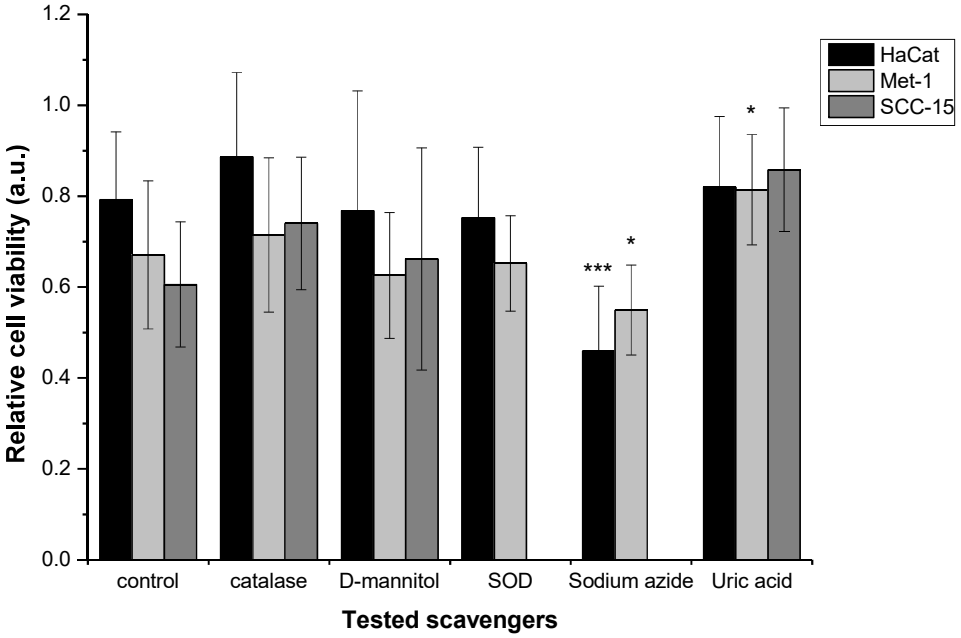

Figure 6.4 Influence on cell viability of the tested scavengers. Results are present as mean±SD, and the significance compared to the first bar (1 min of plasma treatment) is indicated as * $p<0.05$, ** $p<0.01$ and *** $p<0.005$.

6.2.4. Nitrite and nitrate detection

The nitrite and nitrate concentrations are often used as a measure of the plasma-induced reactive nitrogen species produced within the treated liquid. DMEM w/o sodium pyruvate has ingredients that contain nitrate, as it is the case of ferric nitrate monohydrate ($Fe(NO_3)_3 \cdot 9H_2O$), reason why the changes in nitrate concentration induced by plasma are extremely difficult to measure in this cell culture medium. For this reason, and also because of interferences of the detection reactions with the dissolved salt components, in this work, to have an idea how plasma treatments affect the concentration of these reactive species, it was decided to investigate the behavior of nitrate and nitrite produced after the plasma exposure in Milli-Q-water instead of in cell culture medium. In Chapter 7, the production of these reactive species will be studied again using mass spectrometry complemented with IC.

According to the obtained results, the concentration of nitrite in the liquid decreases with the increase of the treatment time, while the nitrate concentration

presents the opposite behavior, as depicted in Figure 6.5. This happens, because when performing plasma treatments in water a small decrease in pH occurs, which favors the disproportionation of nitrites into nitrate and nitric oxide according to reaction 6.9:

$$3NO_2^- + 3H^+ \rightarrow 2NO + NO_3^- + H_3O^+ \quad (6.9)$$

The formation of nitrate may also occur via liquid-phase reaction of NO_2 with $\cdot OH$ radicals to form peroxynitrous acid or its conjugate base peroxynitrite, through reaction 6.10, in a neutral or basic medium, as it is the case of the cell culture medium DMEM w/o sodium pyruvate. Then, the produced unstable moiety isomerizes to the nitrate anion, according to reaction 6.11.

$$OH + NO_2(aq) \rightarrow [O = N - OOH] \rightarrow O = N - OO^- + H^+ \quad (6.10)$$

$$O = N - OO^- \rightarrow NO_3^- \quad (6.11)$$

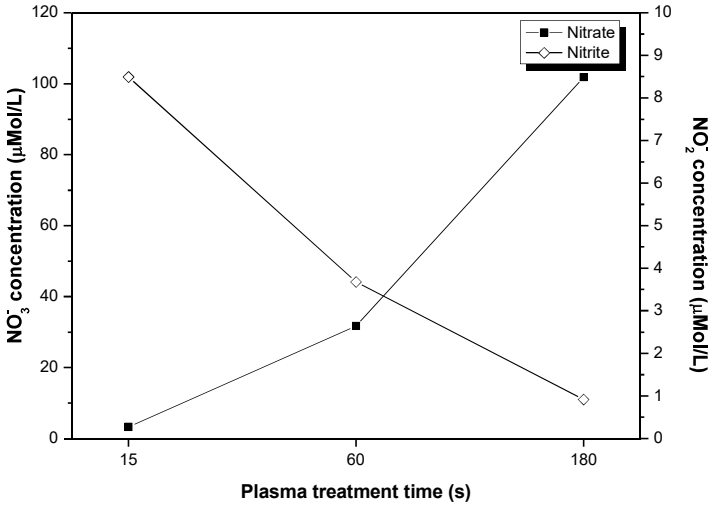

Figure 6.5 The formation of nitrites and nitrates in 2 mL MilliQwater treated with the jet developed during this work at a distance of 7 mm of the upper edge of the well where the treatment was performed using a gas flow of 3 slm of Argon as a function of plasma treatment time. Results of three independent experiments. To note that the solid lines are only represented to allow a better visualization of the obtained results.

Another possible explanation for the decrease of nitrites and the increase of nitrates may be the presence of ozone, which it is known to be produced in a

significant amount during plasma treatments, contributing to the oxidation of nitrites into oxygen and nitrates (reaction 6.12):

$$NO_2^- + O_3 \rightarrow NO_3^- + O_2 \qquad (6.12)$$

For the formation of nitrite and nitrate, both nitrogen and oxygen, are required. Beyond the treatments performed using 3 slm of argon also admixtures of other gases, specifically 0.5% oxygen, 0.5% nitrogen and 0.5% nitrogen-oxygen were also tested, Figure 6.6. The results show an active RNS chemistry independently from the working gas used. As can be seen in Figure 6.6 b), the lowest nitrite concentrations were found for treatments performed adding 0.5% nitrogen. This happens because in this situation there is almost no oxygen from which nitrite species can be produced. Low nitrite concentrations were also found when using 0.5% oxygen as gas admixture. In this case, this is due to the fact that almost no RNS species are being produced in the jet effluent.

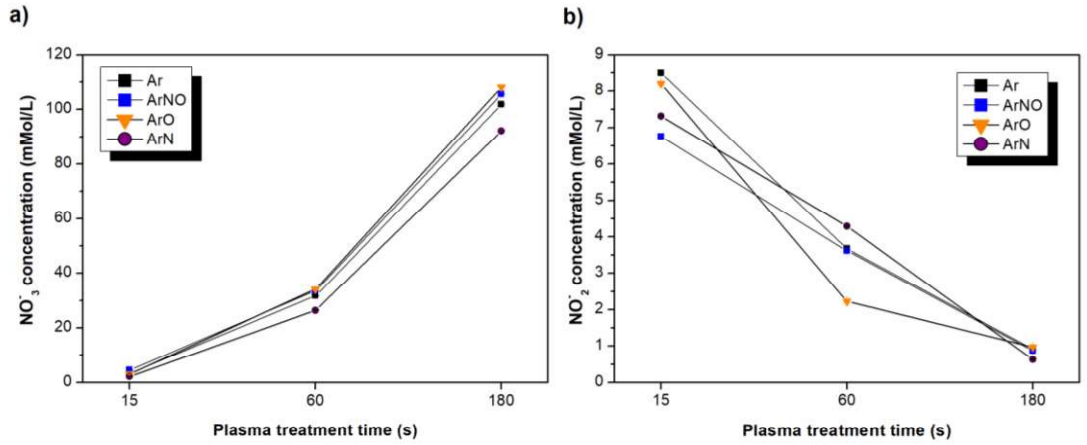

Figure 6.6 Representation of the a) nitrate and b) nitrite concentrations as function of plasma exposure for different working gases. To note that the solid lines are only represented to allow a better visualization of the obtained results.

According to all these results, it can be concluded that there is a strong interaction between the reactive species produced by the plasma jet and the ones present in the ambient air. Otherwise, no nitrite would have been detected in treatments performed using only argon as the working gas as inferred from Figure 6.5. Moreover, the trend for the nitrite and nitrate concentrations in

function of the treatment time is similar for all the tested working gas mixtures as it can be observed in Figure 6.6, and no significant differences were found between the nitrite and nitrate concentrations measured. All these results indicate that the working gas composition almost no affects the total number of RNS produced in treatments performed with the *Jet*, and nitrate seems to have an important role in the cell-killing capacity of the liquids treated by the developed plasma jet. However, it should be noted that in the case of treatments performed with DMEM w/o sodium pyruvate, no pH reduction was observed after plasma exposure, indicating that the transformation of NO_2^- into NO_3^-, that it is accelerated by acidic conditions, cannot be the only responsible for the reduction in cell viability after plasma exposure. This suggests a synergy between all the reactive species (ROS and RNS) generated during plasma exposure, and also between pH and reactive species as pointed by Oehmigen K. *et al*[236] who wrote that "*the action of plasma-based reactive species could cause a higher susceptibility of microorganisms against pH stress"*.

6.3. Summary

In order to understand the mechanisms behind the interactions between plasma-treated medium and the cells, the characterization of the cell culture medium exposed to plasma was performed in terms of pH, temperature, and ROS and RNS production. According to the obtained results, possible effects of thermal damage can be excluded.

Regarding pH, no significant change in pH was found after treating DMEM w/o sodium pyruvate, the medium used to perform the viability assays reported in chapter 5. So, acidification of the medium is not the answer for the decrease in cell viability. However, when treating Milli-Q-water acidification occurs, indicating that probably significant amounts of excited nitrogen species and their end products (NO_2^-, NO_3^-), H_2O_2, and also singlet oxygen are being produced during plasma exposure. For that reason, measures of the H_2O_2, NO_2^- and NO_3^-

produced by plasma exposure were done. It was found that H_2O_2 was formed during treatments however it is not acting alone. By the analysis of the IC results it could be concluded that the liquids treated by the developed jet present a strong RNS chemistry, with nitrite being converted into nitrate over time. The only problem it is that the IC measurements were performed in Milli-Q-water, reason why at this moment only an idea of the behavior of these species can be highlighted, since their quantification in DMEM w/o sodium pyruvate was not performed. The results of scavengers addition also point out to the major influence of RNS species (by addition of uric acid) and H_2O_2 (addition of catalase and sodium pyruvate) on cell viability. It was noted that $ONOO^-$, which is the most reactive and potentially injurious RNS, having powerful oxidizing and nitrating actions, is likely to be abundant in the cell culture medium treated using the *Jet*.

Until now, it can be concluded that the developed jet has a strong RNS chemistry and this illustrates the importance of the RNS species in cell viability reduction. However, more studies need to be performed to fully understand the ROS/RNS chemistry induced by plasma treatment of liquids.

7

Comparison between the developed jet device and the well-characterized Kinpen09

CAPs are under investigation in several research fields, such as surface modification and medical applications. Regarding the last one, it was already shown that they can assist in wound healing, skin disorders, and cancer treatment[6,22,44,184].

As already referred in this thesis, besides the direct application of plasmas, also the treatment of liquids, which are subsequently applied to the biological target has been successfully investigated in the field of plasma medicine. Recently, the injection of plasma-treated medium showed promising results in a peritoneal carcinomatosis model in mice, inducing the apoptosis in cancer cells and reducing tumor size[194]. These *in vitro* and *in vivo* studies strongly indicate that the reactive species (ROS/RNS) produced in plasmas and deposited in the treated liquid interfere with the cellular and intercellular redox signaling processes being essential players in the biological effects of plasmas[7,17,237]. For example, proteins and several amino acids are assumed to be susceptible to plasma-derived oxygen or nitrogen species. Due to the reactivity of the sulfur atom, thiols are potential targets for plasma-derived reactive species and may undergo a number of oxidative and nitrosative modifications with potential bioactivity[238]. However, the origin of these reactive species and its biochemical potential are yet under investigation,

due to the high complexity and diversity of plasma sources and treatment conditions, which often impedes the direct comparison of experimental and clinical results from different plasma devices.

In this chapter, two different plasma sources were investigated: the developed plasma jet device (*Jet*) and the well-characterized Kinpen09. The Kinpen09 was developed at the Leibniz-Institute for Plasma Science and Technology, INP Greifswald, Germany, place where the work presented in this chapter was developed. A physiological buffer solution containing the amino acid cysteine was treated using both set-ups, with and without molecular gas admixtures, and the resulting product pattern was identified via high-resolution mass spectrometry. Cysteine, under controlled conditions, is a sensitive and reactive amino acid, that can be found in almost every biologically-relevant macromolecules from nucleic-acids (DNA and RNA) to lipids and proteins, which makes this amino acid an ideal tracer compound to discriminate between the chemical potential of different plasma sources and working gas mixtures[239,240]. Similarly, to cysteine, also phenol was used to study the interactions between plasma and liquids being treated due to its well-known aromatic form[241,242]. Additionally, long-lived species (NO_2^-, NO_3^-) were quantified by ion chromatography and Pierce™ Quantitative Peroxide Assay kit (H_2O_2). The cell viability was also evaluated using Alamar Blue assay.

7.1. Materials and methods

7.1.1. Cell culture

SCC-15 cells were maintained in DMEM-F12 (Dulbecco's Modified Eagle's Medium: nutrient mixture F-12; ATCC® 30 2006™) supplemented with 10% fetal bovine serum (FBS, Sigma, 102710), 1% antibiotic Penicillin/Streptomycin (Pen/Strep, Sigma, A5955) and 400 ng/mL of hydrocortisone (Sigma, H0888).

Met-1 and HaCaT were kept in DMEM (Dulbecco's Modified Eagle's Medium, Sigma), supplemented with 10% FBS, 1% antibiotic Pen/Strep and 1% L-Glutamine. HaCaT as Met-1, being keratinocytes, presents a high capacity to differentiate and proliferate *in vitro*, being very easy to manipulate.

All cell lines under investigation were maintained under standard conditions (37°C in a humidified atmosphere of 5% CO_2), and to sub-culture cells twice a week they were washed with PBS and trypsinized with 0.025% trypsin/EDTA. To determine the number of cells, a sample was lysed, and the nuclei counted using a Buerker counting chamber. For perform the assays, the cells were collected following the same procedure.

7.1.2. Plasma source

The kINPen09 (kINPen, neoplas GmbH, Germany), an atmospheric pressure plasma jet using argon as main working gas and the jet developed under this project were investigated in parallel. The kINPen consists of a high-voltage needle electrode located in the center of a ceramic capillary with 1.6 mm diameter. The working gas is driven by a radio frequency of around 1 MHz, with an average power of 1.1 W[39,44]. The cold atmospheric plasma (CAP) jet device developed in this research was designed and constructed in our laboratory (Plasmas and Applications laboratory, CEFITEC, Portugal), and it consists of a hand-held principal unit composed by a borosilicate capillary with an outer diameter of 6.93 mm and an inner diameter of 4.94 mm, with a stainless steel electrode in its center (2 mm diameter) and a copper ring around it. The copper ring electrode is connected to a custom-made DC high voltage power supply (2.5 mA, 20 kV).

For the experiments, a gas flow of 3 slm was kept constant and either pure argon was used or 1 % of the feed gas was replaced with O_2 or N_2O_2 (0.3% O_2 and 0.7% N_2). The gap of 7 mm was used in all the treatments performed with both set-ups. To note that in both devices the plasma propagates out of the nozzle, and consequently the atmosphere has an impact on the plasma-induced chemistry of both jets.

7.1.3. Sample preparation and plasma treatments

The cysteine model solution was freshly prepared by dissolving cysteine (L-cysteine, 658057, Sigma-Aldrich) in 5 mM phosphate-buffered saline with pH 7.4, for a final concentration of 300 μM before each analysis, to minimize cysteine spontaneous oxidation. When necessary, a 300 μM phenol solution (Phenol, 108-95-2, Sigma-Aldrich) was also freshly prepared in 5 mM phosphate-buffered saline.

A volume of 2 mL of the desired solution was then treated for different times (15 s, 60 s, and 180 s) in 12-well plates with a fixed distance of 7 mm from both plasma devices to the upper edge of the wells were the treatments were performed. To finalize, the treated samples were divided into aliquots and subjected to subsequent analysis.

7.1.4. Mass spectrometry

The cysteine and phenol derivatives produced by the plasma treatment were analyzed by direct injection into a high-resolution mass spectrometer (TripeTOF5600, Sciex Ltd., Darmstadt, Germany). Isotopically labeled cysteine or phenol, depending on the solution being analyzed, served as internal standard at a fixed concentration of 300 μM. For the mass spectrometry analysis, each sample (control and treated solutions) was diluted 1:1 with 0.3% ammonium hydroxide in methanol (both Sigma, MS grade), to improve negative electrospray ionization. A flow of 10 $\mu L min^{-1}$ was infused by a syringe pump into an electrospray ion source (Turbo Spray V, Sciex Ltd., Darmstadt, Germany), running on 4 kV. The following experimental parameters were used: capillary temperature 150ºC, 35 slm curtain gas, 20 slm N_2 ion source gas 1, and 25 slm N_2 ion source gas 2.

The spectra were acquired in a mass range from 50 to 400 m/z (cycle time of 275 ms, accumulation time of 250 s). Fragmentation spectra (MS/MS) of each peak were acquired to identify the derivatives on the base of its fragmentation pattern (collision energy ±24 eV, declustering potential -10 kV).

7.1.5. Cell viability assay

Cell viability was assessed using the resazurin assay based on the ability of the dehydrogenase enzyme, reduce the resazurin (7- Hydroxy-3H-phenoxazin-3-one 10-oxide) blue dye into a pink-colored and highly red-fluorescent resorufin (3H-phenoxazin-3-one) product. 3500 cells per well were cultured in the inner 60 wells of a 96 well plate, 24 hours prior to each experiment. After this, the medium was removed, the cells were washed with PBS and 100 μL of the treated medium was transferred onto the cells. As control 100 μL of untreated medium was used. To assess cell viability 72 hours after plasma treatments, the medium in the wells was discarded and 100 μL of resazurin (Alfa Aesar, Germany) was added to all the wells in study. The fluorescence intensity was measured at an excitation wavelength of 535 nm and 590 nm emission using a microplate reader. No-cell controls were used to determine assay background and the cell viability was calculated as a percentage of the control.

7.1.6. Quantification of stable reactive species

Hydrogen peroxide was determined for the selected conditions using the xylenol orange assay (Pierce Quantitative Peroxide Assay kit, Thermo Scientific, Germany) according to the manufacturer's protocol. Optical density was recorded at 595 nm (Tecan Infinite M200 Pro, Tecan) and the calibration curves determined using authentic hydrogen peroxide (0-150 μM H_2O_2, in triplicate).

Nitrite and nitrate were determined using a Dionex ICS 5000 ion chromatography system. After treatment, all the treated solutions were diluted threefold by adding ultra-pure water (MilliQ, MilliQ® Merck kGaA, Darmstadt, Germany) before injecting 10 μL onto an IonPac AS23 anion exchange column (2x250 mm, Thermo Fisher Scientific Inc., Waltham, USA). An isocratic mobile phase (4.5 mM Na_2CO_3/0.8 mM $NaHCO_3$) regime and 250 $\mu L min^{-1}$ flow rate was used. The analytes were detected by conductivity and UV detection (210 nm). The instrument was weekly calibrated using the Dionex 7-anions standard (Thermo Fisher Scientific).

7.1.7. Statistics

Values are expressed in terms of mean±SD of three independent experiments carried out at least in duplicates, except for viability assays in which the results were obtained after three independent experiments in sextuplicates. The statistical analysis of the differences was done with ANOVA using Excel, and it was recognized as * $p < 0.05$, ** $p < 0.01$ and *** $p < 0.005$.

7.2. Results

7.2.1. Determination of cysteine derivatives

A way to analyze the biochemistry of CAPs is to monitor the reactions between the species deposited into the treated liquid and small organic molecules, that can be used as chemical traps[240,243]. In this study, high-resolution MS was used to analyze cysteine modifications on a molecular level at different treatment times and gas admixtures. Cysteine is an amino acid with the chemical formula $C_3H_7NO_2S$ that is present in body fluids and cell culture media, e.g. DMEM. It is an important amino acid in proteins, since it undergoes reversible oxidation/reduction under biological conditions, controls proteins function and serves as a biomarker of oxidative damage[244,245]. Additionally, cysteine has shown a strong reactivity through RONS due to the presence of a thiol moiety in its structure[240,245,246]. All these characteristics make this amino acid an ideal model compound to compare and standardize plasma-discharges, since various covalent cysteine derivatives are produced by the impact of plasma-generated reactive species[247]. Moreover, unlike more complex models, like DNA, cysteine has the advantage that it contains each chemical group: amino ($R-NH_2$), carboxyl ($R-COOH$) and thiol ($R-SH$) only once, which enables a more detailed analysis of the modified groups[240,248].

Independently on the device and the working gas used, while in untreated cysteine samples only few signals of unmodified cysteine, its homo-dimer

cystine, and some minor impurities are found, after plasma treatments cysteine is consumed and subsequent production of its derivatives occurs. Table 7-1 shows details of the identified major cysteine derivatives.

Table 7-1 Most abundant compounds, and their respective chemical formula and mass-to-charge ratio.

Compound	Chemical formula	m/z
Cysteine	$C_3H_7NO_2S$	120.0119
Cystine	$C_6H_{12}N_2O_4S_2$	239.016
Cysteine sulfinic acid	$C_3H_7NO_4S$	152.0017
Cysteine sulfonic acid	$C_3H_7NO_5S$	149.0021

Regarding the kINPen09, most of the observed cysteine products include the oxygen dominant oxidation of the thiol group, with cystine and cysteine sulfonic acid being the most abundant derivatives produced after CAPs exposure, followed by cysteine sulfinic acid, which is in good agreement with previous experiments[239,243,248,249] and shows the oxidative nature of this jet device. This is also in accordance with the findings of Zhou et al., who have identified cystine and cysteine sulfonic acid as the major products resulting from cysteine oxidation due to plasma treatments[250].

The change in peak areas normalized to the control group (untreated cysteine solution) is represented in Figure 7.1, where it is visible that the major production of oxidized stable derivatives occurs for longer treatment times and preferably in the presence of oxygen in the used gas, with exception of cystine whose higher production was observed when pure argon was used.

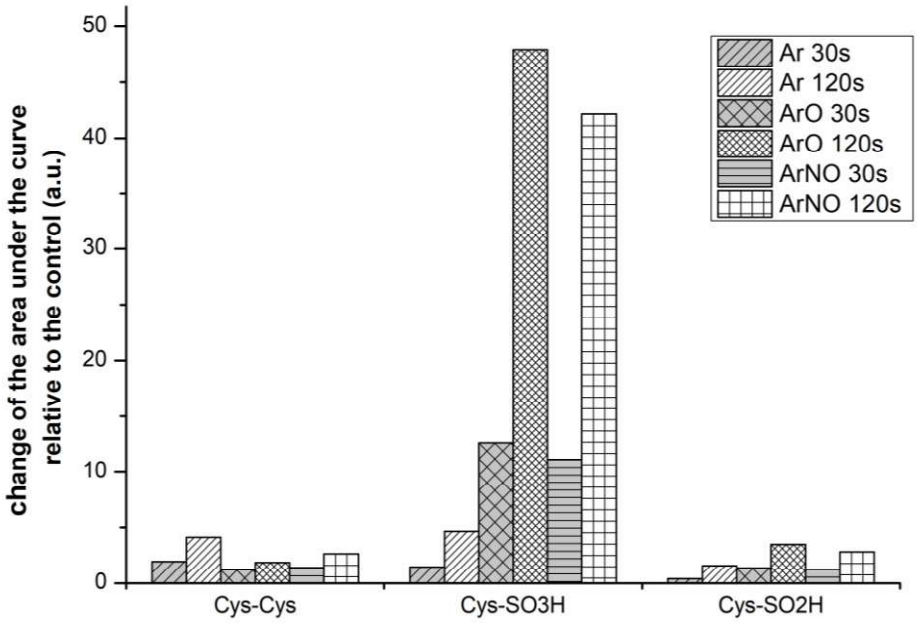

Figure 7.1 Relative quantities of prominent cysteine (Cys) derivates produced through different gas admixtures and treatment times, with focus on cystine (Cys-Cys), cysteine sulfonic acid (Cys-SO_3H) and cysteine sulfinic acid (Cys-SO_2H) using kINPen09.

Treating the cysteine solution with the developed jet (*Jet*) led to a lower oxidation of cysteine (Table A-1 of Appendix). Similarly, to what happens with kINPen09 the major consumption of cysteine occurs for longer treatment times and when oxygen is present in the working gas, as inferred from Figure 7.1. However, as can be observed in Figure 7.2, in the case of the developed jet the consumption of cysteine registered identical values when O_2 and N_2O_2 are admixed to the working gas. This may indicate that in the case of the *Jet*, both oxidation and nitrosylation of cysteine occur, with the plasma-derived nitrogen and oxygen species having a similar role in the effectiveness of plasma-treatments.

Comparing the results obtained for both plasma sources, it can be concluded that cysteine consumption was higher when treatments were performed with the kINPen09 (Table A-2 of Appendix), and for both jet devices, it was favored when using molecular gas admixtures. Interestingly, although cysteine sulfonic acid and cysteine sulfinic acid were detected in all the studied conditions, no traces of cysteine sulfenic acid, their precursor, were found, which

probably is due to its chemical instability. Cysteine sulfenic acid has one of the key roles in redox signaling, and it is rapidly oxidized to cysteine sulfinic acid and cysteine sulfonic acid[239,249]. Additionally, it may react with itself forming oxidized forms of cystine such as di-sulfoxides (m/z=271.0056), which was found for treatments performed with both set-ups but mostly, when kINPen09 was used (see Tables A-1 and A-2 of Appendix). To note, that besides the direct oxidation of cysteine, also the oxidation of cystine and its oxidized disulfides could generate cysteine sulfonic acid[251], which was found to be the most produced cysteine derivative for treatments performed with both studied devices.

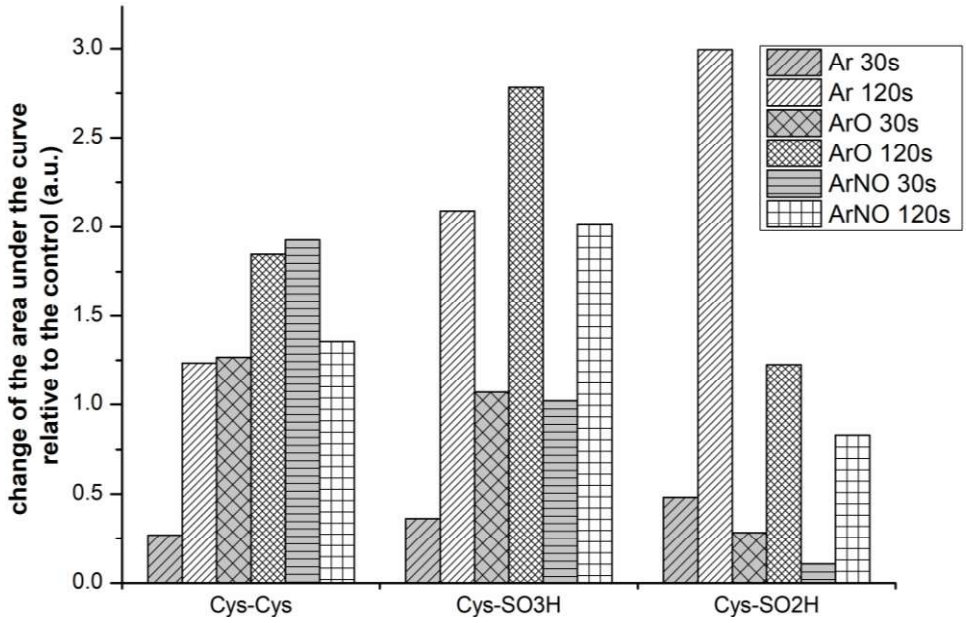

Figure 7.2 Relative quantities of prominent cysteine (Cys) derivates produced by using different gas admixtures and treatment times, with focus on cystine (Cys-Cys), cysteine sulfonic acid (Cys-SO3H) and cysteine sulfinic acid (Cys-SO2H) using the developed jet.

The reaction product S-nitrosocysteine was also found in some of the investigated conditions, as it can be observed in Figure 7.3, with its production increasing for longer treatment times. The appearance of this compound confirms the presence of RNS species, once it is a cysteine derivative in which the

sulfur atom carries a nitroso substituent (Figure 7.4) being formed as a product of S-nytrosilation[243,248].

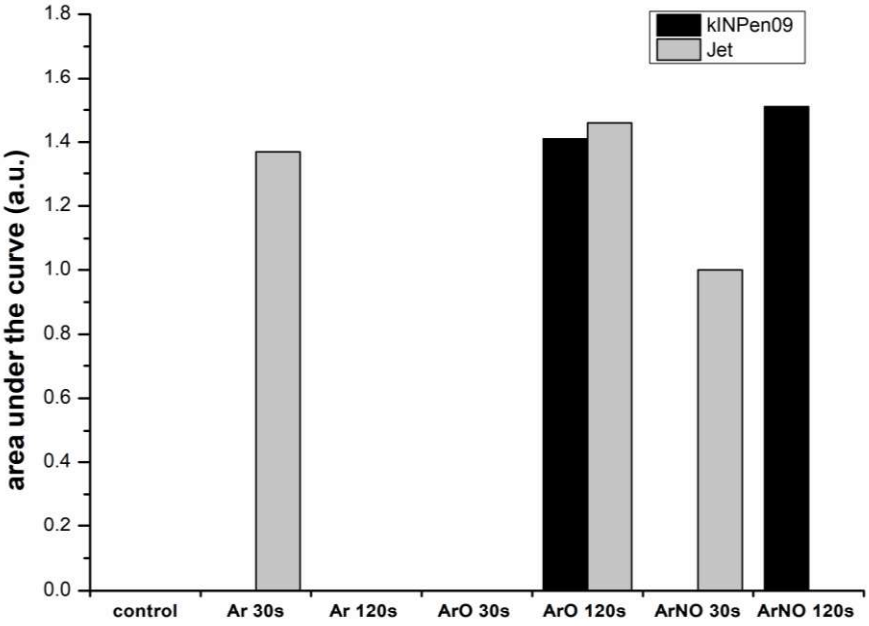

Figure 7.3 Relative quantities of the derivative S-nitrosocysteine produced by using different gas admixtures and treatment times, using kINPen09 and the developed jet (Jet).

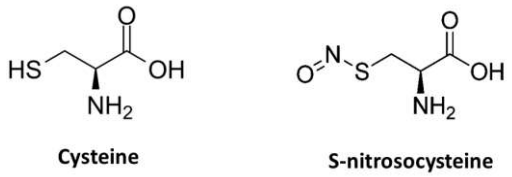

Figure 7.4 Structure representation of cysteine and S-nitrosocysteine

S-nitrosocysteine is known for having a role as hematologic agent, as an inhibitor of platelet aggregation and as a vasodilator agent. It also has a role in the nitric oxide pathway, that makes it essential in wound healing and cancer biology[249]. The Figure 7.3 shows its relative quantities for both set-ups. Although the oxidative modifications of the cysteine's thiol group were dominant, S-nitrosocysteine was only found in small quantities. This might be explained by the direct reaction of plasma-derived RNS species, which facilitate the oxidation but do not form covalent bonds between C or S and N[243,248].

Cysteine-S-sulfanate, an agonist of the NMDA (*N*-methyl-D-aspartate receptor), which the activation leads to calcium influx influencing further cell signaling[252], was also detected in all the analyzed samples including the untreated cysteine. Despite a small increase was registered while increasing plasma treatment time, its production is not significant when compared with the other referred derivatives (see Tables A-1 and A-2 of Appendix). This is an interesting result since the fact that both, cysteine-S-sulfanate and cystine, appeared as products of plasma-treated cysteine solutions, and therefore may indicate that sulfanation and the disulfide-bond formation occur at the same time[245].

In short, it could be seen that regardless of the treatment conditions, several products of cysteine and cystine were observed, which can be used as a fingerprint to identify different plasma sources, with cysteine sulfonic acid being a stable end-product of both devices investigated in this study.

7.2.2. Determination of phenol derivatives

Aromatic hydrocarbons include many organic compounds, such as phenol, that have been treated by different electrical discharge plasmas in gas-liquid environments. Despite that in most of these studies, the oxidation of phenol was achieved through reaction with hydroxyl radicals, phenol may also react at a slower rate by direct reactions with ozone, and with peroxynitrite[233,253]. For that reason, phenol is an adequate compound to try to evaluate the nitrosative profile of cold atmospheric devices.

After plasma exposure two different products resulting from phenol-oxidation, that were not found in untreated phenol solutions, were found in all the tested conditions and for both set-ups (*Jet* and kINPen09), namely, cis-cis-muconic acid and 2-nitrophenol. Muconic acid has been reported as a result of the oxidation mechanism by ozone through direct cleavage of the aromatic ring of phenol[254–256] as shown in Figure 7.5. While 2-nitrophenol is a result of the chemical reactions between phenol and NO (phenol nitration)[233,253]. A possible explanation for the production of 2-nitrophenol is related to the attack of NO_2^- or

$NO^{\cdot}$ radicals, through the formation of a phenoxy radical intermediate[221,241,257], as demonstrated in Figure 7.6. Nitrosation of phenol also occurs, resulting in the production of 4-nitrosophenol[242]. Uppu et al.[253] have reported this compound as the dominant product of the reaction between phenol and peroxynitrite at pH>8. In the case of the treated 0.3 mM phenol solution used in this study, it was prepared in a physiological buffer (pH 7.4) reason why the referred path is not so likely, with the 4-nitrosophenol product probably being a result from the interaction between the phenoxy radical intermediate and the nitric oxide radical, Figure 7.6.

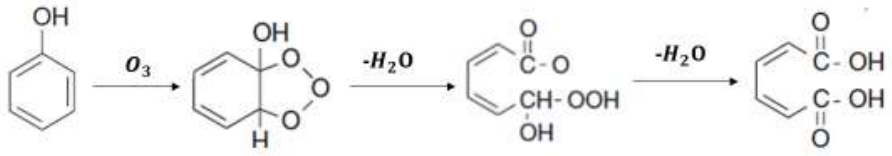

Figure 7.5 Mechanism of ozone attack on phenol ring forming muconic acid.

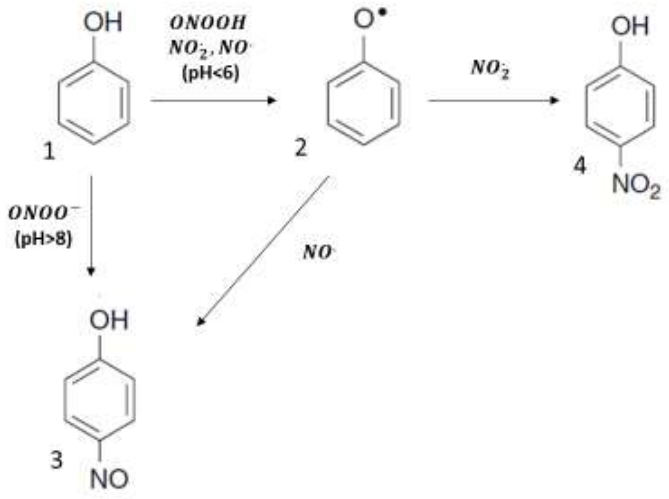

Figure 7.6 Nitration and nitrosation of phenol. 1 - Phenol, 2 -Phenoxy radical intermediate, 3 – 4-nitrosophenol, 4-2-nitrophenol.

The production of all the referred phenol degradation products increases as the time of plasma exposure increases and no apparent relation between the indicated products and the used working gas could be defined. These may be

due to the fact that these compounds are produced in the liquid phase and the influence of the nitrogen and oxygen present in the used working gas cannot be distinguished from that of the oxygen and nitrogen species present in the ambient air[233,258,259]. Moreover, this also helps to explain the appearance of some phenol derivatives such as oxi-phenol, hydroxy-phenol, and nitrosophenol in untreated solutions.

It must be noted that although both, 2-nitrophenol and 4-nitrosophenol, products of nitration and nitrosation of phenol, respectively, were found in treatments performed with both set-ups (see Tables A-3 and A-4 of Appendix), they were mostly produced when the *Jet* was used, which reinforces its nitrosative profile.

7.2.3. Long-lived species deposition in the presence of cysteine

To obtain an idea of the deposition of long-lived species in the presence of cysteine (0.3 mM), nitrite, nitrate, and H_2O_2 were quantified. To note that quantification of H_2O_2 in the presence of cysteine was only performed for the developed jet (*Jet*), since its characterization is the main focus of this work and this quantification was already performed for the kINPen09 with the results being extensively reported in the literature[239,248,249].

According to Figures 7.7 a) and b), which show the nitrite and nitrate profiles, respectively, it can be concluded that for both devices, regardless of the working gas used, the concentration of both species increases for longer treatment times.

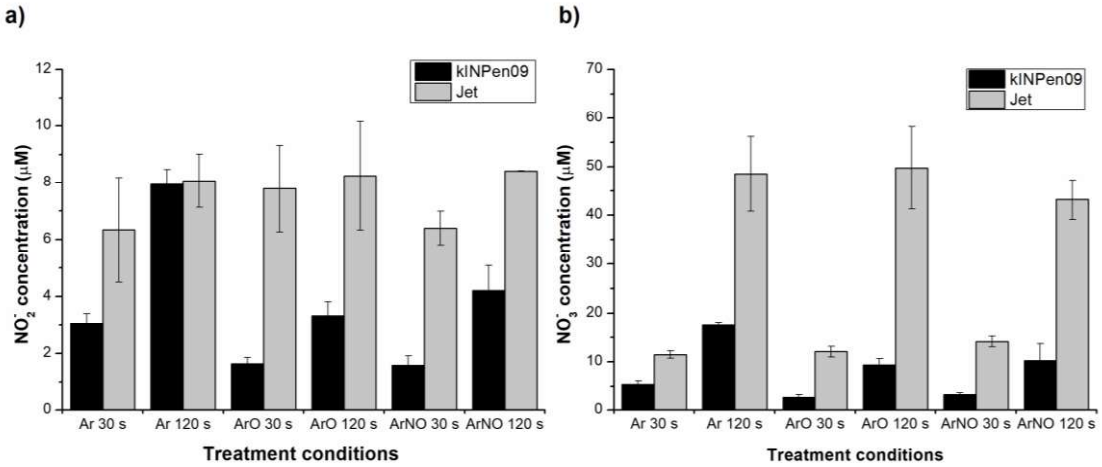

Figure 7.7 a) Nitrite deposition in phosphate buffer in the presence of cysteine. b) Nitrate deposition in phosphate buffer in the presence of cysteine, both using different gas admixtures and treatment times.

For the kINPen09, the working gas composition seems to have a slight impact on the variation of NO_2^- and NO_3^- deposition, with the maximal concentrations being found when pure argon is used.

In contrast, for treatments performed with the developed jet (*Jet*) the deposition of these long-lived species seems to be independent of the working gas used. Regarding nitrate, its deposition markedly increases for longer treated cysteine solutions. Despite this increase, biologically its effects may remain negligible, since no impact on cell proliferation can be observed up to a concentration of 250 µM[249].

One possible explanation for the relatively stable production of nitrite and nitrate may be the fact that these species are predominantly produced in the gas phase by the consumption of the molecular nitrogen and oxygen, and only then are dissolved into the liquid being treated[240]. After generation, further liquid chemistry will affect the final concentration of these species via secondary reactions using reactive nitrogen and oxygen species. For example, the deposited nitrite can contribute to the increase of nitrate concentration in the liquid phase. This occurs via the formation of peroxynitrite by H_2O_2 oxidation, and/or by disproportion, forming nitrogen dioxide (NO_2) and nitric oxide radical ($\cdot NO$)

with the subsequent disproportion of NO_2 and oxidation of $^{\cdot}NO$ by ambient air or CAPs derived oxygen species[243,248]. Moreover, nitrite itself can be directly oxidized to nitrate.

In Figures 7.8 a) and b), the results obtained for the quantification of H_2O_2 in the absence or presence of cysteine, respectively, after treatments performed using the *Jet* are presented. As it is reported for kINPen09[249], using the *Jet*, the H_2O_2 concentration in solution also increases as the treatment time increases, but no significant differences in its concentration were measured in the presence or not of cysteine, immediately after treatments. This is in accordance with the slow direct reaction of H_2O_2 with cysteine at physiological buffer pH[239,249,260]. As it was concluded before, the working gas composition has no effects on the deposition of H_2O_2 after treatments performed with the *Jet*.

Additionally, after one minute of treatment performed with both devices, using 3 slm of pure argon as gas flow, the deposition of H_2O_2 concentration in a physiological buffer solution without cysteine, was investigated. This condition was chosen since it was reported as the one in which the deposition of H_2O_2 is higher for treatments performed using kINPen09[261–263]. A concentration of 2.55±0.47 μM of H_2O_2 was measured for the *Jet*, while a concentration of 44.96±8.29 μM was determined when using kINPen09. These results reinforce the idea that kINPen09 has a more oxidative profile than the *Jet*.

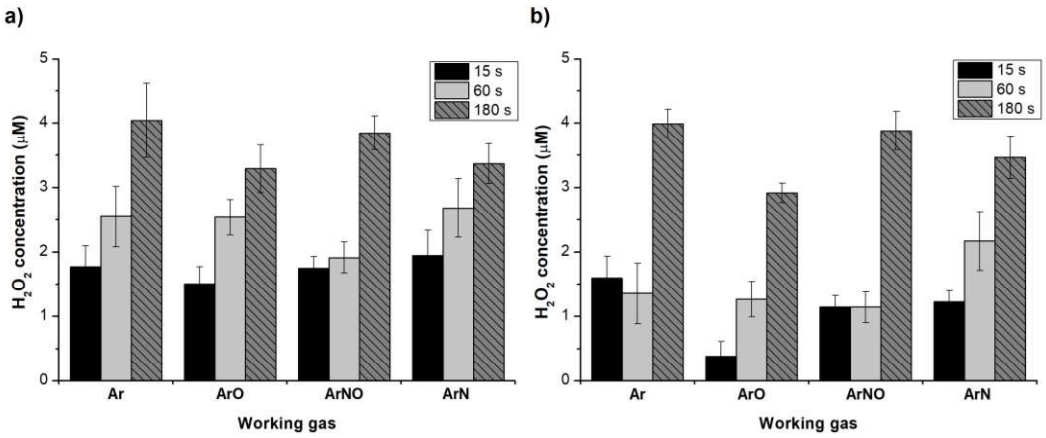

Figure 7.8 H_2O_2 deposition after treatments performed using the Jet in a) absence and b) presence of cysteine, both using different gas admixtures and treatment times.

7.2.4. Influence of plasma treatment on cell viability

In chapter 5 it was observed that the cold plasma produced by the developed jet induces killing-selectivity effects in skin cancer cells. These plasmas created by electrical discharges are a source of a vast number of reactive species that can affect eukaryotic cells through complex biochemical procedures[264]. Here, the effects of cold plasma treatments, performed using the *Jet* and the kINPen09, on Met-1, SCC-15, and HaCaT cells, using the same working parameters (gap, volume, treatment time) were analyzed. In Figure 7.9, the reduction on the cell viability of the referred cells compared to the control group (untreated cells) is registered. Comparing the results obtained using both set-ups, shown in Figures 7.9 a), c), and e) and Figures 7.9 b), d), and f), corresponding to treatments performed using the kINPen09 and the *Jet*, respectively, it seems to be clear that the effects of the plasma produced using the kINPen09 were strongly dependent on the working gas used, while the same does not happen for treatments performed with the *Jet*. A possible explanation for this could be related with the fact that in both set-ups the plasma is produced inside the device and only then driven to the outside. Although, in the case of the *Jet* the plasma is generated just at 2 mm of the opening for the exterior, with this opening being larger than the one observed in the kINPen09. Consequently, contrarily to what happens with the kINPen09, the plasma produced using the *Jet* is more influenced by the ambient air than by the admixtures used in the working gas.

By the analysis of the influence of the working gas on treatments performed using the kINPen09 (Figures 7.9 a), c), and e)), it could be noticed that its killing capacity was higher when pure argon or when small admixtures of oxygen were used. On the other hand, when nitrogen was admixed to the working gas a slight increase in cell viability was observed.

A reduction in cell viability as the treatment time increases has been witnessed for both studied jets, with the steepest reductions being observed when using kINPen09. For example, when treating SCC-15 cells, after a treatment time of 15 seconds using pure argon, the relative cell viability decreases for 0.75±0.19 (a.u.) using the *Jet*, as shown in Figure 7.9 d) and for 0.42±0.19 (a.u)

using kINPen09, Figure 7.9 c). When the time of treatment is increased for 60 seconds the relative cell viability decreases for 0.48±0.19 (a.u.), and 0.07±0.03 (a.u.), using the *Jet* and kINPen09, respectively. This could be explained by the oxidative dominant profile of kINPen09, while the *Jet* induces both oxidation and nitrosylation effects.

The Figure 7.9 also reflects the major vulnerability of cancer cells to CAPs treatment. Regarding the cancerous cells in study, the highest drop in cell viability was registered for SCC-15 cells for a treatment time of 60 seconds using kINPen09 with pure argon used as the feed gas. The lower viability of HaCaT cells was also registered in the referred condition.

All these results seem to indicate that the effects of the indirect plasma treatments are strongly dependent on the used device, reflecting the necessity to optimize the parameters chosen to perform the plasma treatments according to the cell line in study and the device. For example, in the case of this study, the working parameters used were the ones that conducted to a moderate cell response to treatments performed with the *Jet*, leading to a strong impact on cell survival using kINPen09. So, a compromise between all the variables and components involved in plasma treatments must be achieved.

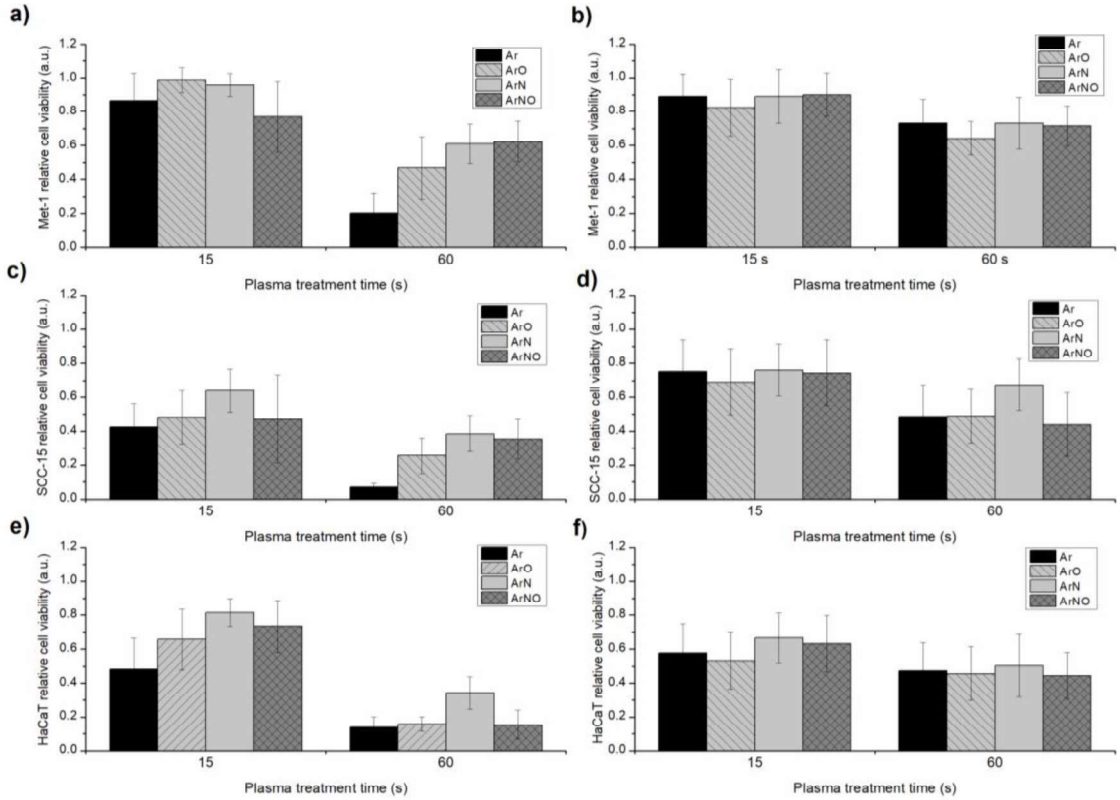

Figure 7.9 Relative cell viability by using different gas admixtures and treatment times of a) Met-1, c) SCC-15, and e) HaCaT for treatments performed using the kINPen09 and of b) Met-1, d) SCC-15, and f) HaCaT for treatments performed using the Jet.

7.3. Summary

Cold plasmas are of interest for the treatment of various medical conditions. Its use is being extensively reported for wound healing treatments, the treatment of pathogen-based and/or inflammatory skin irritation, and also in cancer therapy. In this last case, several reports have shown promising results as CAPs can interact with cancer cells by initializing programmed cell death in them, leading to the reduction of tumor size or even to its complete removal. These seem very promising results, as for example in case of large-scale tumor in which its complete removal is practically impossible, CAPs treatments can be used in combination with surgical tumor resections, by reducing the tumor size before its removal.

One of the biggest advantages of CAPs for biomedical applications is that its active components, as RNOS, are locally produced and can be easily tailored by alteration of the parameters used to perform the treatment (plasma source engineering) or simply by using a different plasma source. As was seen in this chapter, different plasma sources produce different ratios of ROS and RNS species, conducting to different results in which regards to the effects of treated liquids on cells. Small target molecules, such as cysteine, and phenol, are being pointed as target molecules that can act as a sensor system for the study of the plasma-induced chemistry in liquids. In this regard, in this study, it was decided to compare two plasma jet devices, that differ in terms of applied power and its type, in order to prove that these small molecules can be used as a fingerprint of a plasma device. According to the results presented in this chapter, it was apparent that both devices induce chemical modification, both in cysteine and phenol. The intensity of cysteine oxidation, for both devices, increased as the treatment duration increases, being favored when oxygen was admixed to the working gas used. A range of cysteine derivatives was identified for both jets, with cysteine-sulfonic acid being the most produced derivative in both cases. To note, that treatments performed with kINPen09 result in higher production of this derivative as well as higher consumption of cysteine. This indicates that both jets have an oxidative profile with the one of kINPen09 being more effective. S-nitrosocysteine was also found as a cysteine derivative, using both jets, confirming the presence of RNS.

The decomposition of phenol, especially through phenol nitration and nitrosation, was also successfully achieved with both jets, which allowed a better understanding of the chemistry of RNS species. These results indicate that the *Jet* has a RNS chemistry more active than the kINPen09. This seems to be in accordance, with the IC results, which indicate that both, the concentrations of nitrite and nitrate, are higher in liquids treated using the *Jet*. Oppositely, kINPen09 generates higher concentrations of H_2O_2.

Regarding the *in vitro* treatments, it was shown that both devices are effective in killing cancer cells, with the obtained results reinforcing the oxidative

dominant profile of the kINPen09, while the *Jet* seemed to induce both nitrosylation and oxidation resulting in more moderate effects of CAPs application on cells.

Briefly, the plasma effects are strongly related not only with the working parameters but also with the device used to perform the treatments. Small molecules can be successfully used to compare the plasma-chemistry induced in liquids produced by different devices. All these results must be carefully considered, since they point out that when translating these observations to *in vivo* treatments, the application of these plasmas can lead to stronger oxidation of protein thiol groups with subsequent changes in protein biochemistry.

8

Concluding remarks and perspectives of future work

In this section, it is intended to summarize the main conclusions of this thesis and present some perspectives of future work.

8.1. Conclusions

The work of the present thesis was focused on the development and optimization of a cold atmospheric plasma jet device (*Jet*), having as its ultimate aim the study of the interactions between living cells and the generated plasma. In this sense, human skin cancer and non-cancer cells were indirectly treated by the developed *Jet*.

The first part of the work of this thesis consisted in the development of the jet device and of the power supply to which it is connected. As it was shown in chapter 4, the developed jet consists of a hand-held principal unit composed of a borosilicate capillary with an outer diameter of 6.93 mm and an inner diameter of 4.94 mm, with a stainless-steel electrode in its center and a copper ring around it. The copper ring is connected to the developed DC high voltage power supply (20 mA, 20 kV), and usually operates at an argon flow of 3 slm. After the complete

development of the *Jet*, it was necessary to evaluate the conditions that allowed the induction of moderate plasma effects on cells. Based on the obtained results it was found that moderate CAPs effects were achieved using a gap of 7 mm, for treating a volume of 2 mL of medium, from which only 100 μL were transferred to the wells where cells were previously cultured. It was also observed that the plasma effects are time-dependent. At the time of these results, it was already proven that SCC-15 and Met-1 cells (cancer cell lines) are more susceptible to CAPs treatments than HGF-1 (a non-cancer cell line), with a treatment time of 2 minutes being able to reduce SCC-15 and Met-1 cells viability for less than 50%, while the same reduction in HGF-1 cells only was found after 9 minutes of plasma exposure.

Regarding the gas-phase of the plasma produced using the *Jet*, it was observed that when pure argon was used as the working gas, only hydroxyl radicals, nitrogen and argon species were detected by the OES analysis of the gas-phase plasma. While, when small admixtures of O_2, N_2, and N_2O_2 were used also nitric oxide, whose emission occurs in the UV-C range, starts to be produced. Interestingly, the addition of molecular gases does not lead to significant differences in the interaction between the cells and CAPs treated medium. This probably happens due to the strong influence of the atmospheric air in the generated plasma, with interactions between the produced plasma and the atmospheric air constantly occurring. Additionally, the mechanisms of cell death were investigated being found that in the chosen conditions, CAPs are mainly inducing the death of cancer cells by apoptosis. It was also observed that the number of SCC-15 and Met-1 cells in late apoptosis and necrosis increases as the plasma exposure increases. Correlating this finding with the biologically relevant reactive species that were identified in treated medium, it could be pointed that CAPs treatment are driving to apoptosis through oxidative and nitrosative stress, due the high concentration of ROS and RNS species that are formed in the plasma-liquid interactions. The species identified in the liquid phase include mostly long-lived reactive species, namely hydrogen peroxide, nitrite, nitrate, and also the short-lived species peroxynitrite. The concentration of hydrogen

peroxide, which has a key role in the oxidative stress and that is cytotoxic at higher concentrations, was found to increase as the treatment time increases. Although, the response of cells to H_2O_2 solutions is different from the one observed in the presence of CAPs treated medium. This reinforces the idea that even though H_2O_2 has a key role in the induction of oxidative stress and apoptosis induced by CAPs treatments it is not acting alone. Furthermore, the concentration of nitrate was found to increase for higher plasma treatment times, while the one of nitrite decreases.

Besides the developed *Jet* also the well-known kINPen09 was studied in this work. To note, that the referred jets differ in the applied power and its type. It was observed that using the same working parameters (gap, volume of liquid, cell concentration) the effects of kINPen09 are more toxic to cells than the ones of the *Jet*, with higher concentrations of ROS being produced, including H_2O_2. This draws attention to the fact that the conditions used to perform the treatments must be chosen in function of the utilized device, since the same parameters will result in different effects depending on the used source. Moreover, also the treated liquid and cell lines must be taken into account when choosing the treatment conditions.

In the last part of this work, in order to prove that the CAPs effects are dependent on the used plasma source the cysteine was investigated as a target molecule, acting as a sensor system for the study of the plasma chemistry induced by two different CAPs sources (kINPen09, and *Jet*), in liquids. It was observed that both jets led to chemical modifications in cysteine, with cysteine oxidation being favored as the CAPs exposure increases, especially in the presence of oxygen. Cysteine-sulfonic acid was the oxidation product most found after treatments performed with both devices, being found in higher concentrations in liquids treated with the kINPen09. This is in accordance with the quantification of H_2O_2, whose concentration was also higher in liquids treated by kINPen09. Together these results prove the stronger oxidative profile of kINPen09 in comparison to the *Jet*. Besides cysteine-sulfonic acid, S-nitrosocysteine was also detected when using the cysteine model, confirming the

presence of RNS species. This species was achieved in higher concentrations in liquids treated using the *Jet*, indicating that it has a more nitrosative profile than kINPen09.

To confirm the nitrosative profile also the degradation of phenol was evaluated, and it was revealed that it occurs mostly by phenol nitration and nitrosation, being higher when the *Jet* was used.

In sum, all these results highlight to the high importance of the CAPs generated reactive species in cellular biology, with the key roles being attributed to long-lived species, such as H_2O_2, nitrate and nitrite. All of them, constitute species of high importance in essential biological mechanisms, such as oxidative stress, mitochondrial metabolism, and cell signaling.

8.2. Future work perspectives

Looking ahead, more studies need to be done to fully understand the mechanisms behind cell-plasma treated liquids interactions and the plasma-liquid interactions.

Regarding the characterization of the plasma plume some suggestions for future work are:

- Perform a qualitative investigation of the plasma discharge during indirect treatments by means of high-speed (HS) and iCCD imaging;
- Study the influence of the ambient air humidity in the generated plasma;
- Perform absorption measurements for the determination of the particle densities;
- Investigate the temperature of gas-phase plasma.

Concerning the experiments to carried out in cells it would be interesting:

- Try to measure the levels of glutathione mitochondrial membrane depolarization, the caspase-3 activation, the DNA fragmentation and the

exposure of phosphatidylserine, in order to prove the induction of the intrinsic apoptotic pathway;

- Study the cellular oxidation, for example, by incubation of the cells with redox-sensitive probes;
- Study possible changes in cell proliferation and morphology after plasma exposure;
- Study the intracellular ROS and RNS generation;
- Perform western blot analysis for identification of changes in protein expression after plasma exposure.

Additionally, in terms of liquid characterization it would be interesting to use Electron Paramagnetic Resonance Spectroscopy (EPR) to identify short-life species as hydroxyl radical, superoxide anion, singlet oxygen, nitric oxide radical, peroxynitrite, among others.

In vivo studies are also essential to better understand the effects of CAPs on living cells.

8.3. Developed work

8.3.1. Chapters in books

- **Pereira S**., Pinto É., Ribeiro P.A., Sério S. (2020) Non-thermal Atmospheric Pressure Plasmas: Generation, Sources and Applications. In: Raposo M., Ribeiro P., Sério S., Staiano A., Ciaramella A. (eds) Computational Intelligence Methods for Bioinformatics and Biostatistics. CIBB 2018. Lecture Notes in Computer Science, vol 11925. Springer, Cham, Pages 309-318. DOI: 10.1007/978-3-030-34585-3_28;
- **S. Pereira**, P. A. Ribeiro and S. Sério, **Study of a Cold Atmospheric Pressure Plasma jet device for indirect treatment of Squamous Cell Carcinoma**. *in* Clinical Plasma Medicine, (2019), Vol. 13, Pages 9-14. DOI: 10.1016/j.cpme.2018.09.001

8.3.2. Papers in international scientific periodicals with referees

- **S. Pereira**, P. A. Ribeiro and S. Sério**, Optimization of a Cold Atmospheric plasma treatment to selectively affect the viability of skin cancer cells**, (2020), Pages 201-208. DOI: 10.5220/0009373802010208

8.3.3. International peer-reviewed publications in Conference Proceedings

- **S. Pereira**, P. A. Ribeiro and S. Sério**, "Optimization of a Cold Atmospheric plasma treatment to selectively affect the viability of skin cancer cells"**, in 8th international conference in photonics, optics and laser technology, in Valletta, Malta, 27-29 February 2020;
- **S. Pereira**, E. Pinto, P. A. Ribeiro, S. Sério. Poster "**Development and characterization of DC Argon Plasma Jet Device**", at Rabbit Café at NOVA Biophysica, Lisbon, Portugal, 4 September 2019;
- **S. Pereira**, E. Pinto, P. A. Ribeiro and S. Sério, "**Non-thermal atmospheric pressure plasma: generation, sources and applications"**. *in* 15th International Conference on Computational Intelligence methods for Bioinformatics and Biostatistics FCT/UNL, Caparica, Portugal, 6-8 September 2018;
- **S. Pereira**, P. A. Ribeiro and S. Sério, **"Cold Atmospheric Plasmas for Biomedical Applications",** 6th Young Professionals Workshop on Plasma Medicine, in Rostock, Germany, 23-26 October 2017.

8.3.4. Poster communications

- **S. Pereira**, E. Pinto, P. A. Ribeiro, S. Sério. Poster "**Development and characterization of DC Argon Plasma Jet Device**", at NOVA Biophysica, Lisbon, Portugal, 4-6 September 2019.
- **S. Pereira**, E. Pinto, P. A. Ribeiro, S. Sério. Poster "**Study of CAPs treated medium as an in-vitro anti-cancer therapy**", at 3rd NOVA Biomedical Engineering workshop, FCT/UNL, Caparica, Portugal, 9 May 2018;
- E. Pinto, **S. Pereira**, P. A. Ribeiro, S. Sério. Poster "**Development of a Cold Atmospheric Plasma Jet Device for Medical Applications**", at 3rd NOVA

Biomedical Engineering workshop, FCT/UNL, Caparica, Portugal, 9 May 2018;

- J. Brás, **S. Pereira**, P. A. Ribeiro, S. Sério. Poster "**Floating Electrode Dielectric Barrier Discharge for the Treatment of Squamous Cell Carcinoma**", at 3rd NOVA Biomedical Engineering workshop, FCT/UNL, Caparica, Portugal, 9 May 2018;
- **S. Pereira**, E. Pinto, P. A. Ribeiro, S. Sério. Poster "**Development and characterization of a custom-made Argon Plasma Jet Device for medical application**", at EUSpec Cost Action MP1306: Modern Tools for Spectroscopy on Advanced Materials, Final Whole Action Meeting in Lisbon, Caparica, Portugal, 18-22 February 2018;
- **S. Pereira**, P. A. Ribeiro, S. Sério. Poster "**Study the effects of CAPs on skin cells**", at 2nd NOVA Biomedical Engineering workshop, FCT/UNL, Caparica, Portugal, 3 May 2017.

9

References

1. Graham, G. F. & Tuchayi, S. M. Squamous cell carcinoma. in *Dermatological Cryosurgery and Cryotherapy* (2016). doi:10.1007/978-1-4471-6765-5_131
2. Waldman, A. & Schmults, C. Cutaneous Squamous Cell Carcinoma. *Hematology/Oncology Clinics of North America* (2019). doi:10.1016/j.hoc.2018.08.001
3. Miller, D. L. & Weinstock, M. A. Nonmelanoma skin cancer in the United States: Incidence. *J. Am. Acad. Dermatol.* (1994). doi:10.1016/S0190-9622(08)81509-5
4. Brandt, M. G. & Moore, C. C. Nonmelanoma Skin Cancer. *Facial Plastic Surgery Clinics of North America* (2019). doi:10.1016/j.fsc.2018.08.001
5. Apalla, Z., Lallas, A., Sotiriou, E., Lazaridou, E. & Ioannides, D. Epidemiological trends in skin cancer. *Dermatol. Pract. Concept.* (2017). doi:10.5826/dpc.0702a01
6. Weltmann, K. D. & Von Woedtke, T. Plasma medicine - Current state of research and medical application. *Plasma Phys. Control. Fusion* (2017). doi:10.1088/0741-3335/59/1/014031
7. Keidar, M. *et al.* Cold atmospheric plasma in cancer therapy. *Phys. Plasmas* **20**, 057101 (2013).
8. Stoffels, E., Flikweert, A. J., Stoffels, W. W. & Kroesen, G. M. W. Plasma needle: a non-destructive atmospheric plasma source for fine surface treatment of (bio)materials. *Plasma Sources Sci. Technol.* **11**, 383–388 (2002).
9. Keidar, M. Plasma for cancer treatment. *Plasma Sources Sci. Technol.* **24**,

033001 (2015).

10. Crookes, W. On radiant matter. *J. Franklin Inst.* (1879). doi:10.1016/0016-0032(79)90319-3

11. Langmuir, I. Oscillations in Ionized Gases. *Proc. Natl. Acad. Sci.* (1928). doi:10.1073/pnas.14.8.627

12. Burm, K. T. A. L. Plasma: The fourth state of matter. *Plasma Chem. Plasma Process.* (2012). doi:10.1007/s11090-012-9356-1

13. Stoffels, E., Sakiyama, Y. & Graves, D. B. Cold atmospheric plasma: Charged species and their interactions with cells and tissues. *IEEE Trans. Plasma Sci.* (2008). doi:10.1109/TPS.2008.2001084

14. Hoffmann, C., Berganza, C. & Zhang, J. Cold Atmospheric Plasma: methods of production and application in dentistry and oncology. *Med. Gas Res.* **3**, 21 (2013).

15. Ohnuma, T. FUNDAMENTALS OF PLASMAS. in *Radiation Phenomena in Plasmas* 1–18 (WORLD SCIENTIFIC, 1994). doi:10.1142/9789814354035_0001

16. Fridman, A. *Plasma Chemistry*. *Plasma Chemistry* (Cambridge University Press, 2008). doi:10.1017/CBO9780511546075

17. Graves, D. B. The emerging role of reactive oxygen and nitrogen species in redox biology and some implications for plasma applications to medicine and biology. *Journal of Physics D: Applied Physics* (2012). doi:10.1088/0022-3727/45/26/263001

18. Helmke, A., Gerling, T. & Weltmann, K. D. Plasma sources for biomedical applications. in *Comprehensive Clinical Plasma Medicine: Cold Physical Plasma for Medical Application* (2018). doi:10.1007/978-3-319-67627-2_2

19. Fridman, G. *et al.* Applied Plasma Medicine. *Plasma Process. Polym.* **5**, 503–533 (2008).

20. Bárdos, L. & Baránková, H. Cold atmospheric plasma: Sources, processes, and applications. *Thin Solid Films* **518**, 6705–6713 (2010).

21. Morfill, G. E., Kong, M. G. & Zimmermann, J. L. Focus on plasma medicine. *New J. Phys.* (2009). doi:10.1088/1367-2630/11/11/115011

22. von Woedtke, T., Reuter, S., Masur, K. & Weltmann, K.-D. Plasmas for medicine. *Phys. Rep.* **530**, 291–320 (2013).

23. Laroussi, M., Kong, M., Morfill, G. & Stolz, W. *Plasma Medicine*. *Plasma Medicine: Applications of Low-temperature Gas Plasmas in Medicine and Biology* (Cambridge University Press, 2012). doi:10.1017/CBO9780511902598

24. Staack, D., Farouk, B., Gutsol, A. & Fridman, A. Characterization of a dc atmospheric pressure normal glow discharge. *Plasma Sources Sci. Technol.* (2005). doi:10.1088/0963-0252/14/4/009

25. Bruggeman, P. *et al.* Characterization of a direct dc-excited discharge in water by optical emission spectroscopy. *Plasma Sources Sci. Technol.* **18**, 025017 (2009).

26. Machala, Z. *et al.* Emission spectroscopy of atmospheric pressure plasmas for bio-medical and environmental applications. *J. Mol. Spectrosc.* (2007). doi:10.1016/j.jms.2007.03.001

27. Lisovskiy, V. A., Yakovin, S. D. & Yegorenkov, V. D. Low-pressure gas breakdown in uniform dc electric field. *J. Phys. D. Appl. Phys.* **33**, 2722–2730 (2000).

28. R., E. Electricity in Gases. *Nature* (1915). doi:10.1038/095611a0

29. Oppermann, R. H. Gaseous conductors, theory and engineering applications. *J. Franklin Inst.* (1942). doi:10.1016/s0016-0032(42)90330-2

30. Fridman, A., Chirokov, A. & Gutsol, A. Non-thermal atmospheric pressure discharges. *J. Phys. D. Appl. Phys.* **38**, R1–R24 (2005).

31. Meek, J. M. A theory of spark discharge. *Phys. Rev.* (1940). doi:10.1103/PhysRev.57.722

32. Krishnavedala: (https://commons.wikimedia.org/wiki/File:Paschen_curves.svg), https://creativecommons.org/licenses/by-sa/4.0/legalcode

33. Laroussi, M. Plasma Medicine: A Brief Introduction. *Plasma* **1**, 47–60 (2018).

34. Gweon, B., Kim, K., Choe, W. & Shin, J. H. Therapeutic Uses of Atmospheric Pressure Plasma: Cancer and Wound. in *Biomedical Engineering: Frontier Research and Converging Technologies* 357–385 (2016). doi:10.1007/978-3-319-21813-7_15

35. Daeschlein, G. *et al.* In Vitro Susceptibility of Important Skin and Wound Pathogens Against Low Temperature Atmospheric Pressure Plasma Jet (APPJ) and Dielectric Barrier Discharge Plasma (DBD). *Plasma Process. Polym.* **9**, 380–389 (2012).

36. Balzer, J. *et al.* Non-Thermal Dielectric Barrier Discharge (DBD) effects on proliferation and differentiation of human fibroblasts are primary mediated by hydrogen peroxide. *PLoS One* (2015). doi:10.1371/journal.pone.0144968

37. Weltmann, K. D. *et al.* Atmospheric pressure plasma jet for medical

therapy: Plasma parameters and risk estimation. *Contrib. to Plasma Phys.* (2009). doi:10.1002/ctpp.200910067

38. Reuter, S. *et al.* Detection of ozone in a MHz argon plasma bullet jet. *Plasma Sources Sci. Technol.* (2012). doi:10.1088/0963-0252/21/3/034015

39. Reuter, S., von Woedtke, T. & Weltmann, K.-D. The kINPen—a review on physics and chemistry of the atmospheric pressure plasma jet and its applications. *J. Phys. D. Appl. Phys.* **51**, 233001 (2018).

40. Arndt, S., Schmidt, A., Karrer, S. & von Woedtke, T. Comparing two different plasma devices kINPen and Adtec SteriPlas regarding their molecular and cellular effects on wound healing. *Clinical Plasma Medicine* (2018). doi:10.1016/j.cpme.2018.01.002

41. Pipa, A. V., Reuter, S., Foest, R. & Weltmann, K.-D. Controlling the NO production of an atmospheric pressure plasma jet. *J. Phys. D. Appl. Phys.* **45**, 085201 (2012).

42. Hoentsch, M., Von Woedtke, T., Weltmann, K. D. & Barbara Nebe, J. Time-dependent effects of low-temperature atmospheric-pressure argon plasma on epithelial cell attachment, viability and tight junction formation in vitro. *J. Phys. D. Appl. Phys.* (2012). doi:10.1088/0022-3727/45/2/025206

43. Garate, E. *et al.* Atmospheric plasma induced sterilization and chemical neutralization. in *IEEE International Conference on Plasma Science* (1998). doi:10.1109/plasma.1998.677654

44. Bekeschus, S., Schmidt, A., Weltmann, K. D. & von Woedtke, T. The plasma jet kINPen – A powerful tool for wound healing. *Clin. Plasma Med.* (2016). doi:10.1016/j.cpme.2016.01.001

45. Arjunan, K. P. & Clyne, A. M. Non-thermal dielectric barrier discharge plasma induces angiogenesis through reactive oxygen species. in *Proceedings of the Annual International Conference of the IEEE Engineering in Medicine and Biology Society, EMBS* (2011). doi:10.1109/IEMBS.2011.6090680

46. Ngo, M. H. T., Liao, J. Der, Shao, P. L., Weng, C. C. & Chang, C. Y. Increased fibroblast cell proliferation and migration using atmospheric N2/Ar micro-plasma for the stimulated release of fibroblast growth factor-7. *Plasma Process. Polym.* (2014). doi:10.1002/ppap.201300098

47. Arndt, S. *et al.* Cold atmospheric plasma (CAP) changes gene expression of key molecules of the wound healing machinery and improves wound healing in vitro and in vivo. *PLoS One* (2013). doi:10.1371/journal.pone.0079325

48. Dobrynin, D., Wasko, K., Friedman, G., Fridman, A. A. & Fridman, G. Cold

Plasma Sterilization of Open Wounds: Live Rat Model. *Plasma Med.* **1**, 109–114 (2011).

49. Dobrynin, D. *et al.* Live pig skin tissue and wound toxicity of cold plasma treatment. *Plasma Med.* (2011). doi:10.1615/PlasmaMed.v1.i1.80

50. García-Alcantara, E. *et al.* Accelerated mice skin acute wound healing in vivo by combined treatment of argon and helium plasma needle. *Arch. Med. Res.* (2013). doi:10.1016/j.arcmed.2013.02.001

51. Kramer, A. *et al.* Suitability of tissue tolerable plasmas (TTP) for the management of chronic wounds. *Clinical Plasma Medicine* (2013). doi:10.1016/j.cpme.2013.03.002

52. Martines, E. *et al.* A novel plasma source for sterilization of living tissues. *New J. Phys.* **11**, 115014 (2009).

53. Keidar, M. *et al.* Cold plasma selectivity and the possibility of a paradigm shift in cancer therapy. *Br. J. Cancer* **105**, 1295–1301 (2011).

54. Arndt, S. *et al.* Cold atmospheric plasma, a new strategy to induce senescence in melanoma cells. *Exp. Dermatol.* (2013). doi:10.1111/exd.12127

55. Yan, D. *et al.* The Specific Vulnerabilities of Cancer Cells to the Cold Atmospheric Plasma-Stimulated Solutions. *Sci. Rep.* (2017). doi:10.1038/s41598-017-04770-x

56. Ahn, H. J. *et al.* Targeting Cancer Cells with Reactive Oxygen and Nitrogen Species Generated by Atmospheric-Pressure Air Plasma. *PLoS One* **9**, e86173 (2014).

57. Joh, H. M., Choi, J. Y., Kim, S. J., Chung, T. H. & Kang, T.-H. Effect of additive oxygen gas on cellular response of lung cancer cells induced by atmospheric pressure helium plasma jet. *Sci. Rep.* **4**, 6638 (2015).

58. Lee, S. Y. *et al.* Nonthermal Plasma Induces Apoptosis in ATC Cells: Involvement of JNK and p38 MAPK-Dependent ROS. *Yonsei Med. J.* **55**, 1640 (2014).

59. Volotskova, O., Hawley, T. S., Stepp, M. A. & Keidar, M. Targeting the cancer cell cycle by cold atmospheric plasma. *Sci. Rep.* (2012). doi:10.1038/srep00636

60. Bartek, J., Lukas, C. & Lukas, J. Checking on DNA damage in S phase. *Nature Reviews Molecular Cell Biology* (2004). doi:10.1038/nrm1493

61. Kastan, M. B. & Bartek, J. Cell-cycle checkpoints and cancer. *Nature* (2004). doi:10.1038/nature03097

62. Segurado, M. & Tercero, J. A. The S-phase checkpoint: targeting the

replication fork. *Biol. Cell* (2009). doi:10.1042/bc20090053

63. Nasruddin *et al.* Cold plasma on full-thickness cutaneous wound accelerates healing through promoting inflammation, re-epithelialization and wound contraction. *Clin. Plasma Med.* (2014). doi:10.1016/j.cpme.2014.01.001

64. Vandamme, M. *et al.* Response of human glioma U87 xenografted on mice to non thermal plasma treatment. *Plasma Med.* (2011). doi:10.1615/PlasmaMed.v1.i1.30

65. Yajima, I. *et al.* Non-equilibrium atmospheric pressure plasmas modulate cell cycle-related gene expressions in melanocytic tumors of RET-transgenic mice. *Exp. Dermatol.* (2014). doi:10.1111/exd.12415

66. El-Aouar Filho, R. A. *et al.* Heterogeneous family of cyclomodulins: Smart weapons that allow bacteria to hijack the eukaryotic cell cycle and promote infections. *Frontiers in Cellular and Infection Microbiology* (2017). doi:10.3389/fcimb.2017.00208

67. Heinlin, J. *et al.* Randomized placebo-controlled human pilot study of cold atmospheric argon plasma on skin graft donor sites. in *Wound Repair and Regeneration* (2013). doi:10.1111/wrr.12078

68. Lademann, O. *et al.* Antisepsis of the follicular reservoir by treatment with tissue-tolerable plasma (TTP). *Laser Phys. Lett.* **8**, 313–317 (2011).

69. Noori, S. An Overview of Oxidative Stress and Antioxidant Defensive System. *J. Clin. Cell. Immunol.* (2012). doi:10.4172/scientificreports.413

70. Sies, H. Oxidative stress: oxidants and antioxidants. *Exp. Physiol.* **82**, 291–295 (1997).

71. Apel, K. & Hirt, H. REACTIVE OXYGEN SPECIES: Metabolism, Oxidative Stress, and Signal Transduction. *Annu. Rev. Plant Biol.* (2004). doi:10.1146/annurev.arplant.55.031903.141701

72. Zhang, J. *et al.* ROS and ROS-Mediated Cellular Signaling. *Oxidative Medicine and Cellular Longevity* (2016). doi:10.1155/2016/4350965

73. Sosa, V. *et al.* Oxidative stress and cancer: An overview. *Ageing Research Reviews* (2013). doi:10.1016/j.arr.2012.10.004

74. Son, Y. *et al.* Mitogen-Activated Protein Kinases and Reactive Oxygen Species: How Can ROS Activate MAPK Pathways? *J. Signal Transduct.* (2011). doi:10.1155/2011/792639

75. Son, Y., Kim, S., Chung, H. T. & Pae, H. O. Reactive oxygen species in the activation of MAP kinases. in *Methods in Enzymology* (2013).

doi:10.1016/B978-0-12-405881-1.00002-1

76. Halliwell, B. & Gutteridge, J. M. C. Free radicals in biology and medicine, second edition. *Free Radic. Biol. Med.* **10**, 449–450 (1991).

77. Kohen, R. & Nyska, A. Oxidation of biological systems: Oxidative stress phenomena, antioxidants, redox reactions, and methods for their quantification. *Toxicologic Pathology* (2002). doi:10.1080/01926230290166724

78. Kalghatgi, S. U. Mechanisms of interaction of non-thermal plasma with living cells. *ProQuest Diss. Theses* (2010).

79. Matés, J. M., Segura, J. A., Alonso, F. J. & Márquez, J. Intracellular redox status and oxidative stress: Implications for cell proliferation, apoptosis, and carcinogenesis. *Archives of Toxicology* (2008). doi:10.1007/s00204-008-0304-z

80. Mushtaq, B. Wound Healing. *Nurs. Heal. Care* 41–41 (2018). doi:10.33805/2573.3877.115

81. Sen, C. K. & Roy, S. Redox signals in wound healing. *Biochimica et Biophysica Acta - General Subjects* (2008). doi:10.1016/j.bbagen.2008.01.006

82. Wlaschek, M. & Scharffetter-Kochanek, K. Oxidative stress in chronic venous leg ulcers. *Wound Repair and Regeneration* (2005). doi:10.1111/j.1067-1927.2005.00065.x

83. D'Autréaux, B. & Toledano, M. B. ROS as signalling molecules: Mechanisms that generate specificity in ROS homeostasis. *Nature Reviews Molecular Cell Biology* (2007). doi:10.1038/nrm2256

84. Dan Dunn, J., Alvarez, L. A. J., Zhang, X. & Soldati, T. Reactive oxygen species and mitochondria: A nexus of cellular homeostasis. *Redox Biology* (2015). doi:10.1016/j.redox.2015.09.005

85. Zorov, D. B., Juhaszova, M. & Sollott, S. J. Mitochondrial Reactive Oxygen Species (ROS) and ROS-Induced ROS Release. *Physiol. Rev.* **94**, 909–950 (2014).

86. Lisanti, M. P. *et al.* Hydrogen peroxide fuels aging, inflammation, cancer metabolism and metastasis: The seed and soil also needs 'fertilizer'. *Cell Cycle* (2011). doi:10.4161/cc.10.15.16870

87. N, A. Cell Injury, Cell Death and Adaptations. in *Synopsis of Pathology* 1–1 (Jaypee Brothers Medical Publishers (P) Ltd., 2013). doi:10.5005/jp/books/11992_1

88. Birben, E., Sahiner, U. M., Sackesen, C., Erzurum, S. & Kalayci, O. Oxidative stress and antioxidant defense. *World Allergy Organization*

Journal (2012). doi:10.1097/WOX.0b013e3182439613

89. Lee, H.-Y. *et al.* Targeted Expression of Catalase to Mitochondria Prevents Age-Associated Reductions in Mitochondrial Function and Insulin Resistance. *Cell Metab.* **12**, 668–674 (2010).

90. Spitz, D. R., Azzam, E. I., Li, J. J. & Gius, D. Metabolic oxidation/reduction reactions and cellular responses to ionizing radiation: A unifying concept in stress response biology. *Cancer and Metastasis Reviews* (2004). doi:10.1023/B:CANC.0000031769.14728.bc

91. Kohen, R. & Gati, I. Skin low molecular weight antioxidants and their role in aging and in oxidative stress. in *Toxicology* (2000). doi:10.1016/S0300-483X(00)00206-7

92. Kurutas, E. B. The importance of antioxidants which play the role in cellular response against oxidative/nitrosative stress: Current state. *Nutrition Journal* (2016). doi:10.1186/s12937-016-0186-5

93. Bickers, D. R. & Athar, M. Oxidative stress in the pathogenesis of skin disease. *J. Invest. Dermatol.* (2006). doi:10.1038/sj.jid.5700340

94. Moreira, P. *et al.* Oxidative Stress: The Old Enemy in Alzheimers Disease Pathophysiology. *Curr. Alzheimer Res.* (2005). doi:10.2174/156720505774330537

95. Singh, U. & Jialal, I. Oxidative stress and atherosclerosis. *Pathophysiology* (2006). doi:10.1016/j.pathophys.2006.05.002

96. Golstein, P. & Kroemer, G. Cell death by necrosis: towards a molecular definition. *Trends Biochem. Sci.* **32**, 37–43 (2007).

97. Proskuryakov, S. Y., Konoplyannikov, A. G. & Gabai, V. L. Necrosis: A specific form of programmed cell death? *Experimental Cell Research* (2003). doi:10.1016/S0014-4827(02)00027-7

98. Galluzzi, L., Kepp, O., Krautwald, S., Kroemer, G. & Linkermann, A. Molecular mechanisms of regulated necrosis. *Semin. Cell Dev. Biol.* **35**, 24–32 (2014).

99. Vanlangenakker, N., Berghe, T., Krysko, D., Festjens, N. & Vandenabeele, P. Molecular Mechanisms and Pathophysiology of Necrotic Cell Death. *Curr. Mol. Med.* (2008). doi:10.2174/156652408784221306

100. Rock, K. L. & Kono, H. The Inflammatory Response to Cell Death. *Annu. Rev. Pathol. Mech. Dis.* (2008). doi:10.1146/annurev.pathmechdis.3.121806.151456

101. Bottone, M. *et al.* Morphological Features of Organelles during Apoptosis:

An Overview. *Cells* (2013). doi:10.3390/cells2020294

102. Edinger, A. L. & Thompson, C. B. Death by design: Apoptosis, necrosis and autophagy. *Current Opinion in Cell Biology* (2004). doi:10.1016/j.ceb.2004.09.011

103. Reiners, J. J. *et al.* Release of cytochrome c and activation of pro-caspase-9 following lysosomal photodamage involves bid cleavage. *Cell Death Differ.* (2002). doi:10.1038/sj.cdd.4401048

104. Jimbo, A. *et al.* ER stress induces caspase-8 activation, stimulating cytochrome c release and caspase-9 activation. *Exp. Cell Res.* (2003). doi:10.1016/S0014-4827(02)00033-2

105. Cho, S. G. & Choi, E. J. Apoptotic signaling pathways: Caspases and stress-activated protein kinases. *Journal of Biochemistry and Molecular Biology* (2002). doi:10.5483/bmbrep.2002.35.1.024

106. Tummers, B. & Green, D. R. Caspase-8: regulating life and death. *Immunol. Rev.* **277**, 76–89 (2017).

107. Gnesutta, N. & Minden, A. Death Receptor-Induced Activation of Initiator Caspase 8 Is Antagonized by Serine/Threonine Kinase PAK4. *Mol. Cell. Biol.* **23**, 7838–7848 (2003).

108. Schäfer, M. & Werner, S. Oxidative stress in normal and impaired wound repair. *Pharmacological Research* (2008). doi:10.1016/j.phrs.2008.06.004

109. Kruidering, M. & Evan, G. Caspase-8 in Apoptosis: The Beginning of 'The End'? *IUBMB Life* (2000). doi:10.1080/713803693

110. Redza-Dutordoir, M. & Averill-Bates, D. A. Activation of apoptosis signalling pathways by reactive oxygen species. *Biochim. Biophys. Acta - Mol. Cell Res.* **1863**, 2977–2992 (2016).

111. Simon, H. U., Haj-Yehia, A. & Levi-Schaffer, F. Role of reactive oxygen species (ROS) in apoptosis induction. *Apoptosis* (2000). doi:10.1023/A:1009616228304

112. Cooke, M. S., Evans, M. D., Dizdaroglu, M. & Lunec, J. Oxidative DNA damage: Mechanisms, mutation, and disease. *FASEB Journal* (2003). doi:10.1096/fj.02-0752rev

113. De Bont, R. & van Larebeke, N. Endogenous DNA damage in humans: A review of quantitative data. *Mutagenesis* (2004). doi:10.1093/mutage/geh025

114. Ames, B. N., Shigenaga, M. K. & Hagen, T. M. Oxidants, antioxidants, and the degenerative diseases of aging. *Proceedings of the National Academy of Sciences of the United States of America* (1993). doi:10.1073/pnas.90.17.7915

115. Cadet, J. & Davies, K. J. A. Oxidative DNA damage & repair: An introduction. *Free Radical Biology and Medicine* (2017). doi:10.1016/j.freeradbiomed.2017.03.030

116. Kasprzak, K. S. Oxidative DNA and protein damage in metal-induced toxicity and carcinogenesis. *Free Radic. Biol. Med.* (2002). doi:10.1016/S0891-5849(02)00809-2

117. Halliwell, B. Oxygen and nitrogen are pro-carcinogens. Damage to DNA by reactive oxygen, chlorine and nitrogen species: Measurement, mechanism and the effects of nutrition. *Mutat. Res. - Genet. Toxicol. Environ. Mutagen.* (1999). doi:10.1016/S1383-5742(99)00009-5

118. Klotz, L. O. Oxidant-induced signaling: Effects of peroxynitrite and singlet oxygen. *Biological Chemistry* (2002). doi:10.1515/BC.2002.047

119. Epe, B. DNA damage by peroxynitrite characterized with DNA repair enzymes. *Nucleic Acids Res.* **24**, 4105–4110 (1996).

120. Hirst, A. M. *et al.* Low-temperature plasma treatment induces DNA damage leading to necrotic cell death in primary prostate epithelial cells. *Br. J. Cancer* (2015). doi:10.1038/bjc.2015.113

121. Ciriolo, M. R. *et al.* Loss of GSH, oxidative stress, and decrease of intracellular pH as sequential steps in viral infection. *J. Biol. Chem.* (1997). doi:10.1074/jbc.272.5.2700

122. Halliwell, B. & Gutteridge, J. M. C. Oxygen toxicity, oxygen radicals, transition metals and disease. *Biochemical Journal* (1984). doi:10.1042/bj2190001

123. Alam, M. & Ratner, D. Cutaneous squamous-cell carcinoma. *New England Journal of Medicine* (2001). doi:10.1056/NEJM200103293441306

124. Firnhaber, J. M. Diagnosis and treatment of Basal cell and squamous cell carcinoma. *Am. Fam. Physician* **86**, 161–8 (2012).

125. Madan, V., Lear, J. T. & Szeimies, R. M. Non-melanoma skin cancer. *The Lancet* (2010). doi:10.1016/S0140-6736(09)61196-X

126. Brash, D. E. *et al.* A role for sunlight in skin cancer: UV-induced p53 mutations in squamous cell carcinoma. *Proc. Natl. Acad. Sci. U. S. A.* (1991). doi:10.1073/pnas.88.22.10124

127. Leibovitch, I. *et al.* Cutaneous squamous cell carcinoma treated with Mohs micrographic surgery in Australia I. Experience over 10 years. *J. Am. Acad. Dermatol.* (2005). doi:10.1016/j.jaad.2005.02.059

128. Leibovitch, I. *et al.* Cutaneous squamous cell carcinoma treated with Mohs

micrographic surgery in Australia II. Perineural invasion. *J. Am. Acad. Dermatol.* (2005). doi:10.1016/j.jaad.2005.03.048

129. Leibovitch, I., Huilgol, S. C., Selva, D., Paver, R. & Richards, S. Cutaneous lip tumours treated with Mohs micrographic surgery: clinical features and surgical outcome. *Br. J. Dermatol.* **153**, 1147–1152 (2005).

130. Sheridan, A. T. & Dawber, R. P. R. Curettage, electrosurgery and skin cancer. *Australasian Journal of Dermatology* (2000). doi:10.1046/j.1440-0960.2000.00383.x

131. Zimmerman, E. E. & Crawford, P. Cutaneous cryosurgery. *Am. Fam. Physician* (2012). doi:10.1201/b17660

132. Juarranz, Á., Jaén, P., Sanz-Rodríguez, F., Cuevas, J. & González, S. Photodynamic therapy of cancer. Basic principles and applications. *Clin. Transl. Oncol.* **10**, 148–154 (2008).

133. Agostinis, P. *et al.* Photodynamic therapy of cancer: An update. *CA. Cancer J. Clin.* **61**, 250–281 (2011).

134. Huang, Z. A Review of Progress in Clinical Photodynamic Therapy. *Technol. Cancer Res. Treat.* **4**, 283–293 (2005).

135. Van Herk, M. Errors and Margins in Radiotherapy. *Semin. Radiat. Oncol.* (2004). doi:10.1053/j.semradonc.2003.10.003

136. Van Herk, M., Remeijer, P., Rasch, C. & Lebesque, J. V. The probability of correct target dosage: Dose-population histograms for deriving treatment margins in radiotherapy. *Int. J. Radiat. Oncol. Biol. Phys.* (2000). doi:10.1016/S0360-3016(00)00518-6

137. Babington, P. *et al.* Use of cold atmospheric plasma in the treatment of cancer. *Biointerphases* (2015). doi:10.1116/1.4915264

138. Bekeschus, S. *et al.* Human Mononuclear Cell Survival and Proliferation is Modulated by Cold Atmospheric Plasma Jet. *Plasma Process. Polym.* **10**, 706–713 (2013).

139. Laroussi, M. & Lu, X. Room-temperature atmospheric pressure plasma plume for biomedical applications. *Appl. Phys. Lett.* **87**, 113902 (2005).

140. Fridman, A. & Friedman, G. Introduction to Fundamental and Applied Aspects of Plasma Medicine. in *Plasma Medicine* 1–17 (John Wiley & Sons Ltd, 2013). doi:10.1002/9781118437704.ch1

141. Langheinrich, A. P. & Roberts, D. B. Optical Emission Spectroscopy. in *Modern Methods of Geochemical Analysis* (1971). doi:10.1007/978-1-4684-1830-9_7

142. Coburn, J. W. & Chen, M. Optical emission spectroscopy of reactive plasmas: A method for correlating emission intensities to reactive particle density. *J. Appl. Phys.* (1980). doi:10.1063/1.328060

143. Fantz, U. Basics of plasma spectroscopy. *Plasma Sources Sci. Technol.* **15**, S137–S147 (2006).

144. Longo-Sorbello, G. S. A., Saydam, G., Banerjee, D. & Bertino, J. R. Cytotoxicity and cell growth assays. in *Cell Biology, Four-Volume Set* (2006). doi:10.1016/B978-012164730-8/50039-3

145. Adan, A., Kiraz, Y. & Baran, Y. Cell Proliferation and Cytotoxicity Assays. *Curr. Pharm. Biotechnol.* (2016). doi:10.2174/1389201017666160808160513

146. Rampersad, S. N. Multiple applications of alamar blue as an indicator of metabolic function and cellular health in cell viability bioassays. *Sensors (Switzerland)* (2012). doi:10.3390/s120912347

147. Al-Nasiry, S., Hanssens, M., Luyten, C. & Pijnenborg, R. The use of Alamar Blue assay for quantitative analysis of viability, migration and invasion of choriocarcinoma cells. *Hum. Reprod.* (2007). doi:10.1093/humrep/dem011

148. Uzarski, J. S., DiVito, M. D., Wertheim, J. A. & Miller, W. M. Essential design considerations for the resazurin reduction assay to noninvasively quantify cell expansion within perfused extracellular matrix scaffolds. *Biomaterials* (2017). doi:10.1016/j.biomaterials.2017.02.015

149. Riss, T. L. *et al. Cell Viability Assays*. *Assay Guidance Manual* (2004).

150. Kuete, V., Karaosmanoğlu, O. & Sivas, H. Anticancer Activities of African Medicinal Spices and Vegetables. in *Medicinal Spices and Vegetables from Africa: Therapeutic Potential Against Metabolic, Inflammatory, Infectious and Systemic Diseases* (2017). doi:10.1016/B978-0-12-809286-6.00010-8

151. Borra, R. C., Lotufo, M. A., Gagioti, S. M., Barros, F. de M. & Andrade, P. M. A simple method to measure cell viability in proliferation and cytotoxicity assays. *Braz. Oral Res.* **23**, 255–262 (2009).

152. Sauer, H., Wartenberg, M. & Hescheler, J. Reactive Oxygen Species as Intracellular Messengers During Cell Growth and Differentiation. *Cell. Physiol. Biochem.* **11**, 173–186 (2001).

153. Anoopkumar-Dukie, S. *et al.* Resazurin assay of radiation response in cultured cells. *Br. J. Radiol.* **78**, 945–947 (2005).

154. O'Brien, J., Wilson, I., Orton, T. & Pognan, F. Investigation of the Alamar Blue (resazurin) fluorescent dye for the assessment of mammalian cell cytotoxicity. *Eur. J. Biochem.* **267**, 5421–5426 (2000).

155. Hamid, R., Rotshteyn, Y., Rabadi, L., Parikh, R. & Bullock, P. Comparison of alamar blue and MTT assays for high through-put screening. *Toxicol. Vitr.* **18**, 703–710 (2004).

156. Wlodkowic, D., Skommer, J. & Darzynkiewicz, Z. Flow cytometry-based apoptosis detection. *Methods Mol. Biol.* (2009). doi:10.1007/978-1-60327-017-5_2

157. Manti, A., Papa, S. & Boi, P. What Flow Cytometry can Tell Us About Marine Micro-Organisms – Current Status and Future Applications. in *Flow Cytometry - Recent Perspectives* (InTech, 2012). doi:10.5772/38616

158. Hawley, T. S. & Hawley, R. G. *Flow Cytometry Protocols*. *Flow Cytometry Protocols* **263**, (Humana Press, 2004).

159. Quirke, P. Introduction to Flow Cytometry. *J. Clin. Pathol.* **45**, 275–276 (1992).

160. Dass, C. *Fundamentals of Contemporary Mass Spectrometry*. *Fundamentals of Contemporary Mass Spectrometry* (2006). doi:10.1002/9780470118498

161. Yue, Y. F., Mohades, S., Laroussi, M. & Lu, X. Measurements of Plasma-Generated Hydroxyl and Hydrogen Peroxide Concentrations for Plasma Medicine Applications. *IEEE Trans. Plasma Sci.* **44**, 2754–2758 (2016).

162. Mohanty, J. G., Jaffe, J. S., Schulman, E. S. & Raible, D. G. A highly sensitive fluorescent micro-assay of H2O2 release from activated human leukocytes using a dihydroxyphenoxazine derivative. *J. Immunol. Methods* (1997). doi:10.1016/S0022-1759(96)00244-X

163. Ghasempur, S. *et al.* Optimization of peroxidase-catalyzed oxidative coupling process for phenol removal from wastewater using response surface methodology. *Environ. Sci. Technol.* (2007). doi:10.1021/es070626q

164. Hynninen, P. H., Kaartinen, V. & Kolehmainen, E. Horseradish peroxidase-catalyzed oxidation of chlorophyll a with hydrogen peroxide. *Biochim. Biophys. Acta - Bioenerg.* **1797**, 531–542 (2010).

165. Smith, S. A., Smith, R. W., Xia, Y. & Ouyang, Z. Introduction to Mass Spectrometry. *Characterization of Impurities and Degradants Using Mass Spectrometry* (2011). doi:10.1002/9780470921371.ch1

166. Mass spectrometry: a textbook. *Choice Rev. Online* (2011). doi:10.5860/choice.49-1469

167. Paces, J. B., Weis, D. & Ireland, T. R. Mass spectrometry. in *Encyclopedia of Earth Sciences Series* (2015). doi:10.5650/jos1956.11.600

168. Finehout, E. J. & Lee, K. H. An Introduction to Mass Spectrometry

Applications in Biological Research. *Biochemistry and Molecular Biology Education* (2004). doi:10.1002/bmb.2004.494032020331

169. Mass spectrometry: principles and applications. *Choice Rev. Online* **45**, 45-4389-45–4389 (2008).

170. Guilhaus, M. Special feature: Tutorial. Principles and instrumentation in time-of-flight mass spectrometry. Physical and instrumental concepts. *J. Mass Spectrom.* **30**, 1519–1532 (1995).

171. Wollnik, H. Time-of-flight mass analyzers. *Mass Spectrom. Rev.* (1993). doi:10.1002/mas.1280120202

172. Wiley, W. C. & McLaren, I. H. Time-of-Flight Mass Spectrometer with Improved Resolution. *Rev. Sci. Instrum.* **26**, 1150–1157 (1955).

173. Colby, S. M., King, T. B., Reilly, J. P. & Lubman, D. M. Improving the resolution of matrix-assisted laser desorption/ionization time-of-flight mass spectrometry by exploiting the correlation between ion position and velocity. *Rapid Commun. Mass Spectrom.* **8**, 865–868 (1994).

174. Brown, R. S. & Lennon, J. J. Mass Resolution Improvement by Incorporation of Pulsed Ion Extraction in a Matrix-Assisted Laser Desorption/Ionization Linear Time-of-Flight Mass Spectrometer. *Anal. Chem.* (1995). doi:10.1021/ac00109a015

175. Li, D. & Liu, S. Drinking Water Detection. in *Water Quality Monitoring and Management* (2019). doi:10.1016/b978-0-12-811330-1.00010-7

176. Ion Exchange Chromatography & Chromatofocusing - Principles and Methods. Ion Exchange Chromatography & Chromatofocusing - Principles and Methods. *GE Healthc.* (2004).

177. Grönberg, A. Ion Exchange Chromatography. in *Biopharmaceutical Processing* 379–399 (Elsevier, 2018). doi:10.1016/B978-0-08-100623-8.00018-9

178. Jungbauer, A. & Hahn, R. Chapter 22 Ion-Exchange Chromatography. in *Methods in Enzymology* 349–371 (2009). doi:10.1016/S0076-6879(09)63022-6

179. Nesterenko, P. N. & Paull, B. Ion chromatography. in *Liquid Chromatography* 205–244 (Elsevier, 2017). doi:10.1016/B978-0-12-805393-5.00009-9

180. Coskun, O. Separation Tecniques: CHROMATOGRAPHY. *North. Clin. Istanbul* (2016). doi:10.14744/nci.2016.32757

181. Biotech, A. P. Chromatography Ion Exchange Chromatography. *Ion Exch. Chromatogr. Princ. Methods* (1991). doi:10.1002/0471140864.ps0802s15

182. Wilson, B., Gandhi, J. & Zhang, C. Analysis of inorganic nitrogen and

related anions in high salinity water using ion chromatography with tandem UV and conductivity detectors. *J. Chromatogr. Sci.* (2011). doi:10.1093/chrsci/49.8.596

183. Braithwaite, N. S. J. Introduction to gas discharges. *Plasma Sources Sci. Technol.* (2000). doi:10.1088/0963-0252/9/4/307

184. Heinlin, J. *et al.* Plasma applications in medicine with a special focus on dermatology. *Journal of the European Academy of Dermatology and Venereology* (2011). doi:10.1111/j.1468-3083.2010.03702.x

185. Hoentsch, M. *et al.* Persistent effectivity of gas plasma-treated, long time-stored liquid on epithelial cell adhesion capacity and membrane morphology. *PLoS One* (2014). doi:10.1371/journal.pone.0104559

186. Pereira, S., Pinto, E., Ribeiro, P. A. & Sério, S. Study of a Cold Atmospheric Pressure Plasma jet device for indirect treatment of Squamous Cell Carcinoma. *Clin. Plasma Med.* **13**, 9–14 (2019).

187. Lukes, P. & Locke, B. R. Plasmachemical oxidation processes in a hybrid gas-liquid electrical discharge reactor. *J. Phys. D. Appl. Phys.* (2005). doi:10.1088/0022-3727/38/22/010

188. The Principles of Humane Experimental Technique. *Med. J. Aust.* (1960). doi:10.5694/j.1326-5377.1960.tb73127.x

189. Flecknell, P. Replacement, reduction and refinement. *ALTEX* **19**, 73–8 (2002).

190. Fridman, G. *et al.* Comparison of direct and indirect effects of non-thermal atmospheric-pressure plasma on bacteria. *Plasma Process. Polym.* (2007). doi:10.1002/ppap.200600217

191. Duchesne, C., Frescaline, N., Lataillade, J.-J. & Rousseau, A. Comparative Study between Direct and Indirect Treatment with Cold Atmospheric Plasma on In Vitro and In Vivo Models of Wound Healing. *Plasma Med.* (2018). doi:10.1615/plasmamed.2019028659

192. Babaeva, N. Y. & Kushner, M. J. Direct and indirect treatment of living tissue: Dielectric barrier discharges VS. plasma jets. in (2011). doi:10.1109/plasma.2011.5993038

193. Tanaka, H. *et al.* Plasma-activated medium selectively kills glioblastoma brain tumor cells by down-regulating a survival signaling molecule, AKT kinase. *Plasma Med.* (2011). doi:10.1615/PlasmaMed.2012006275

194. Liedtke, K. R. *et al.* Non-thermal plasma-treated solution demonstrates antitumor activity against pancreatic cancer cells in vitro and in vivo. *Sci. Rep.* **7**, 8319 (2017).

195. Deberardinis, R. J. & Thompson, C. B. Cellular metabolism and disease: What do metabolic outliers teach us? *Cell* (2012). doi:10.1016/j.cell.2012.02.032

196. Pal, S. & Shil, K. Metabolic Toxicity and Alteration of Cellular Bioenergetics by Hexavalent Chromium. in *Handbook of Environmental Materials Management* 1–28 (Springer International Publishing, 2018). doi:10.1007/978-3-319-58538-3_58-1

197. Masters, J. R. & Stacey, G. N. Changing medium and passaging cell lines. *Nat. Protoc.* (2007). doi:10.1038/nprot.2007.319

198. Long, L. H. & Halliwell, B. Artefacts in cell culture: Pyruvate as a scavenger of hydrogen peroxide generated by ascorbate or epigallocatechin gallate in cell culture media. *Biochem. Biophys. Res. Commun.* (2009). doi:10.1016/j.bbrc.2009.08.069

199. Salahudeen, A. K., Clark, E. C. & Nath, K. A. Hydrogen peroxide-induced renal injury a protective role for pyruvate in vitro and in vivo. *J. Clin. Invest.* (1991). doi:10.1172/JCI115511

200. Yan, D. *et al.* Principles of using Cold Atmospheric Plasma Stimulated Media for Cancer Treatment. *Sci. Rep.* **5**, 18339 (2015).

201. Nakamura, K. *et al.* Novel Intraperitoneal Treatment With Non-Thermal Plasma-Activated Medium Inhibits Metastatic Potential of Ovarian Cancer Cells. *Sci. Rep.* (2017). doi:10.1038/s41598-017-05620-6

202. Chauvin, J., Judée, F., Yousfi, M., Vicendo, P. & Merbahi, N. Analysis of reactive oxygen and nitrogen species generated in three liquid media by low temperature helium plasma jet. *Sci. Rep.* (2017). doi:10.1038/s41598-017-04650-4

203. Ayala, A., Muñoz, M. F. & Argüelles, S. Lipid Peroxidation: Production, Metabolism, and Signaling Mechanisms of Malondialdehyde and 4-Hydroxy-2-Nonenal. *Oxid. Med. Cell. Longev.* **2014**, 1–31 (2014).

204. He, L. *et al.* Antioxidants Maintain Cellular Redox Homeostasis by Elimination of Reactive Oxygen Species. *Cellular Physiology and Biochemistry* (2017). doi:10.1159/000485089

205. Kalghatgi, S. *et al.* Effects of Non-Thermal Plasma on Mammalian Cells. *PLoS One* **6**, e16270 (2011).

206. Davies, M. J. Protein oxidation and peroxidation. *Biochemical Journal* (2016). doi:10.1042/BJ20151227

207. Wende, K. *et al.* Identification of the biologically active liquid chemistry induced by a nonthermal atmospheric pressure plasma jet. *Biointerphases*

(2015). doi:10.1116/1.4919710

208. Wende, K. *et al.* Risk assessment of a cold argon plasma jet in respect to its mutagenicity. *Mutat. Res. - Genet. Toxicol. Environ. Mutagen.* (2016). doi:10.1016/j.mrgentox.2016.02.003

209. Yan, D. *et al.* Controlling plasma stimulated media in cancer treatment application. *Appl. Phys. Lett.* (2014). doi:10.1063/1.4902875

210. Reineke, K., Langer, K., Hertwig, C., Ehlbeck, J. & Schlüter, O. The impact of different process gas compositions on the inactivation effect of an atmospheric pressure plasma jet on Bacillus spores. *Innov. Food Sci. Emerg. Technol.* **30**, 112–118 (2015).

211. Schmidt, A. *et al.* Role of Ambient Gas Composition on Cold Physical Plasma-Elicited Cell Signaling in Keratinocytes. *Biophys. J.* (2017). doi:10.1016/j.bpj.2017.04.030

212. Chen, Q. M., Tu, V. C., Wu, Y. & Bahl, J. J. Hydrogen peroxide dose dependent induction of cell death or hypertrophy in cardiomyocytes. *Arch. Biochem. Biophys.* (2000). doi:10.1006/abbi.1999.1558

213. Turrini, E. *et al.* Cold Atmospheric Plasma Induces Apoptosis and Oxidative Stress Pathway Regulation in T-Lymphoblastoid Leukemia Cells. *Oxid. Med. Cell. Longev.* **2017**, 1–13 (2017).

214. Kanduc, D. *et al.* Cell death: Apoptosis versus necrosis (Review). *Int. J. Oncol.* (2002). doi:10.3892/ijo.21.1.165

215. Krysko, D. V., Berghe, T. Vanden, Parthoens, E., D'Herde, K. & Vandenabeele, P. Chapter 16 Methods for Distinguishing Apoptotic from Necrotic Cells and Measuring Their Clearance. in *Methods in Enzymology* 307–341 (2008). doi:10.1016/S0076-6879(08)01416-X

216. Boehm, D., Heslin, C., Cullen, P. J. & Bourke, P. Cytotoxic and mutagenic potential of solutions exposed to cold atmospheric plasma. *Sci. Rep.* **6**, 21464 (2016).

217. Lu, X. *et al.* Reactive species in non-equilibrium atmospheric-pressure plasmas: Generation, transport, and biological effects. *Phys. Rep.* **630**, 1–84 (2016).

218. Bauer, G., Sersenová, D., Graves, D. B. & Machala, Z. Cold Atmospheric Plasma and Plasma-Activated Medium Trigger RONS-Based Tumor Cell Apoptosis. *Sci. Rep.* **9**, 14210 (2019).

219. Surre, J. *et al.* Strong increase in the autofluorescence of cells signals struggle for survival. *Sci. Rep.* (2018). doi:10.1038/s41598-018-30623-2

220. Maziveyi, M. & Alahari, S. K. Cell matrix adhesions in cancer: The proteins that form the glue. *Oncotarget* (2017). doi:10.18632/oncotarget.17265

221. Hanahan, D. & Weinberg, R. A. Hallmarks of cancer: The next generation. *Cell* (2011). doi:10.1016/j.cell.2011.02.013

222. Matyas, Z. Comparative Oncology. *Veterinary Pathology* (1982). doi:10.1177/030098588201900101

223. Alibert, C., Goud, B. & Manneville, J. B. Are cancer cells really softer than normal cells? *Biology of the Cell* (2017). doi:10.1111/boc.201600078

224. Rumbach, P., Bartels, D. M., Sankaran, R. M. & Go, D. B. The solvation of electrons by an atmospheric-pressure plasma. *Nat. Commun.* (2015). doi:10.1038/ncomms8248

225. Bundscherer, L. *et al.* Viability of Human Blood Leukocytes Compared with Their Respective Cell Lines after Plasma Treatment. *Plasma Med.* **3**, 71–80 (2013).

226. Rhee, S. G. *et al.* Intracellular messenger function of hydrogen peroxide and its regulation by peroxiredoxins. *Curr. Opin. Cell Biol.* **17**, 183–189 (2005).

227. Eruslanov, E. & Kusmartsev, S. Identification of ROS Using Oxidized DCFDA and Flow-Cytometry. in *Methods in Molecular Biology* 57–72 (2010). doi:10.1007/978-1-60761-411-1_4

228. Anbar, M. On the sonochemical formation of hydrogen peroxide in water. *J. Phys. Chem.* (1964). doi:10.1021/j100784a025

229. Anbar, M., Guttmann, S. & Stein, G. Radiolysis of Aqueous Solutions Highly Enriched in O 18. *J. Chem. Phys.* **34**, 703–711 (1961).

230. Jablonowski, H. & von Woedtke, T. Research on plasma medicine-relevant plasma–liquid interaction: What happened in the past five years? *Clin. Plasma Med.* **3**, 42–52 (2015).

231. Adachi, T. *et al.* Plasma-activated medium induces A549 cell injury via a spiral apoptotic cascade involving the mitochondrial-nuclear network. *Free Radic. Biol. Med.* (2015). doi:10.1016/j.freeradbiomed.2014.11.014

232. Houot, V. *et al.* Hydrogen peroxide induces programmed cell death features in cultured tobacco BY-2 cells, in a dose-dependent manner. *J. Exp. Bot.* (2001). doi:10.1093/jxb/52.361.1721

233. Lukes, P., Locke, B. R. & Brisset, J.-L. Aqueous-Phase Chemistry of Electrical Discharge Plasma in Water and in Gas-Liquid Environments. in *Plasma Chemistry and Catalysis in Gases and Liquids* 243–308 (Wiley-VCH Verlag GmbH & Co. KGaA, 2012). doi:10.1002/9783527649525.ch7

234. Kim, S. J. & Chung, T. H. Cold atmospheric plasma jet-generated RONS and their selective effects on normal and carcinoma cells. *Sci. Rep.* **6**, 20332 (2016).

235. van Gils, C. A. J., Hofmann, S., Boekema, B. K. H. L., Brandenburg, R. & Bruggeman, P. J. Mechanisms of bacterial inactivation in the liquid phase induced by a remote RF cold atmospheric pressure plasma jet. *J. Phys. D. Appl. Phys.* **46**, 175203 (2013).

236. Oehmigen, K. *et al.* The role of acidification for antimicrobial activity of atmospheric pressure plasma in liquids. *Plasma Process. Polym.* (2010). doi:10.1002/ppap.200900077

237. Khlyustova, A., Labay, C., Machala, Z., Ginebra, M.-P. & Canal, C. Important parameters in plasma jets for the production of RONS in liquids for plasma medicine: A brief review. *Front. Chem. Sci. Eng.* **13**, 238–252 (2019).

238. Giles, G. I., Nasim, M. J., Ali, W. & Jacob, C. The reactive sulfur species concept: 15 years on. *Antioxidants* (2017). doi:10.3390/antiox6020038

239. Lackmann, J. W. *et al.* Chemical fingerprints of cold physical plasmas - An experimental and computational study using cysteine as tracer compound. *Sci. Rep.* (2018). doi:10.1038/s41598-018-25937-0

240. Kogelheide, F. *et al.* FTIR spectroscopy of cysteine as a ready-to-use method for the investigation of plasma-induced chemical modifications of macromolecules. *J. Phys. D. Appl. Phys.* (2016). doi:10.1088/0022-3727/49/8/084004

241. Vione, D., Belmondo, S. & Carnino, L. A kinetic study of phenol nitration and nitrosation with nitrous acid in the dark. *Environ. Chem. Lett.* (2004). doi:10.1007/s10311-004-0088-1

242. Yan, J. H. *et al.* Plasma chemical degradation of phenol in solution by gas-liquid gliding arc discharge. *Plasma Sources Sci. Technol.* (2005). doi:10.1088/0963-0252/14/4/001

243. Lackmann, J.-W. *et al.* Nitrosylation vs. oxidation – How to modulate cold physical plasmas for biological applications. *PLoS One* **14**, e0216606 (2019).

244. Salazar, A., Keusgen, M. & Von Hagen, J. Amino acids in the cultivation of mammalian cells. *Amino Acids* (2016). doi:10.1007/s00726-016-2181-8

245. Takai, E. *et al.* Chemical modification of amino acids by atmospheric-pressure cold plasma in aqueous solution. *J. Phys. D. Appl. Phys.* **47**, 285403 (2014).

246. Poole, L. B. The basics of thiols and cysteines in redox biology and

chemistry. *Free Radical Biology and Medicine* (2015). doi:10.1016/j.freeradbiomed.2014.11.013

247. Klämpfl, T. G. *et al.* Cold Atmospheric Air Plasma Sterilization against Spores and Other Microorganisms of Clinical Interest. *Appl. Environ. Microbiol.* **78**, 5077–5082 (2012).

248. Bruno, G. *et al.* Cold physical plasma-induced oxidation of cysteine yields reactive sulfur species (RSS). *Clin. Plasma Med.* (2019). doi:10.1016/j.cpme.2019.100083

249. Heusler, T. *et al.* Can the effect of cold physical plasma-derived oxidants be transported via thiol group oxidation? *Clin. Plasma Med.* (2019). doi:10.1016/j.cpme.2019.100086

250. Zhou, R. *et al.* Interaction of atmospheric-pressure air microplasmas with amino acids as fundamental processes in aqueous solution. *PLoS One* (2016). doi:10.1371/journal.pone.0155584

251. Alcock, L. J., Perkins, M. V. & Chalker, J. M. Chemical methods for mapping cysteine oxidation. *Chem. Soc. Rev.* **47**, 231–268 (2018).

252. Kumar, A. *et al.* S-sulfocysteine/NMDA receptor–dependent signaling underlies neurodegeneration in molybdenum cofactor deficiency. *J. Clin. Invest.* (2017). doi:10.1172/JCI89885

253. Uppu, R. M. *et al.* Nitrosation by peroxynitrite: Use of phenol as a probe. *Arch. Biochem. Biophys.* (1998). doi:10.1006/abbi.1998.0825

254. Wu, J., Rudy, K. & Spark, J. Oxidation of aqueous phenol by ozone and peroxidase. *Adv. Environ. Res.* (2000). doi:10.1016/S1093-0191(00)00034-4

255. Gurol, M. D. & Vatistas, R. Oxidation of phenolic compounds by ozone and ozone + u.v. radiation: A comparative study. *Water Res.* (1987). doi:10.1016/S0043-1354(87)80006-4

256. Esplugas, S., Giménez, J., Contreras, S., Pascual, E. & Rodríguez, M. Comparison of different advanced oxidation processes for phenol degradation. *Water Res.* (2002). doi:10.1016/S0043-1354(01)00301-3

257. Yenes, S. & Messeguer, A. A study of the reaction of different phenol substrates with nitric oxide and peroxynitrite. *Tetrahedron* **55**, 14111–14122 (1999).

258. Challis, B. C. & Lawson, A. J. The chemistry of nitroso-compounds. Part II. The nitrosation of phenol and anisole. *J. Chem. Soc. B Phys. Org.* 770 (1971). doi:10.1039/j29710000770

259. Daiber, A., Mehl, M. & Ullrich, V. New Aspects in the Reaction Mechanism

of Phenol with Peroxynitrite: The Role of Phenoxy Radicals. *Nitric Oxide* **2**, 259–269 (1998).

260. Luo, D., Smith, S. W. & Anderson, B. D. Kinetics and Mechanism of the Reaction of Cysteine and Hydrogen Peroxide in Aqueous Solution. *J. Pharm. Sci.* **94**, 304–316 (2005).

261. Wende, K., Reuter, S., Von Woedtke, T., Weltmann, K. D. & Masur, K. Redox-based assay for assessment of biological impact of plasma treatment. *Plasma Process. Polym.* (2014). doi:10.1002/ppap.201300172

262. Winter, J. *et al.* Feed gas humidity: A vital parameter affecting a cold atmospheric-pressure plasma jet and plasma-treated human skin cells. *J. Phys. D. Appl. Phys.* (2013). doi:10.1088/0022-3727/46/29/295401

263. Reuter, S. *et al.* The Influence of Feed Gas Humidity Versus Ambient Humidity on Atmospheric Pressure Plasma Jet-Effluent Chemistry and Skin Cell Viability. *IEEE Trans. Plasma Sci.* (2015). doi:10.1109/TPS.2014.2361921

264. Canal, C. *et al.* Plasma-induced selectivity in bone cancer cells death. *Free Radic. Biol. Med.* (2017). doi:10.1016/j.freeradbiomed.2017.05.023

A

Appendix

Figure A.1 Schematics of the developed DC power supply.

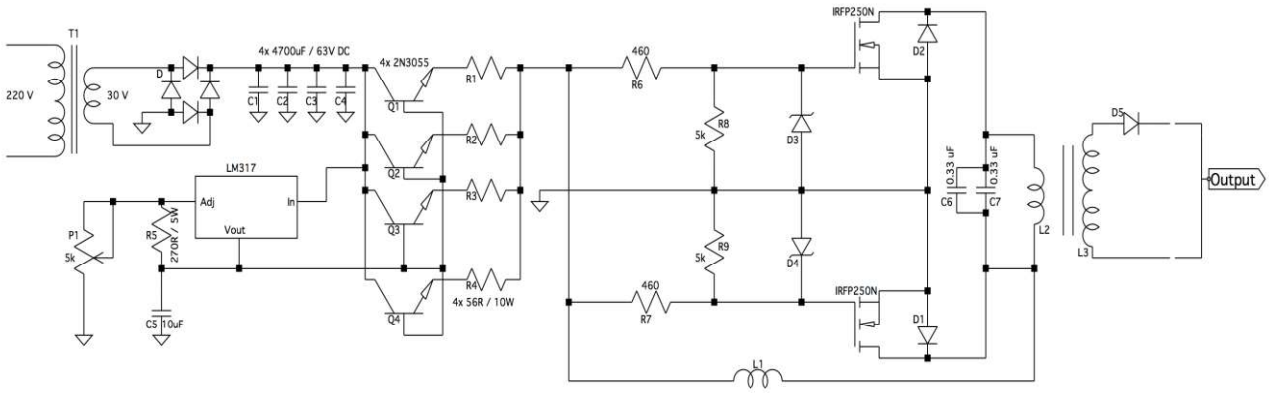

Table A-1 Cysteine derivatives found using the developed Jet.

	Control	Ar 30 s	Ar120 s	ArO 30 s	ArO 120 s	ArNO 30 s	ArNO 120 s
Sulfite (m/z=79.96)	*	*	*	*	1.21	*	1.02
Sulfate (m/z=96.96)	23.60	30.45	25.65	25.65	34.33	30.13	29.22
Cysteine (m/z=120.01)	1165.11	1040.44	1030.66	1040.10	914.03	915.09	925.21
S-nitrosocysteine (m/z =19.01)	*	1.37	*	*	1.46	1.00	*
Dehydro- sulfinic acid (m/z=149.99)	*	*	*	*	1.76	*	1.76
Deamino-sulfonic acid (m/z=150.97)	*	1.92	3.12	2.00	2.31	2.53	2.26
Cysteine Sulfinic acid (m/z=152)	12.08	17.92	48.25	15.49	26.87	13.36	22.09
Cysteine sulfonic acid (m/z=168)	22.29	30.40	68.90	46.11	84.31	45.01	67.16
Cysteine S-sulfonate (m/z=199.95)	3.50	6.98	4.49	5.21	9.13	8.01	9.09
Cystine (m/z=239.02)	246.97	312.98	551.90	559.98	703.40	722.92	581.60
Cysteine disulfoxide (m/z=271.01)	6.31	6.59	8.04	7.79	7.73	5.67	7.16

Table A-2 Cysteine derivatives found using the developed kINPen09.

	Control	Ar 30 s	Ar120 s	ArO 30 s	ArO 120 s	ArNO 30 s	ArNO 120 s
Sulfite (m/z=79.96)	*	*	1.05	2.10	6.04	1.77	5.21
Sulfate (m/z=96.96)	23.60	24.98	25.14	33.71	60.74	25.59	50.21
Cysteine (m/z=120.01)	1165.11	934.89	834.05	885.12	758.08	924.97	725.07
S-nitrosocysteine (m/z =19.01)	*	*	*	*	1.41	*	1.51
Dehydro- sulfinic acid (m/z=149.99)	*	1.40	3.47	8.40	30.44	7.71	28.91
Deamino-sulfonic acid (m/z=150.97)	*	2.10	2.64	5.21	16.56	4.83	15.42
Cysteine Sulfinic acid (m/z=152)	12.08	16.91	30.94	28.42	53.96	27.18	45.94
Cysteine sulfonic acid (m/z=168)	22.29	54.71	125.87	303.46	1090.52	269.74	962.51
Cysteine S-sulfonate (m/z=199.95)	3.50	7.72	6.14	9.89	10.40	7.87	9.62
Cystine (m/z=239.02)	246.97	724.06	1260.38	546.06	707.12	586.02	901.44
Cysteine disulfoxide (m/z=271.01)	6.31	6.56	10.79	26.80	67.41	24.16	57.56

Table A-3 Phenol derivatives found using the developed Jet.

	m/z	control	Ar 15 s	Ar 60 s	ArO 15 s	ArO 60 s	ArNO 15 s	ArNO 60 s
Phenol	93.03	2019.71	2948.81	2871.76	3239.62	2931.89	2886.72	2773.01
Oxi-phenol	108.02	16.69	33.14	53.25	47.27	120.35	65.47	145.10
Hydroxy-phenol	109.03	39.27	49.04	56.11	53.63	90.03	63.61	100.21
Nitroso-phenol	122.03	3.38	3.79	4.86	3.91	6.47	6.88	4.62
2Oxi-phenol	124.02	1.88	1.82	3.38	2.11	4.29	2.76	5.85
2Hydroxy-phenol	125.03	1.99	2.29	2.64	2.13	3.40	2.62	3.62
Nitro-phenol	138.03	*	2.65	6.12	2.17	4.88	2.86	3.88
Muconic acid	141.02	*	1.07	1.74	1.43	2.54	1.46	2.80
2Nitroso-phenol	151.04	2.06	3.23	2.88	2.29	2.85	2.37	2.03

Table A-4 Phenol derivatives found using the kINPen09.

	m/z	control	Ar 15 s	Ar 60 s	ArO 15 s	ArO 60 s	ArNO 15 s	ArNO 60 s
Phenol	93.03	2019.71	3029.91	3137.78	3125.02	2668.51	2934.28	2299.16
Oxi-phenol	108.02	16.69	29.81	50.72	44.09	104.16	44.57	88.79
Hydroxy-phenol	109.03	39.27	44.06	55.33	50.38	69.07	46.93	67.35
Nitroso-phenol	122.03	3.38	5.87	5.77	5.02	4.71	4.89	6.29
2Oxi-phenol	124.02	1.88	1.65	2.42	3.02	3.15	2.07	3.22
2Hydroxy-phenol	125.03	1.99	1.90	2.14	2.17	2.55	1.89	2.39
Nitro-phenol	138.03	*	2.24	4.88	1.89	1.97	1.56	1.86
Muconic acid	141.02	*	1.35	1.62	1.96	2.62	1.37	2.64
2Nitroso-phenol	151.04	2.06	2.24	2.15	1.87	1.89	1.98	2.19